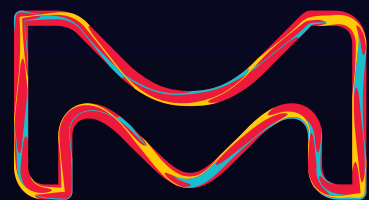


Photoredox Catalysis

Desk Reference and User's Guide

Nathan J. Gesmundo, Megan H. Shaw, Jack Twilton,
John C. Tellis, David W. C. MacMillan, David A. Nicewicz



The life science
business of Merck
operates as
MilliporeSigma in
the U.S. and Canada.

Sigma-Aldrich[®]
Lab & Production Materials

Photoredox Catalysis

Introduction,
Desk Reference,
and Users Guide



Nathan Gesmundo. Nathan was raised in Kalamazoo, MI. Nathan pursued his undergraduate degree at Michigan State University, graduating in 2009 with a B.S. in Chemistry after conducting research in the laboratory of Professor Robert E. Maleczka, Jr.

In 2010 Nathan began his graduate studies in the laboratory of Professor David A. Nicewicz at the University of North Carolina at Chapel Hill. Nathan's research in the Nicewicz laboratory focused on the discovery and development of new methods using organic photoredox catalysis, and he graduated with his Ph.D. in 2015.



Megan Shaw. Megan conducted her undergraduate studies at the University of Sheffield, obtaining her MChem degree in 2010. Following this, she began her Ph.D studies under the supervision of Dr. John Bower, with co-supervision from Dr. William Whittingham at Syngenta,

focusing on the development of new methodologies for *N*-heterocycle synthesis via C–C bond activation of aminocyclopropanes. In 2015, she began a postdoctoral appointment with Professor David MacMillan at Princeton University where she has been conducting research in the area of photoredox catalysis with an emphasis on C–H functionalization strategies.



Jack Twilton. Jack obtained his MChem degree from the University of Oxford in 2014, undertaking research in the laboratory of Professor Veronique Gouverneur, where he worked on the development of a novel strategy for the ^{18}F radiolabeling of novel fluorinated pharmacophores.

In 2014, Jack subsequently joined the laboratory of Professor David MacMillan at Princeton University for his doctoral studies. He is currently working on the development of dual photoredox transition metal-catalyzed processes with an emphasis on the use of native functionality in cross-coupling.



John Tellis. John was born and raised in Pottstown, Pennsylvania and received his B.S. in biochemistry from Elizabethtown College in 2012. He subsequently completed graduate studies in organic chemistry at the University of Pennsylvania in 2016.

There, he contributed to the genesis of photoredox/nickel dual catalytic cross-coupling of oxidatively activated pro-radicals in the laboratory of Professor Gary Molander. He is currently a Scientist in Discovery Chemistry at Genentech, Inc.



Professor David MacMillan. David MacMillan received his undergraduate degree in chemistry from the University of Glasgow, where he worked with Dr. Ernie Colvin. In 1990, he began his doctoral studies under the direction of Professor Larry Overman at the University of California, Irvine, before

undertaking a postdoctoral position with Professor Dave Evans at Harvard University. He began his independent career at the University of California, Berkeley, in July of 1998 before moving to Caltech in June 2000 (Earle C. Anthony Chair of Organic Chemistry). In 2006, Dave moved to the east coast and is currently the James S. McDonnell Distinguished University Professor at Princeton University, where he served as Department Chair from 2010 to 2015. Research in the MacMillan laboratory focuses on photoredox catalysis, organocatalysis, and the synthesis of natural products and pharmaceuticals.



Professor David Nicewicz. David Nicewicz is an Associate Professor of Chemistry at the University of North Carolina at Chapel Hill. David began his independent career at UNC-Chapel Hill in 2009, after completing his Ph.D. under the advisement of Professor Jeffrey S. Johnson and

postdoctoral research in the laboratory of Professor David MacMillan. Research in the Nicewicz laboratory is focused on photoredox catalysis; especially the development of organic photoredox systems using acridinium and pyrylium catalysts. The group is broadly interested in employing this technology in synthetic method development, natural product synthesis, and mechanistic investigation. These efforts have culminated in a suite of alkene and arene functionalization reactions.

Table of Contents

I.	Introduction	2
II.	Standard Reaction Setup	4
III.	High-Throughput Experimentation and Introduction to Scaling Up via Flow	9
IV.	Photoinduced Electron Transfer	12
V.	Synthesis of Photoredox Catalysts	16
VI.	Metallaphotoredox Cross-Couplings	17
VII.	Late-Stage Functionalization and Trifluoromethylation	33
VIII.	Alkene and Arene Functionalization Using Organic Photoredox Systems	39
IX.	Recent Cyclization Strategies Enabled by Photoredox Catalysis	45
X.	Conclusion	48
XI.	Abbreviations and Symbols	49
XII.	References	50
XIII.	Appendix Table 1: Photoredox catalysts	54
XIV.	Appendix Table 2: Excited state photooxidants	55
XV.	Appendix Table 3: Excited state photoreductants	56
XVI.	Appendix Table 4: Catalyst references and properties	57

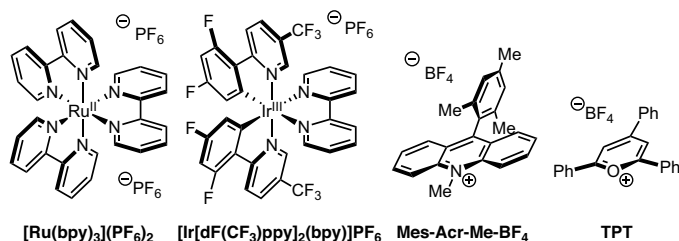
I. Introduction

Over the last decade visible light photoredox catalysis has emerged as a powerful tool in organic synthesis, building upon the foundation set by early pioneers in the areas of radical chemistry and photochemistry. Photoredox chemistry allows one to forge new bonds via open shell pathways and facilitates the rapid assembly of complex products en route to new areas of chemical space (**Figure 1**).¹⁻⁷

A strength of photoredox catalysis lies in the ability to generate reactive open shell intermediates via single electron transfer in a controlled manner under mild conditions. The requisite oxidant or reductant for electron transfer is generated upon catalyst excitation with visible light (photoredox catalyst examples, **Figure 1A**). This permits one to selectively add energy to a light-harvesting system as most organic substrates/reagents do not absorb in the visible region of the electromagnetic spectrum. This is in contrast to irradiation with ultraviolet (UV) light where deleterious radical side reactions can occur through substrate/reagent photoexcitation, and heating where energy is applied uniformly to the system. That a photoredox catalyst can act as both an oxidant and a reductant allows for the development of net oxidative processes, net reductive reactions, and redox neutral processes where the catalyst acts as a transiently generated oxidant and reductant at different points in the cycle.⁴

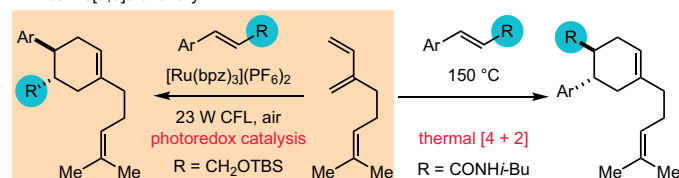
The reactivity or selectivity imparted by photoredox activation can be complementary to other established reaction paradigms (**Figure 1B**). Yoon and co-workers showed that Diels-Alder cycloadditions proceeding through cation radicals (photoredox-mediated) and thermal pathways display opposite regioselectivity in related systems.⁸ Additionally, the cation radical-mediated pathway represents an electronically mismatched reaction, counter to thermal or Lewis acid-catalyzed cycloadditions.⁸ Nicewicz showed that cation radical-mediated photoredox alkene hydrofunctionalization yields anti-Markovnikov products, in contrast to the Markovnikov selectivity observed in Brønsted acid-catalyzed systems.⁹ The Molander Group observed orthogonal reactivity for a Ni/photoredox cross-coupling compared to a palladium-catalyzed Suzuki cross-coupling.¹⁰ The photoredox step was selective for coupling of an aryl halide to an alkyltrifluoroborate salt in the presence of an aryl boronic ester. The aryl boronic ester was then used in a downstream Pd-catalyzed Suzuki cross-coupling reaction. Finally, MacMillan and co-workers showed that the established α -functionalization reactivity observed in enamine catalysis can be modified via the merger of photoredox and organocatalysis to facilitate β -functionalization of aldehydes (via β -enaminy radical generation).^{11,12}

A. Representative Visible Light Photoredox Catalysts



B. Complementary Reactivity Imparted by Photoredox Catalysis

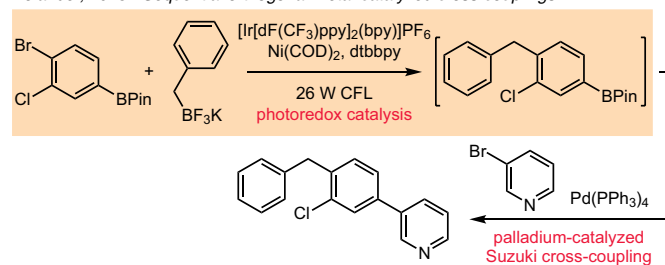
Yoon, 2011 - Electronically mismatched Diels-Alder [4+2] cycloaddition
Ar = benzo[1,3]dioxol-5-yl



Nicewicz, 2012 - anti-Markovnikov alkene hydrofunctionalization



Molander, 2015 - Sequential orthogonal metal-catalyzed cross-couplings



MacMillan, 2014 - β -alkylation via photoredox organocatalysis

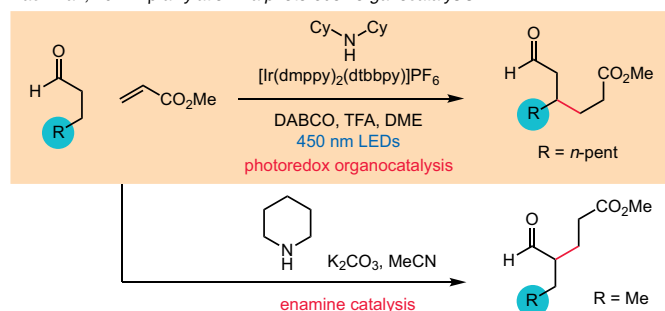
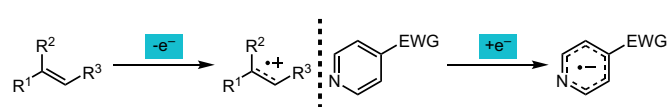


Figure 1. Photoredox Catalysts and Complementary Reactivity

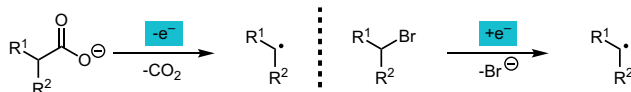
Importantly, photoredox catalysis can provide access to entirely new, previously inaccessible bond formations. Key examples will be highlighted in this guide. The powerful nature of photoredox catalysis arises, in part, from the ability to activate readily accessible, simple starting materials via single electron transfer pathways to provide access to reactive open shell species under mild reaction conditions (**Figure 2**). Direct substrate oxidation or reduction can form radical ion intermediates (radical cations and radical anions, respectively, **Figure 2A**).^{9,13-16} In addition, radical intermediates can be accessed through fragmentation/mesolytic cleavage induced by oxidation or reduction (**Figure 2B**).¹⁷⁻²² As shown, carboxylate oxidation leads to CO₂ extrusion, while alkyl halide reduction leads to halide loss. Radical intermediates can also be accessed through proton-coupled electron transfer (PCET, **Figure 2C**), both oxidative (e.g. amidyl radical formation)²³ and reductive (e.g. ketyl radical formation).²⁴ α -Amino radicals have found use in many photoredox methodologies and can be generated through sequential amine oxidation and deprotonation (**Figure 2D**).¹⁸ Upon formation, these distinct open shell species can be engaged in a wide variety of radical trapping/quenching events to, ultimately, deliver high value products. While this list is not exhaustive, it does highlight the diversity of pathways accessible through redox chemistry.

Photoredox catalysis has been successfully employed by academic research groups, by industrial chemists, and in academic-industrial collaborations. These efforts have produced innovative methods, new synthetic disconnections, and have improved our mechanistic understanding of photoredox pathways. We sought to develop this visible light photoredox catalysis guide for four reasons:

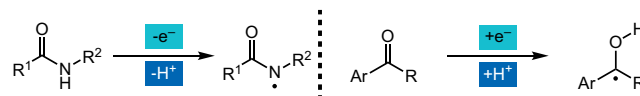
A. Formation of Radical Ion Intermediates



B. Formation of Radical Intermediates Upon Fragmentation



C. Radical Formation via PCET



D. Radical Formation Upon Sequential Oxidation/Deprotonation

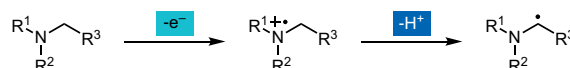


Figure 2. Photoredox SET Substrate Activation Pathways

1. To provide a foundation and introduction to the field for practitioners of synthetic and medicinal chemistry not familiar with photoredox catalysis.
2. To empower chemists to deploy photoredox catalysis when it is advantageous and adopt it in their synthetic repertoire.
3. To serve as a reference tool. This guide will cover fundamental principles of photoinduced electron transfer and highlight recent applications and advances in the field of photoredox catalysis.
4. To highlight how coupling photoredox catalysis and high-throughput experimentation can impact reaction discovery and optimization.

II. Standard Reaction Setup

Photoreactor Setup

The optimum light source for a reaction depends on the catalyst local absorption maxima, λ_{max} , but generally the light source should possess a high luminous flux and output light in the visible region in which the catalyst absorbs. Compact fluorescent lamps (CFL) can be used for the photoexcitation of many common catalysts.^{8,25} Lamps include the GE Lighting Spiral 26 W CFL and the Bayco SL-908 26 W fluorescent work light. An example of CFL reaction setup from the Molander group is shown below (**Figure 3**). A CFL may

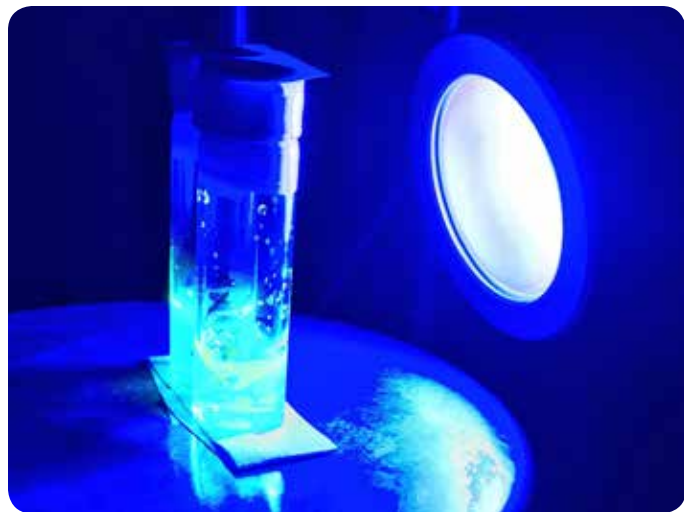


Figure 5. Kessil H150 Lamp Arranged to Irradiate Reactions



Figure 3. Photoreactor Setup With a 26 W CFL Lamp



Figure 4. Ecoxotic Lamps Aligned to Irradiate Reactions

not be ideal for all applications (e.g. may be too diffuse due to the existence of multiple emission bands). To target a catalyst more directly, LED lamps can be used which emit high intensity light in a specific region of the visible spectrum. Catalysts such as eosin Y ($\lambda_{\text{max}} = 520 \text{ nm}$) and rhodamine B ($\lambda_{\text{max}} = 550 \text{ nm}$), which absorb in the green region, can be excited with green LED lamps in addition to CFL lamps.^{4,26,27} High intensity blue LED lamps can be used for the photoexcitation of catalysts which absorb in the violet-blue region of the spectrum. Lamps that emit light around 450 nm, such as the Ecoxotic 455 nm 21 W LED lamp (**Figure 4**) or the EagleLight 450 nm 15 W LED lamp, have been used for the photoexcitation of acridinium (Mes-Acr-Me-BF₄, $\lambda_{\text{max}} = 425 \text{ nm}$) and pyrylium (TPT, $\lambda_{\text{max}} = 416 \text{ nm}$) catalysts, respectively.^{14,28,29}

Similarly, high luminosity Kessil aquarium and horticulture lamps have been used for the photoexcitation of iridium complexes which absorb in the violet-blue region. The 36 W Kessil H150 Blue lamp and the 40 W Kessil A160WE Tuna Blue lamp both output high intensity blue light which overlaps with the absorption bands of many iridium photoredox catalysts.^{30,31} Shown in **Figure 5** is a setup using a Kessil H150 Blue LED lamp.

Commercially available lamps represent a quick and effective point of entry into the field of photoredox catalysis. For those looking to standardize photoreactor setup, optimize light exposure, and broadly deploy photoredox catalysis, the Penn Photon Devices Photoreactor m1 presents an alternative to the disparate light sources currently used (**Figure 6**). Developed in a collaboration between the MacMillan laboratory and scientists at MSD,

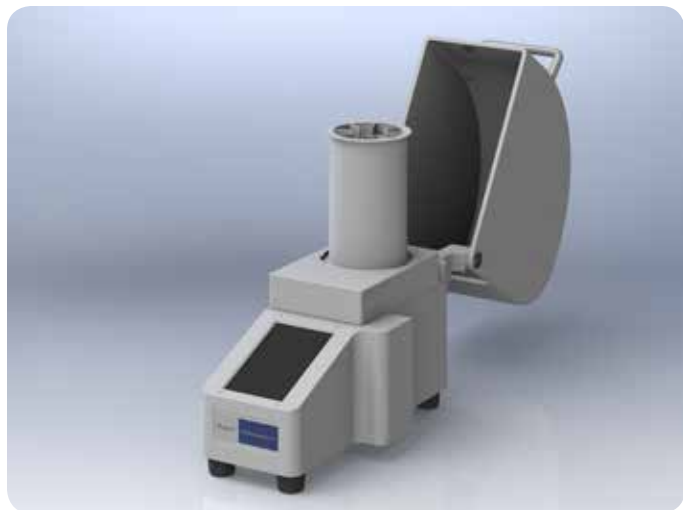
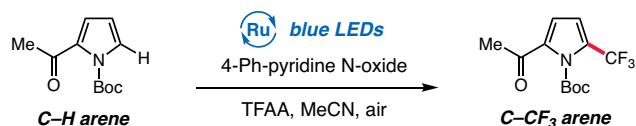


Figure 6. Penn PhD Photoreactor m1

the Photoreactor m1 was designed to standardize parameters such as reaction temperature and LED wavelength/output, and maximize reaction photon exposure.³² The optical power of various reactor prototypes was evaluated, ultimately leading to the development of a photoreactor that provided a 10-fold increase in total radiant power versus standard LED setups. Two key design elements contributed to this increase in light exposure: placement of the reaction vessel 6 mm above an array of four LEDs and the use of a reflective chamber optimized with respect to the distance between the reflective surface and the reaction medium (Figure 6). In addition to providing enhanced photon flux, the integrated photoreactor delivers stirring, cooling and high reaction consistency. The modular design of the photoreactor allows the reflective chamber and vial holder to be readily exchanged, thereby enabling batch photochemical reactions from milligram to gram scale to be run. This device incorporates an interchangeable LED module that allows access to a variety of wavelengths — 365, 420 and 450 nm. Light intensity can be precisely controlled using the touchscreen interface, thereby allowing facile evaluation of the impact of photonic flux on reaction efficiency — a challenging reaction parameter to investigate using typical photochemical reaction setups.

To evaluate the capability of the integrated photoreactor, scientists at the Center for Catalysis at Princeton University examined eight photochemical reactions widely employed by medicinal chemists.³² Improved reaction times, yields, and reproducibility were observed when using this integrated reactor. As shown in Figure 7, changing



LED Strip Setup

62% yield, 60 min

Photoreactor

64% yield, 3 min



34 W LED lamp

58% yield, 3 h

Photoreactor

64% yield, 20 min

Figure 7. Examples from Evaluation of the Photoreactor m1

from the standard LED setup (as reported in the original publications) to the Photoreactor m1 resulted in significantly reduced reaction times for both mono- and dual photoredox-catalyzed transformations. These examples demonstrate the importance of the integrated photoreactor for both enhancing photon exposure to small-scale photochemical reactions and providing a means for standardization and high reproducibility across the field of photocatalysis.

When looking to set up multiple reactions simultaneously, one can align multiple vials in front of the previously described LED lamps or one can use a parallel photoreactor. One such option for photoredox or photochemical library synthesis is the Sigma-Aldrich SynLED parallel photoreactor (Figure 8). Developed by SynLED, this photoreactor was designed to facilitate rapid library synthesis and will allow for 16 simultaneous reactions in 2 dram or smaller scintillation or microwave vials. The setup was designed to fit on a conventional stir plate, including a round cutout to fit firmly on IKA brand stir plates. Each well contains a 1W LED centered at 467.5 nm with a 45 degree lens. A built-in cooling fan and heat sink help maintain reaction temperatures at approximately 30 °C.



Figure 8. Sigma-Aldrich SynLED Parallel Photoreactor

Lamps and photoreactors highlighted throughout this section are tabulated below, however equivalent products from other vendors should also work in reaction setup. Additionally, one can construct a custom LED lamp or photoreactor from individual components if commercially available lamps do not meet one's needs. Vendors such as Rapid LED (www.rapidled.com) offer multiple brands of individual LEDs (e.g. CREE and Philips), multiple colors/wavelengths (e.g. white, blue, green), and other necessary components or accessories.

Product Description	Vendor	Product Number
26 W Spiral CFL	GE	75408
26 W CFL Work Light	Bayco	SL-908
21 W 455 nm PAR38	Ecoxotic	6851
15 W 450 nm PAR38	EagleLight	PAR38-E27-15W42S-BL
36 W H150 Blue LED	Kessil	KSH150B
40 W Tuna Blue LED	Kessil	A160WE Tune Blue
Penn PhD Photoreactor m2	Sigma-Aldrich	Z744035
Sigma-Aldrich SynLED Photoreactor	Sigma-Aldrich	Z742680

When constructing a photoreactor, attention should be paid to maximizing reaction irradiation as this can reduce reaction times. Increasing the surface area exposed to light can be beneficial as light may not penetrate far beyond the surface of a reaction medium.³³ Strategies for maximizing irradiation include flanking reactions with multiple lamps, using more powerful or focused lamps, increasing the surface area-to-volume ratio of a reaction, and covering the photoreactor with a reflective shield to minimize light escape. Reactions should be placed close to the light source(s) to ensure maximum irradiation (positioning can be optimized). An overhead cooling fan can be used to maintain room temperature and prevent heating of the reactions. However, when heating is desired or necessary, these cooling measures can be omitted (see temperature control, below).^{30,34} Finally, reactions should be stirred, especially if they are heterogeneous (e.g. using sparingly soluble/insoluble reagents or relying on a liquid-gas interface).

Materials

Reactions are typically carried out in 2 mL, 4 mL, 8 mL, 20 mL, or 40 mL clear glass screw top vials equipped with PTFE/silicone-coated septum screw caps and appropriately sized PTFE-coated magnetic stir bars. Round-bottom flasks and pressure-build-up resistant microwave vials can also be used.

Note: Practitioners running photoredox transformations may be exposed to high intensity blue light during the process of reaction setup and monitoring. While ambient blue light irradiation does not present a significant health hazard for scientists, the use of blue light blocking safety glasses will prevent direct eye exposure to high intensity lamps.

Presence of Oxygen in a Reaction

The effect of oxygen on photoredox systems may be worth exploring, as it can sometimes have interesting beneficial effects,³⁵⁻³⁷ however it is often best to control the presence of molecular oxygen due to potential deleterious pathways. Molecular oxygen is redox active and its presence can facilitate undesired oxidative degradation pathways. Some photocatalysts (e.g. rose bengal) can also act as sensitizers for the formation of singlet oxygen.^{38,39} For these reasons it may be best to exclude oxygen from photoredox systems and this can be done by setting up and running reactions under an inert atmosphere. This requirement does not apply when one is deliberately designing an oxidative process.^{13,14,40-43}

Solvents and Reagents

Common solvents for photoredox reactions are tabulated below. Solvents should be purified (following published procedures)⁴⁴ and degassed before use (again, unless oxygen is required). Solvent degassing can be done through freeze-pump-backfill-thaw cycles or sparging with N₂ or Ar. If the solvent in question is of sufficiently high purity out of the bottle (e.g. many Sure/Seal™ solvents) only degassing may be necessary. Solvents can be stored under an inert atmosphere for future use. Purified and anhydrous solvents are available in Sigma-Aldrich® Sure/Seal™ bottles and common degassed anhydrous solvents are available under the ZerO₂™ label (below).

Common solvents and associated part numbers

Solvent	Sure/Seal™	ZerO ² ™
Acetonitrile (MeCN)	271004	900644
Acetone	N/A	N/A
Dichloromethane (DCM)	270997	900633
1,2-Dichloroethane (DCE)	284505	900637
Chloroform (CHCl ₃)	288306	N/A
Dimethylacetamide (DMA)	271012	900634
Dimethylformamide (DMF)	227056	900638
Dimethyl sulfoxide (DMSO)	276855	900645
Nitromethane (MeNO ₂)	N/A	N/A
1,2-Dimethoxyethane (DME)	259527	900646
1,4-Dioxane	296309	900640
Toluene (PhMe)	244511	900522

These solvents represent good starting points for reaction development. Solvent screening and optimization may yield an improved solvent or solvent/cosolvent system.^{25,30,45,46}

Reagents and substrates should be purified before use to remove potentially non-innocent impurities. Reagent or substrate purification can be done by recrystallization, distillation, or chromatography following published procedures.⁴⁷ Sensitive species can be stored under an inert atmosphere at low temperatures for future use if necessary.

Reaction Setup: Inert Atmosphere Protocol

1. Weigh all solid reagents (e.g. photoredox catalyst, cocatalysts, or substrates) into a suitable oven-dried reaction vessel equipped with a PTFE-coated stir bar and cap the vial (screw-top cap equipped with septum).
2. Place the reaction under an inert atmosphere. This can be done by moving the reaction to a glove box or by vessel evacuation followed by backfilling with N₂ or Ar (cycle three times).
3. Dispense degassed solvent into the reaction vessel via syringe under inert atmosphere.
4. Dispense all liquid reagents (e.g. liquid cocatalysts, bases, liquid substrates, or reagent stock solutions) into the vessel via syringe under inert atmosphere.
5. Seal the reaction vessel, remove it from the inert environment, and place it in front of the appropriate lamp(s). Stir and irradiate until complete. If an oxygen atmosphere is required see **Note 1**.

Reaction Setup: Sparging Protocol

1. Weigh all solid reagents (e.g. photoredox catalyst, cocatalysts, or substrates) into a suitable oven-dried reaction vessel equipped with a PTFE-coated stir bar and cap the vial (screw-top cap equipped with septum).
2. Dispense solvent into the reaction vessel via syringe.
3. Dispense all liquid reagents (e.g. bases, liquid catalyst, liquid substrates, or reagent stock solutions) into the vessel via syringe.
4. Degas the reaction mixture by sparging with N₂ or Ar for a predetermined amount of time (e.g. 10 minutes). This can be done using a long needle to pierce the septum and bubble gas through the reaction medium and a shorter vent needle. If using a volatile solvent or reagent, sparging can be performed at 0 °C to minimize loss of the volatile component. Alternatively, a volatile reagent can be added after sparging.
5. Seal the reaction vessel and place it in front of the appropriate lamp(s). Stir and irradiate until complete. If an oxygen atmosphere is required see **Note 1**. See **Note 2** for alternative freeze-pump-backfill-thaw technique.

Note 1: For protocols that require oxygen (1 atm O₂) the reaction mixture should be sparged by bubbling with O₂ from an overhead balloon before irradiation.¹⁴ The oxygen atmosphere is then sustained by retaining the overhead O₂ balloon during the reaction. This parameter obviates the need for inert conditions during reaction setup.

Note 2: An alternative freeze-pump-backfill-thaw degassing strategy may be advised for some transformations^{48,49} and this protocol is conducted in the following manner: The reaction vessel is equipped with a N₂ inlet and submerged in a dry ice/acetone bath for 2-5 minutes until the reaction mixture is frozen. The reaction vessel is then degassed via vacuum evacuation for 5 minutes, backfilled with N₂ and warmed to ambient temperature with stirring. This process is repeated (as specified in the protocol) and then the vial is sealed and irradiated. It should be noted that, while degassing via freeze-pump-backfill-thaw may be specified, often sparging the reaction mixture with N₂ will provide comparable yields.

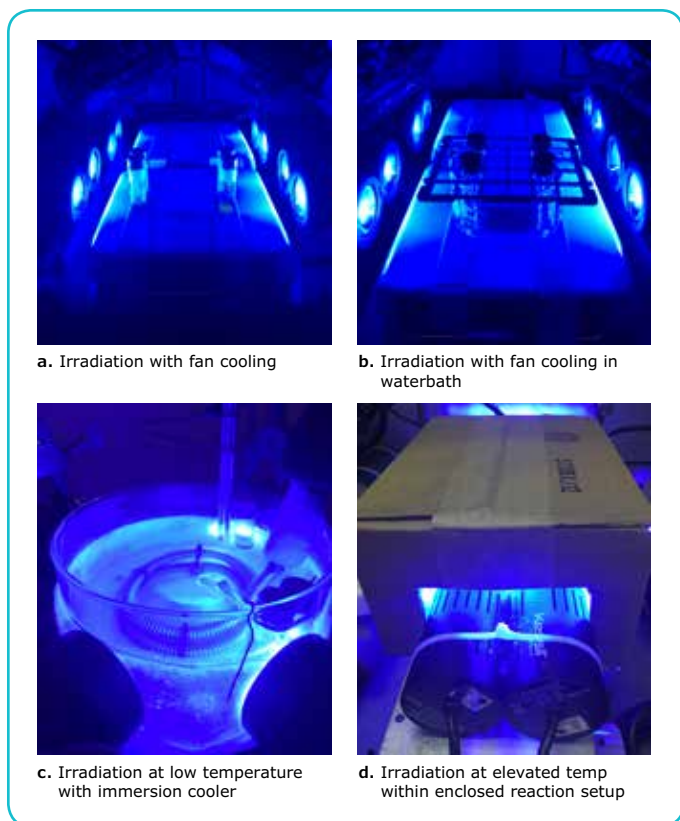


Figure 9. Temperature Control in Photoredox Catalysis

Temperature Control

Photoredox-catalyzed reactions often proceed under mild reaction conditions without the requirement for external heating. However, in certain instances, altering the reaction temperature can have a beneficial effect on the reaction efficiency and/or selectivity (e.g. low temperatures can enhance selectivity in enantioselective transformations,⁵⁰ elevated temperatures can improve reaction efficiency in some metallaphotoredox reactions^{30,49}). Strategies for conducting photoredox transformations at low or high temperatures are outlined below (**Figure 9**, images courtesy of the MacMillan group).

Room temperature: The LED lamps/strips produce heat and, without cooling, irradiation tends to elevate the reaction temperature. Household fans can be used to cool photoredox reactions (**Figure 9a**). Alternatively, photoredox reactions can be maintained at room temperature by suspending the reaction vessel in a water bath (with fan cooling) and irradiating the reaction mixture through the side of the water bath (**Figure 9b**).⁵¹

Low temperature: Reduced reaction temperatures can be achieved by placing the reaction vessel in a cooling bath with exposure to an appropriate light source. For instance, blue LED Kessil lamps can be positioned against the wall of a cooling bath, with the reaction

vials suspended in an appropriate solvent system cooled via the use of an immersion cooler (**Figure 9c**). The use of a cryocooler or immersion cooler enables precise control over low temperature photoredox reactions.

High temperature: Elevated temperatures can be achieved using the heat from the LED lamps, without the requirement for an additional heat source.³⁰ Adjustment of a number of reaction setup parameters, namely (i) the distance between the LED lamp and the reaction mixture, (ii) the number of lamps per reaction vessel, and (iii) use of an enclosed reaction set up (*i.e.* enclosure within a box with foil covering the inside of the box, **Figure 10d**), can provide access to elevated reaction temperatures anywhere between room temperature and 80 °C (see **Note** below). Alternatively, precise control at elevated temperatures can be achieved by using an external heating source and placing the reaction vessel in a heated water/oil bath.³⁴

Note: While altering the position/number of the LED lamps provides a means to adjust reaction temperature, it should be noted that changing these parameters will also vary light exposure to the reaction medium. The Photoreactor m1 provides the opportunity to determine the impact of photon flux on reaction efficiency independently from reaction temperature and enables precise control over light intensity.

Reaction Monitoring, Workup, and Purification

Vial caps with PTFE-coated septa allow for reaction monitoring. Aliquots can be removed from a reaction using a nitrogen-flushed syringe while maintaining positive N₂ or Ar pressure. Reactions can be monitored using conventional laboratory techniques such as thin layer chromatography, GC-MS, or LC-MS, observing the disappearance of starting material or presence of product. When puncturing the PTFE septum, take care to minimize introduction of oxygen to the system. Seal the vessel afterwards with laboratory tape, electrical tape, and/or thread seal PTFE tape.

Product formation or substrate conversion can be measured at the optimization/screening stage against an internal standard using techniques such as NMR, GC, or HPLC.

Frequently, upon completion, crude reactions can be concentrated *in vacuo* and the products isolated directly by column chromatography on silica gel. If advantageous, a quench/extraction/workup or short silica plug with DCM can be performed in advance of crude residue concentration to remove impurities or byproducts (e.g. water soluble salts or bases). Product isolation is then accomplished using the purification method of choice (e.g. column chromatography).

III. High-Throughput Experimentation and Introduction to Scaling Up via Flow

High-Throughput Experimentation

High-throughput experimentation (HTE) is a powerful tool that allows for rapid reaction optimization through parallel reaction screening. Miniaturizing reaction optimization to the micromole-scale allows for reactions to be run in 24- or 96-wells to screen multiple variables simultaneously, while minimizing consumption of precious substrates. The development of new transformations can be significantly expedited using HTE by both reducing the number of operations required to set up large numbers of experiments, and allowing a more diverse array of reaction conditions to be evaluated simultaneously thereby increasing the likelihood of obtaining a successful “hit” with fewer experimental iterations. The strength of this parallel optimization approach was exemplified by the development of high yielding, general conditions for reactions such as S_NAr , Buchwald-Hartwig amination, Suzuki cross-coupling, and hydrogenation for discovery and process applications.⁵²⁻⁵⁹ To facilitate the adoption of parallel reaction screening, a suite of pre-dosed 4×6 24-well kits were developed (KitAlysis™ series, **Figure 10**) for screening challenging reactions such as ring closing metathesis (KITALYSIS-RCM), Suzuki cross-coupling (KITALYSIS-SM), and Buchwald-Hartwig amination (KITALYSIS-CN-1KT). Coupling parallel reaction screening technology to high-throughput analytical techniques, such as GC-MS or LC-MS, minimizes time requirements and allows one to quickly form conclusions from a complete reactivity data set.



Figure 10. KitAlysis™ Kit

Miniaturized reaction screening technology was recently extended to photochemistry through the use of purpose-built 24-well and 96-well reaction assemblies which sit over 4×6 or 8×12 blue LED arrays.⁶⁰ This advance allows one to probe challenging photoredox systems at a miniaturized scale. Screening photoredox catalysts, redox-active reagents, and additives in parallel has allowed scientists to develop conditions for late-stage heterocycle methylation,⁶⁰ photoredox heterocycle hydroxymethylation,⁶¹ photocatalytic C-H fluorination,⁶² and cross-couplings.⁶³ These tools are available from Analytical Sales and Services, Inc. and are listed below. A high-throughput screening kit designed to interrogate photoredox catalyst effects (starter kit: Z742612, pre-dosed vials: KITALYSIS-PHO-2PAK) is shown below in **Figure 11**. Notably, this kit comes with a 24-well arrays of vials pre-dosed with the latest photocatalysts, and with the option of three separate LED sources with differing wavelengths: green (Z742608-1EA), white (Z742609-1EA) and blue (Z742610-1EA) light LEDs.



Figure 11. High-Throughput Screening in Photoredox Catalysis

Product Description	Product Number
Photo KitAlysis™ Starter Kit: LED Photoreactor Controller with Blue LED Array and 24-well reaction block for LED and screwdriver for LED array	Z742612
Photo KitAlysis™ 24-Green LED Array	Z742608
Photo KitAlysis™ 24-White LED Array	Z742609
Photo KitAlysis™ High-Throughput Reaction Screening Kit	KITALYSIS-PHO

The merger of photoredox catalysis and a second mode of catalysis has proven to be highly effective for the development of entirely new catalytic platforms.^{3,5} A high-throughput approach can be particularly valuable when evaluating multicatalytic platforms due to the high degree of catalyst interdependence in these systems. There are several important points to consider when utilizing commercial high-throughput setups. Below is a list of important considerations and a brief outline regarding the use of these reaction block assemblies.

- Without access to specialized equipment, HTE using these commercially available reaction blocks is best suited to the evaluation of categorical variables. It is possible to evaluate anywhere between 3 and 6 variables in a single plate (typically 3 or 4 variables are evaluated simultaneously).

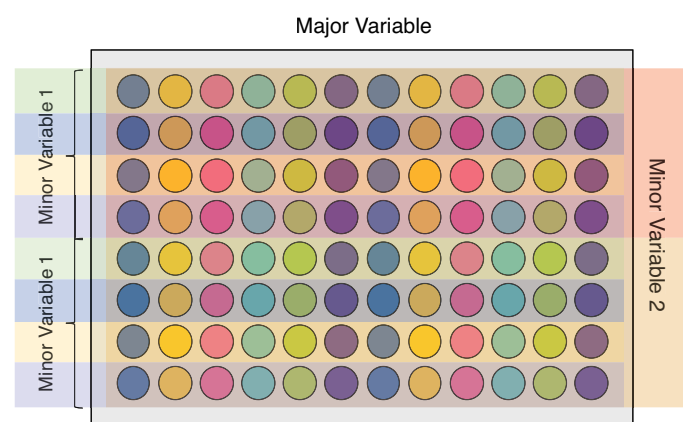


Figure 12. Typical Layout of a 96-Well Plate Optimization Study

- For 24-well and 96-well reaction blocks the light source is an LED array which is placed underneath the reaction block. Consequently, the reaction volume should be restricted to 50–100 μL to maintain an optimal path length (or 25 μL in microvials) and the scale of the reaction should be adjusted accordingly.
- Common operations such as the dosing of substrates and catalysts to the reaction block should be done utilizing liquid handling techniques, ideally using stock solutions. Solvent from the stock solution can be removed from the plate using a Genevac. When using reagents that are not hydroscopic or air and moisture sensitive, solvent removal can be conducted outside the glovebox/inert atmosphere. When using hydroscopic or sensitive reagents, solvent removal should be carried out inside a glovebox (either using a Genevac or a blow down block). The reaction solvent and any volatile reagents can then be added at the end before sealing the plate. Dispensing of solids to individual vials is typically less accurate or requires access to specialized robotics.

- Stock solutions of substrates and catalysts can be dosed using pipettes and, when using a homogenous solution, the use of a multichannel pipette can further decrease the number of operations. When addition of a heterogenous solution is required, one should “slurry dose” the mixture using a single channel pipette with a small portion of the tip end cut off (1-2 mm). It is important to stir the mixture vigorously to make sure the slurry is a uniform suspension and to ensure accurate reagent dispensing. Inorganic bases are often insoluble in organic solvents and should be ground finely before slurry dosing.
- The plate should be sealed carefully in a glovebox with a disposable solvent-compatible PFA mat positioned between the rubber section of the lid and the vials. When sealing the plate begin with the central screw, then those in the corners, before finally those at the sides of the plate (**Figure 13**). It is recommended that the screws are first tightened with an electric screw driver before finally being hand-tightened at the end. Be careful not to strip the screws and replace screws as necessary.

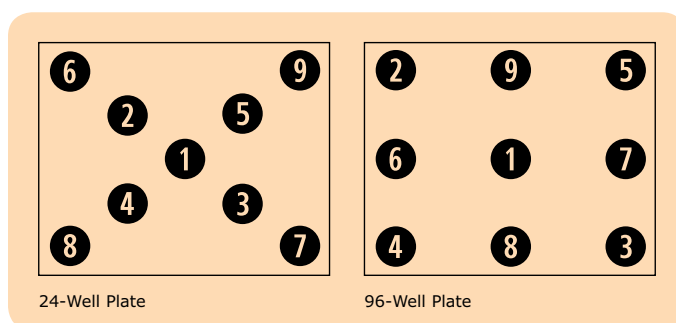


Figure 13. Order of Screw Tightening When Sealing a 24- or 96-Well Plate

- When the chemistry is known to be air sensitive, the reaction plate should be irradiated inside a glovebox to maintain air-free conditions, as the PFA liner seal is slightly permeable to molecular oxygen over time.
- Efficient stirring across a 96-well plate can be achieved using an orbital shaker or tumble stirrer (V&P Scientific). Obtaining efficient stirring using a conventional stir plate can sometimes be difficult.
- Heating or cooling the plate is possible utilizing either a heating block (available from V&P Scientific), or a recirculating chiller, respectively. In the absence of a heat sink or external heating, the LED array will typically heat a 96-well reaction assembly to 40-45 $^{\circ}\text{C}$.

Photoredox Catalysis at the Preparative Scale: Flow Chemistry

Continuous-flow synthesis is an attractive option when looking to increase from the laboratory/test scale batch reactions in vials, to the preparative scale.⁶⁴ As stated previously, increasing reaction surface area is one strategy for increasing irradiation, as most photons are absorbed at or near the surface of a reaction.^{33,65} Flow reactors often possess high surface area-to-volume ratios, which increases irradiation and improves reaction efficiency.⁶⁴⁻⁶⁶ This is in contrast to batch reactors (e.g. flasks), where scaling up generally decreases surface area-to-volume ratio and results in extended reaction times for photochemical transformations. Reactions requiring a liquid-gas interface can also be scaled up in flow^{67,68} and flow chemistry permits the safe handling/use of reactive reagents, reactive intermediates, and high temperatures. Reactions such as the photoredox Newman-Kwart rearrangement²⁹ and arene perfluoroalkylation^{69,70} have been demonstrated in flow at the multigram scale. Flow chemistry has also been leveraged in photoredox fragmentations and oxidative iminium formation/trapping to both improve throughput and increase safety.^{33,65,71} Consult referenced manuscripts and reviews for details on flow reactor setup, applications, and reaction conditions.

- The choice of reaction solvent is very important. When working with the small volumes of solvent required by HTE, solvent evaporation becomes a significant issue. Low boiling solvents such as DCM should be replaced by similar solvents with higher boiling points (e.g. DCE, dichlorobenzene). Below is a short list of solvents which can present difficulties in a high-throughput setting and appropriate alternatives. When working with volatile solvents, sealing the plate carefully is especially important.
 - DCM → DCE, dichlorobenzene
 - Et₂O → MTBE
 - Acetone → Methyl ethyl ketone
- Work-up of a 24-well or 96-well reaction block typically involves dilution of the reaction mixtures, addition of an internal standard stock solution and transfer of an aliquot to an appropriate 96-well microplate designed to interface directly with the analytical instrument of choice.
- Reaction analysis can often be the bottleneck of HTE reaction optimization. Reverse-phase UPLC analysis is optimal, with runtimes of 1-2 minutes possible with modern instruments and methods. GC analysis can take longer but is also a possible analytical technique. Concomitant MS analysis can be helpful in determining the identity of byproducts and confirming the formation of product.
- Oftentimes catalysts loadings must be adjusted when transitioning between the 96-well reaction assemblies and conventional reaction vessels.

Another useful application of HTE is parallel-in-parallel screening: the assessment of the generality of a new procedure with respect to a wide range of substrates. By evaluating a set of conditions against a range of substrates it is possible to both investigate the generality of a new reaction, or conduct optimization on a new reaction against multiple substrates to facilitate development of a highly general protocol.⁵⁹ This technique was demonstrated by scientists from the MacMillan laboratory, Buchwald laboratory, and MSD in the development of a dual photoredox nickel-catalyzed aryl amination reaction.⁴⁹ In this report, parallel-in-parallel screening showed that the amination protocol was general across a range of medically relevant aryl halide coupling partners.

IV. Photoinduced Electron Transfer

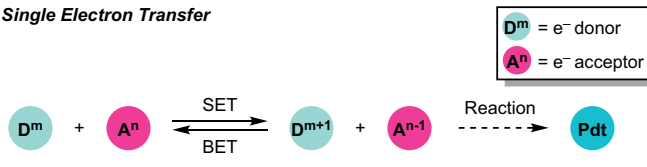
Single electron transfer (SET), as depicted in **Figure 14A**, is a redox event between an electron donor ($D^m \rightarrow D^{m+1}$) and an electron acceptor ($A^n \rightarrow A^{n-1}$). The reverse of a SET event, back electron transfer (BET), is the process of reforming the ground state donor (D^m) and acceptor (A^n) species. Ground state chemical oxidants or reductants can be employed to access some SET pathways, however a photoinduced electron transfer (PET) pathway may be advantageous for reasons such as oxidant/reductant strength or the ability to utilize an oxidant and reductant in concert. PET begins with photoexcitation of one of the redox partners (generally the photoredox catalyst) with visible light. Absorption of a photon of light produces a singlet excited state species (S_1), as shown in the simplified Jablonski diagram in **Figure 15B**. From here, a variety of radiative (light emitting) and non-radiative processes are possible including relaxation through fluorescence (radiative) and spin-forbidden intersystem crossing to the triplet excited state T_1 (ISC, non-radiative). Analogous radiative relaxation from the triplet excited state occurs through spin-forbidden phosphorescence.^{1,3,4,41,72} In the ground state, electron transfer with the catalyst (**cat**) is endergonic; however photoexcitation to the excited state (**[cat]***) promotes an electron to the LUMO and creates a vacancy in the HOMO, producing a stronger redox agent (**Figure 14B**). Quenching can occur through electron transfer: in the presence of a suitable donor, the catalyst can act as an excited state photooxidant and accept an electron resulting in formation of a reduced catalyst (**[cat]⁻**) and oxidized donor (D^{m+1}). Similarly, in the presence of a suitable acceptor, the catalyst can act as an excited state photoreductant, donating an electron to form the oxidized catalyst (**[cat]⁺**) and reduced acceptor (A^{n-1}).⁴ Photoinduced electron transfer can occur with a singlet excited state catalyst, triplet excited state catalyst, or species produced upon charge transfer (e.g. metal-to-ligand charge transfer, MLCT). The dominant process is catalyst dependent and the nature of the excited state species can impact properties such as excited state lifetime and redox potentials. Consult referenced reviews for greater detail on photophysics and catalyst properties.^{1,4}

An oxidative quenching cycle is operative when an acceptor (A^n) quenches the excited state catalyst, resulting in catalyst oxidation (to **[cat]⁺**, **Figure 14C**). A second redox event between the oxidized catalyst and a donor (D^m) closes the cycle to regenerate the ground state photoredox catalyst (**cat**). In this scheme, direct substrate activation occurs when a substrate (A^n) engages the excited catalyst and accepts an electron. Also possible are systems where a redox-active reagent (e.g. methyl viologen) or cocatalyst quenches the excited state catalyst. The reduced reagent/cocatalyst could be used to activate a substrate, or, a donor substrate (D^m) could be activated by the more strongly oxidizing intermediate **[cat]⁺** in the catalyst turnover step (secondary quenching).

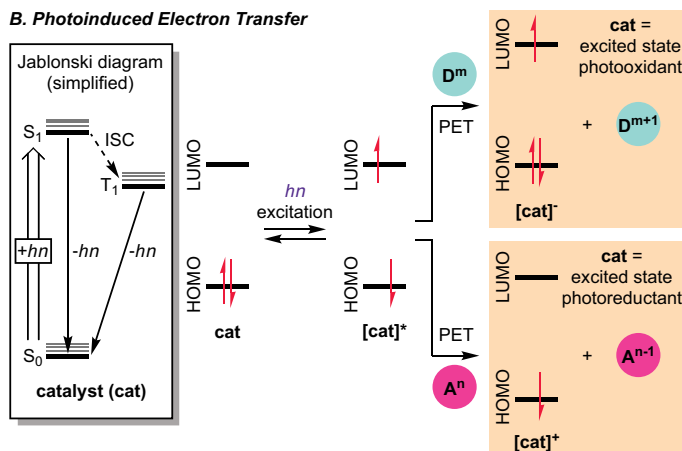
A reductive quenching cycle is operative when the excited state catalyst engages an electron donor (D^m), resulting in catalyst reduction (to **[cat]⁻**, **Figure 14D**). A redox event between the reduced catalyst and an acceptor (A^n) closes the cycle and regenerates the ground state photoredox catalyst (**cat**) as depicted. Direct substrate activation occurs when a donor substrate releases an electron upon engaging an excited state catalyst (e.g. producing a cation radical intermediate from an olefin substrate). In systems where a substrate is not directly activated by PET, a redox-active donor reagent (e.g. an amine) or cocatalyst may quench the excited catalyst. This oxidized species could then activate the substrate (e.g. via H-atom abstraction), or, secondary quenching could be operative if an acceptor substrate is instead activated by the strongly reducing intermediate **[cat]⁻** in the turnover step. These complementary quenching cycles highlight a catalyst's ability to act as both an oxidant and a reductant in concert.

The operative mechanism and optimum photoredox catalyst for a system will depend on the transformation, mode of substrate activation, and the electronic nature and redox properties of all components of the system. These factors can inform the user on how to improve a photoredox system.

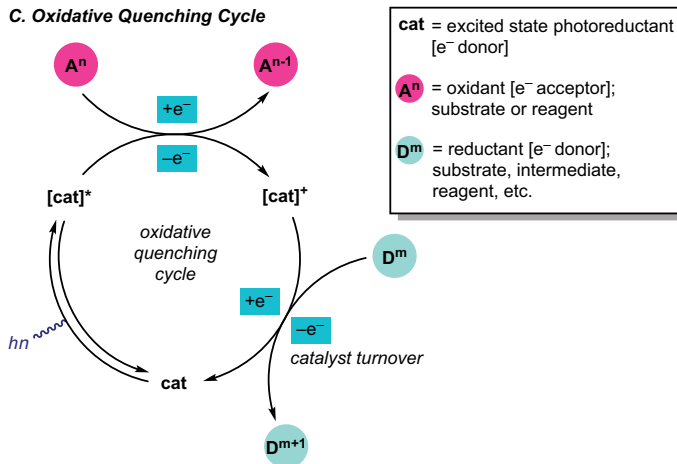
A. Single Electron Transfer



B. Photoinduced Electron Transfer



C. Oxidative Quenching Cycle



D. Reductive Quenching Cycle

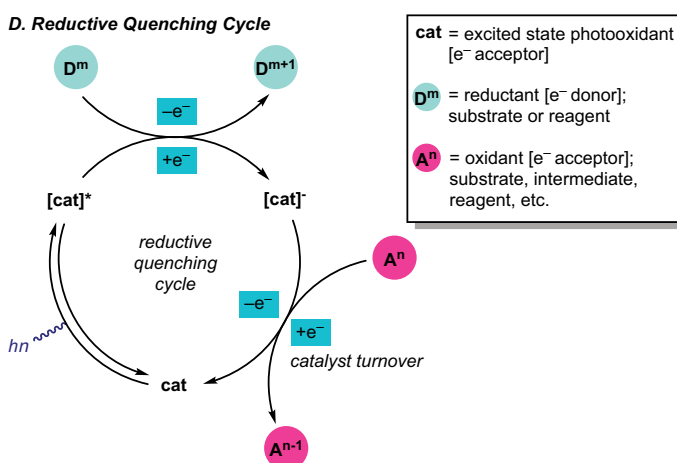


Figure 14. Photoinduced Electron Transfer Pathways

Redox Potentials: A Predictive Tool for Electron Transfer

The redox potentials of species participating in a redox reaction can help predict the thermodynamic feasibility of electron transfer. The redox potential of an electron acceptor (acceptor reduction potential, E_{red} , measured in volts, V) measures its ability to accept an electron and thereby be reduced ($A^n \rightarrow A^{n-1}$). Likewise, the redox potential of an electron donor measures how readily that donor will give up an electron, and hence be oxidized ($D^m \rightarrow D^{m+1}$, donor oxidation potential, E_{ox} , measured in volts, however technically representing the reverse $D^{m+1} \rightarrow D^m$ reduction event). Species that are more easily oxidized possess lower (more negative) oxidation potentials whereas species that are more readily reduced possess higher (more positive) reduction potentials. The equations below connects these two values to Gibbs free energy of electron transfer.^{40,73,4}

$$\Delta G_{ET} = -nF[\Delta E]$$

$$\Delta G_{ET} = -nF[E_{red}(A^n/A^{n-1}) - E_{ox}(D^{m+1}/D^m)]$$

Where, F is the Faraday constant (23.061 kcal V⁻¹ mol⁻¹) and n the moles of electrons transferred ($n = 1$ for SET). For a favorable, exergonic, redox reaction an acceptor should be used whose reduction potential exceeds (is more positive than) the oxidation potential of the donor ($\Delta E > 0$ V). Conversely, an endergonic redox reaction is likely one where the reduction potential of the acceptor is lower (more negative) than the oxidation potential of the donor ($\Delta E < 0$ V).

Extending this relationship to photoinduced electron transfer requires excited state redox potentials for the catalyst(s) in use: $*E_{red}(cat^*/cat^-)$ for a reductive quenching process and $*E_{ox}(cat^+/cat^*)$ for an oxidative quenching process. Solvent-dependent Coulombic impact, w , can also be factored into the free energy relationship however it is frequently omitted for clarity due to negligible impact ($w = 0.06$ eV in MeCN). For thermodynamically favorable PET through an oxidative quenching cycle, a catalyst should be used whose excited state oxidation potential is more negative (lower) than the reduction potential of the acceptor (see below).⁴

$$\Delta G_{PET} = -nF[E_{red}(A^n/A^{n-1}) - E_{ox}(cat^+/cat^*)]$$

An example of this PET pathway is the direct allylic arylation published by MacMillan and co-workers in 2015.¹⁶ The excited state reductant $fac-Ir(ppy)_3$ ($*E_{ox}(Ir^{IV}/*Ir^{III}) = -1.73$ V vs. saturated calomel electrode, SCE, in MeCN) was used to reduce arene substrates to arene anion radicals (Figure 15). As shown, PET with 1,4-dicyanobenzene (1,4-DCB, $E_{red} = -1.61$ V vs. SCE) is exergonic ($\Delta E = +0.12$ V, $\Delta G = -2.77$ kcal/mol). In a separate step, ground state catalyst $fac-Ir(ppy)_3$ is regenerated through thiolate oxidation, forming a thiyl radical which is necessary for downstream H-atom transfer (HAT) with the allylic substrate.

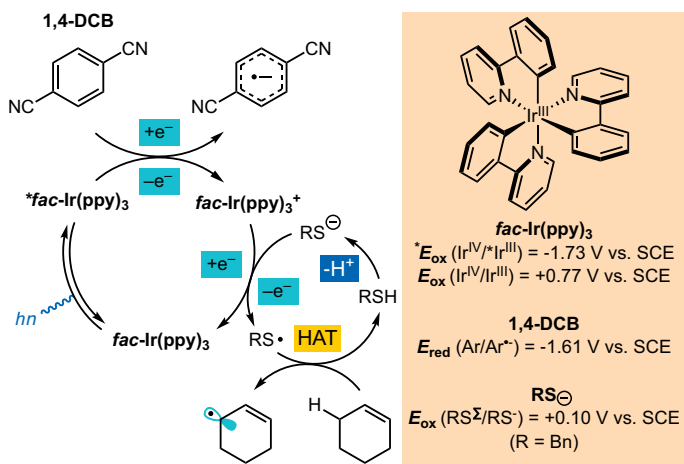


Figure 15. PET via Oxidative Quenching

In a reductive quenching cycle, where a donor quenches the excited state catalyst, a catalyst whose excited state reduction potential is more positive (higher) than the oxidation potential of the donor should be used (see below).⁴

$$\Delta G_{PET} = -nF[E_{red}(cat^+/cat^*) - E_{ox}(D^{m+1}/D^m)]$$

Direct reductive quenching of an excited state acridinium catalyst was utilized by Nicewicz and coworkers to access olefin cation radical intermediates (Figure 16).^{74,75} Here, excited state oxidant *Mes-Acr-Me-BF₄ (*E_{red}(*Acr⁺/Acr^{•+}) = +2.08 V vs. SCE in MeCN) acts as the acceptor for olefin donors. *Mes-Acr-Me⁺ efficiently oxidizes β-methylstyrene (E_{ox}(D^{•+}/D) = +1.74 V vs. SCE, ΔE = +0.34 V, ΔG = -7.84 kcal/mol) as the catalyst's excited state reduction potential exceeds the olefin oxidation potential. In the depicted scheme the ground state acridinium catalyst (E_{red}(Acr⁺/Acr^{•+}) = -0.57 V vs. SCE) is regenerated in an acridine radical/thiyl radical (E_{red}(PhS[•]/PhS⁻) = +0.16 V vs. SCE) redox event (ΔE = +0.73 V, ΔG = -16.83 kcal/mol), culminating in thiolate formation. However, PET is endergonic for some less electron-rich donors such as 2-methyl-1-pentene (E_{ox}(D^{•+}/D) = +2.50 V vs. SCE). Here, the donor oxidation potential exceeds the acridinium excited state reduction potential (ΔE = -0.42 V, ΔG = +9.68 kcal/mol).

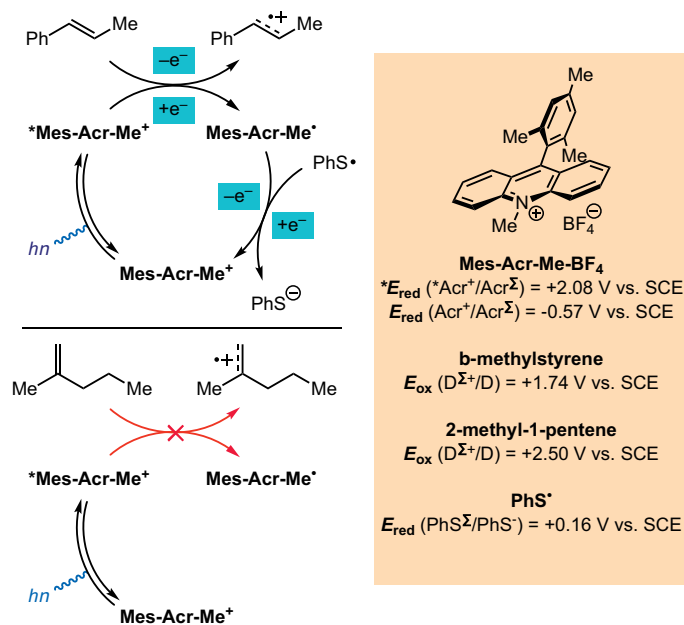
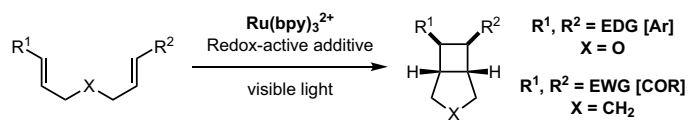
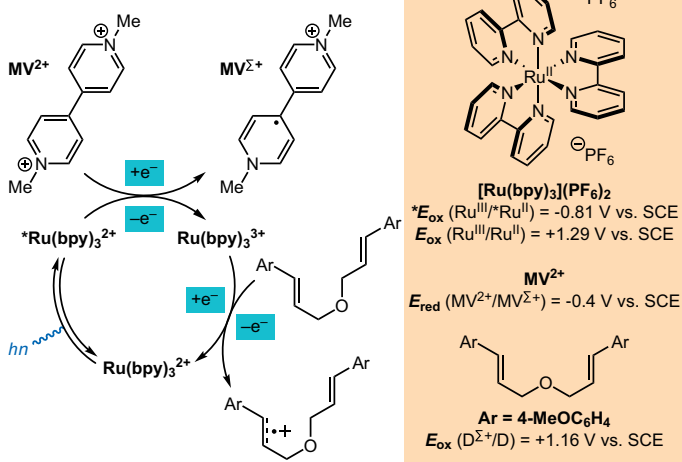


Figure 16. PET via Reductive Quenching

PET methods relying on secondary oxidative and reductive quenching modes were demonstrated by Yoon and coworkers in intramolecular [2+2] PET cycloadditions.^{76,77} Olefin activation was achieved using Ru(bpy)₃²⁺ as a photoredox catalyst (Figure 17). *Ru(bpy)₃²⁺ is only capable of activating the most electron-rich substrates via reductive quenching (*E_{red}(*Ru^{II}/Ru^I) = +0.77 V vs. SCE). Methyl viologen (MV²⁺), an electron acceptor, was utilized to cyclize tethered bis(styrenyl) olefin substrates which lay at elevated oxidation potentials by facilitating generation of the oxidant Ru(bpy)₃³⁺. In this scheme (Figure 17A), methyl viologen (E_{red}(MV²⁺/MV^{•+}) = -0.4 V vs. SCE) quenches the excited state catalyst (*E_{ox}(Ru^{III}*/Ru^{II}) = -0.81 V vs. SCE, ΔE = +0.41 V, ΔG = -9.46 kcal/mol) to form the more strongly oxidizing species Ru(bpy)₃³⁺ (E_{ox}(Ru^{III}/Ru^{II}) = +1.29 V vs. SCE). Ru(bpy)₃³⁺ then oxidizes the shown olefin substrate (E_{ox}(D^{•+}/D) = +1.16 V vs. SCE, ΔE = +0.13 V, ΔG = -3.00 kcal/mol). Electron-deficient tethered alkenes were cyclized to form cyclobutanes through a reductive quenching mechanism employing a redox-active amine electron donor (Figure 17B).⁷⁶ Again *Ru(bpy)₃²⁺ cannot activate the diene substrate directly through reduction, however, excited state quenching (*E_{red}(*Ru^{II}/Ru^I) = +0.77 V vs. SCE) by amine donor *i*-Pr₂NEt (E_{ox}(R₃N^{•+}/R₃N) = +0.68 V vs. SCE, ΔE = +0.09 V, ΔG = -2.08 kcal/mol) generates Ru(bpy)₃^{•+} which is a demonstrably stronger reductant (E_{red}(Ru^{II}/Ru^I) = -1.33 V vs. SCE). This species reduces the olefin substrate to a reactive radical ion (ΔE = +0.13 V, ΔG = -2.99 kcal/mol), regenerating the ground state photocatalyst.



A. Oxidative Quenching



B. Reductive Quenching

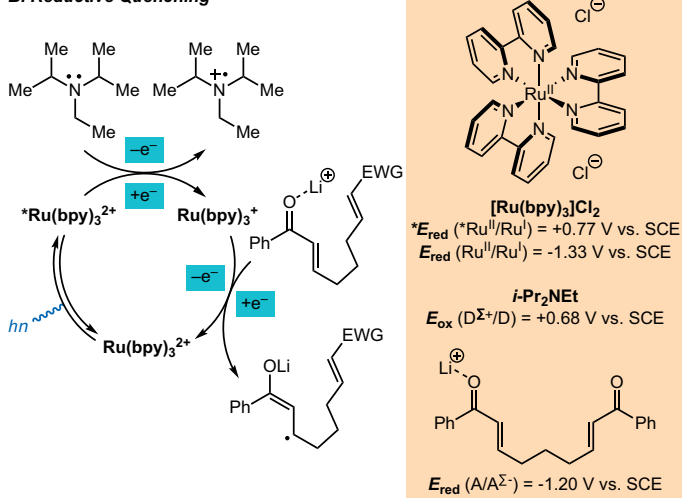


Figure 17. Secondary Quenching

The catalyst for a photoredox system is chosen based on a variety of factors including (but not limited to) substrate redox potential(s), catalyst redox properties, excited state lifetime, or possible catalyst degradation pathways. Taking these variables into account can direct one to relevant catalyst classes and it can be productive at the optimization stage to screen multiple catalysts that possess a range of properties, to generate a detailed map of reactivity.

Knowledge of catalyst, cocatalyst, substrate, and reagent redox potentials allows one to predict the thermodynamic feasibility of electron transfer. To aid in this endeavor, redox potential and property tables have been compiled to shed light on common photoredox catalysts, potential substrates, and redox-active reagents. These tables can serve as guides but it should be noted that redox potentials can be affected by solvent.

Appendix Table 1 – Photoredox catalysts

Appendix Table 2 – Excited state photooxidants

Appendix Table 3 – Excited state photoreductants

Appendix Table 4 – Catalyst references and properties

For a recent detailed compilation of redox potentials for common organic molecules and substrates:

Roth, H. G.; Romero, N. A.; Nicewicz, D. A. Experimental and Calculated Electrochemical Potentials of Common Molecules for Applications to Single-Electron Redox Chemistry. *Synlett* **2016**, *27*, 714-723.

For more detailed surveys of photoredox catalysis in organic synthesis, photophysical properties, and recent applications consult the following reviews and collections:

Prier, C. K.; Rankic, D. A.; MacMillan, D. W. C. Visible Light Photoredox Catalysis with Transition Metal Complexes: Applications in Organic Synthesis. *Chem. Rev.* **2013**, *113*, 5322-5363.

Skubi, K. L.; Blum, T. R.; Yoon, T. P. Dual Catalysis Strategies in Photochemical Synthesis. *Chem. Rev.* **2016**, *116*, 10035-10074 (part of the 2016 *Chemical Reviews* special issue described below)

Romero, N. A.; Nicewicz, D. A. Organic Photoredox Catalysis. *Chem. Rev.* **2016**, *116*, 10075-10166 (part of the 2016 *Chemical Reviews* special issue described below)

Chemical Reviews 2016 Special Issue "Photochemistry in Organic Synthesis"

<http://pubs.acs.org/toc/chreay/116/17>

Accounts of Chemical Research 2016 Special Issue "Photoredox Catalysis in Organic Chemistry"

<http://pubs.acs.org/page/achre4/photoredox-catalysis.html?ref=si>

Journal of Organic Chemistry 2016 Special Issue "Photocatalysis"

<http://pubs.acs.org/toc/joaceh/81/16>

V. Synthesis of Photoredox Catalysts

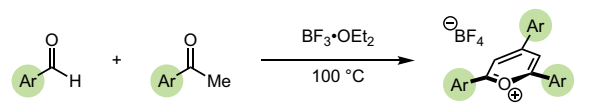
Publications continue to expand the catalyst library, resulting in uniquely effective catalysts for many applications. While many catalysts are commercially available, one may encounter a scenario where catalyst synthesis is required in order to access a catalyst with tuned steric or electronic properties. Catalysts from the pyrylium, acridinium, ruthenium polypyridyl, and heteroleptic iridium families are constructed via modular syntheses making customization possible (**Figure 18**).

Pyrylium catalysts can be prepared in one step via a $\text{BF}_3 \cdot \text{OEt}_2$ -mediated condensation/cyclization reaction from aryl aldehydes and aryl ketones (**Figure 18A**).⁴⁰ The redox properties of a pyrylium catalyst can be tuned through substitution on the aryl ketone and aryl aldehyde precursors.^{40,78} Acridinium dyes can be constructed via a modular three-step synthesis from *N*-phenylanthranilic acid derivatives as depicted in **Figure 18B**.^{14,42,45,79} H_2SO_4 -mediated cyclization is followed by *N*-alkylation or C–N coupling to give *N*-alkyl or *N*-aryl acridones, as shown. Finally, mesityl addition into the ketone (with Grignard reagent or aryl lithium reagent) followed by treatment with $\text{HBF}_4 \cdot \text{OEt}_2$ to effect dehydration produces the acridinium catalyst. Increasing substitution on the acridinium core can render the catalyst less susceptible to nucleophilic deactivation and, again, incorporating electron-donating or withdrawing groups can impact catalyst excited state properties.^{14,45,79}

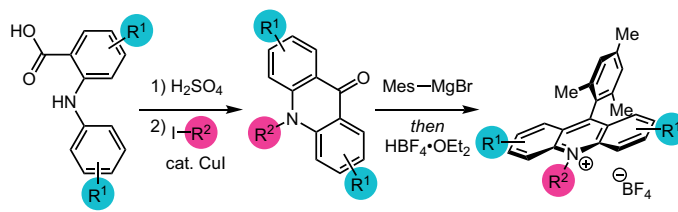
Ruthenium polypyridyl complexes such as $[\text{Ru}(\text{bpy})_3](\text{PF}_6)_2$ and $[\text{Ru}(\text{bpz})_3](\text{PF}_6)_2$ can be synthesized in one step, treating a Ru^{III} salt with the desired bidentate ligand at elevated temperatures followed by a KPF_6 wash (**Figure 18C**).^{80–82} Electronically different chelating ligands can impact catalyst redox properties.⁸³ Finally, heteroleptic iridium complexes can be constructed in three steps from an Ir^{III} salt via a bridged intermediate (**Figure 18D**).⁸⁴ Catalyst redox property modification again arises from differential ligand substitution.^{82,84–88} Treating an Ir^{III} salt with a phenyl-substituted pyridine ligand at reflux produces the bridged Ir^{III} dimer shown.

The desired iridium complex is then constructed from this intermediate in a two-step process comprised of silver salt metathesis and treatment with a chelating bipyridine ligand. If available, microwave-assisted synthesis has been shown to lower reaction times and increase yields.⁸⁹ It is also worth noting that, in many cases (*i.e.* for the synthesis of the commonly employed $[\text{Ir}(\text{dF}(\text{CF}_3)\text{ppy})_2(\text{dtbbpy})]\text{PF}_6$ photocatalyst), the catalysts can be synthesized by directly cracking the bridged Ir^{III} dimer with the desired bipyridine ligand, followed by salt exchange.⁸⁴ Homoleptic iridium complexes can be constructed using a similar strategy.^{87,90} See references for detailed protocols.

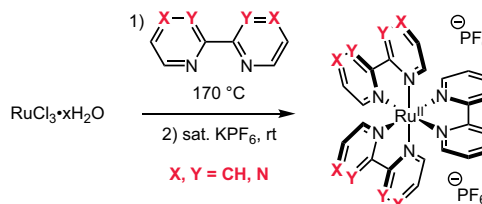
A. Pyrylium Catalyst Synthesis



B. Acridinium Catalyst Synthesis [Mes = 2,4,6-trimethylphenyl]



C. Ruthenium Polypyridyl Complex Synthesis



D. Synthesis of Heteroleptic Iridium Complexes

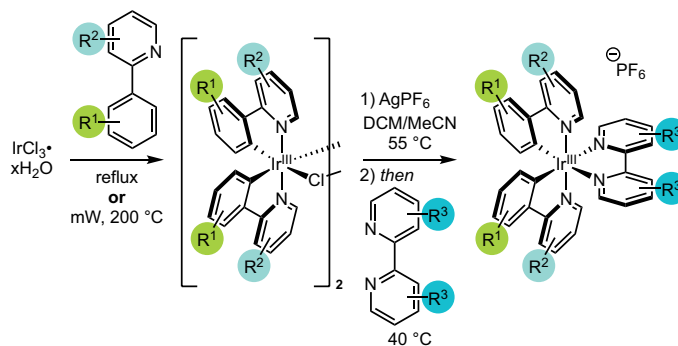


Figure 18. Photoredox Catalyst Synthesis

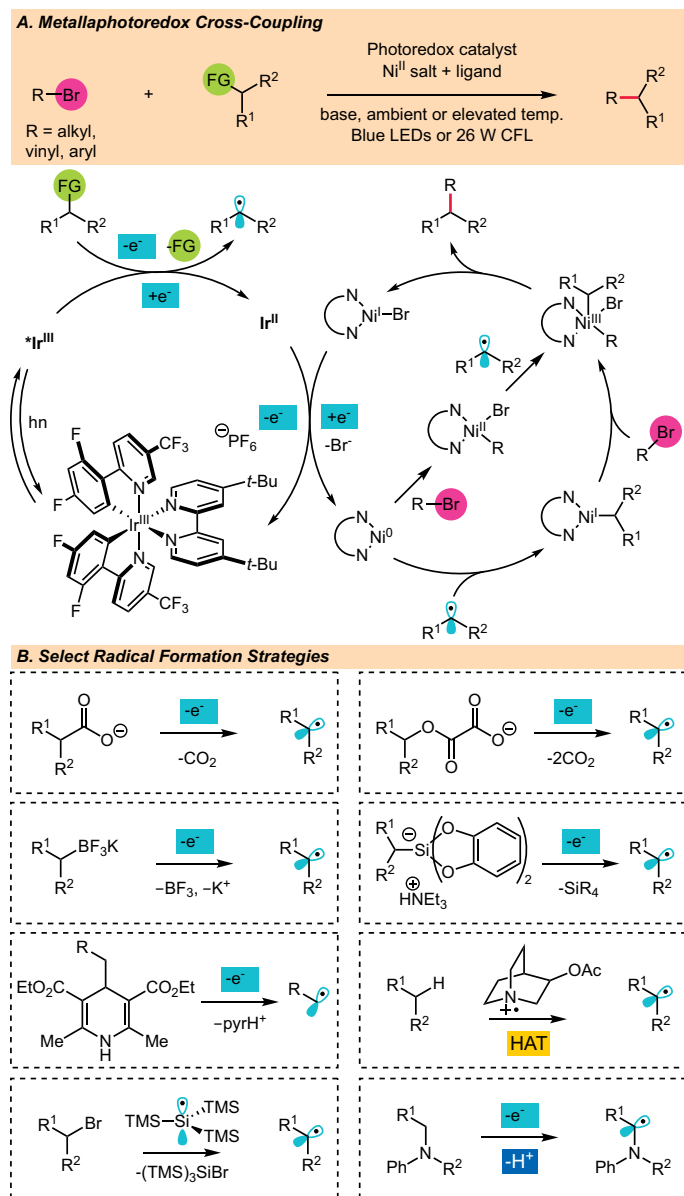
VI. Metallaphotoredox Cross-Couplings

Synergistic Metallaphotoredox C(sp²)-C(sp³) and C(sp³)-C(sp³) Cross-Coupling

Dual photoredox nickel-catalyzed cross-coupling has emerged as a powerful tool for the construction of C(sp²)-C(sp³) and C(sp³)-C(sp³) bonds (**Figure 19**). This coupling strategy utilizes an aryl/vinyl/alkyl halide coupling partner, a photoredox catalyst involved in carbon-centered radical coupling partner formation (and/or nickel oxidation state manipulation), and a nickel salt to couple the two fragments together. The general mechanism is shown in **Figure 19A**: excitation of the photoredox catalyst, followed by electron transfer with the radical precursor generates the requisite radical species after fragmentation. The alkyl radical intermediate then enters the nickel coupling cycle, where the desired bond is ultimately formed after a radical addition/oxidative addition/reductive elimination process (via a Ni⁰/Ni^I/Ni^{III} or Ni⁰/Ni^{II}/Ni^{III} pathway). Electron transfer between a transient L_nNi^I intermediate and the reduced photocatalyst reforms the L_nNi⁰ species and the ground state photoredox catalyst.^{18,25,91}

Pioneering work by the MacMillan, Doyle, and Molander groups has led to the disclosure of a diverse range of readily available, abundant radical precursors which provide access to open shell coupling partners that can be engaged in the aforementioned metallaphotoredox platform (**Figure 19B**). Oxidation of carboxylate or oxalate species results in decarboxylation and alkyl radical formation.^{18,30,92} Similarly, single electron oxidation of alkyltrifluoroborate salts, alkylsilicate salts, and alkyl-1,4-dihydropyridines results in fragmentation and alkyl radical formation.^{25,63,93-96} Hydrogen-atom transfer and halogen-atom abstraction can also be powerful tools in alkyl radical formation.^{48,97} In the cited examples, the relevant abstracting agents (e.g. shown quinuclidinium radical cation or silyl radical) are formed via a photoredox-mediated SET event. Finally, α-amino radicals are accessible through sequential amine oxidation and deprotonation.^{18,98,99} That so many functional groups can be used to access diverse radical species highlights the potential utility of this platform in discovery space and in quickly accessing new areas of chemical space.

Five examples of this cross-coupling platform will be elaborated on further: the decarboxylative photoredox cross-coupling using carboxylic acid radical precursors (**Figure 20-Figure 22**), the double decarboxylative photoredox cross-coupling using oxalate half ester radical precursors (**Figure 23**), the cross-coupling of alkyltrifluoroborate salts (**Figure 24**), cross-electrophile coupling via silyl radical-mediated halogen abstraction (**Figure 25**), and hydrogen atom transfer-mediated C-H functionalization (**Figure 26**).



Decarboxylative Cross-Coupling

The merger of photoredox and nickel catalysis has facilitated the development of a toolbox of new cross-coupling methods utilizing carboxylic acids as the nucleophilic coupling partner in lieu of more traditional organoboron, organotin, organozinc, or organomagnesium reagents. These new metallaphotoredox protocols have been shown to be competent for the construction of C(sp²)-C(sp³) and C(sp³)-C(sp³) bonds.^{18,92,100-102} A broad array of carboxylic acids have been employed in these technologies, including α -heteroatom, α -oxo, benzylic and simple aliphatic acids. The optimal photocatalyst, nickel source, ligand, base, and solvent differs depending on the substrate class. An outline of the most generally applicable reaction conditions for the decarboxylative arylation, vinylation, alkylation and the double decarboxylative cross-coupling of alcohols (via the intermediacy of the corresponding oxalate half esters) is given below. When the published conditions give low levels of efficiency for a given substrate combination, the suggested modifications can in many instances restore the yield.

Common Conditions for Decarboxylative Arylation

- **Solvent:** DMA (0.1 M), degassed and anhydrous.
- **Stoichiometry:** 1 equiv. aryl halide and 1.5 equiv. carboxylic acid and base are typically employed. Comparable efficiency is observed when the stoichiometry is inverted.
- **Photoredox catalyst:** [Ir[dF(CF₃)ppy]₂(dtbbpy)]PF₆ (1 mol %) or [Ir[dF(Me)ppy]₂(dtbbpy)]PF₆ (1-2 mol %) for simple aliphatic substrates.
- **Nickel catalyst:** NiCl₂•glyme (5 mol %)
- **Ligand:** dtbbpy (4,4'-di-*tert*-butyl-2,2'-bipyridine, 5 mol %)
- **Base:** Cs₂CO₃ (1.5 equiv., stored in glovebox), DBU (1.5 equiv., distilled and stored under inert atm) or Barton's Base (2-*tert*-butyl-1,1,3,3-tetramethylguanidine, 1.5 equiv., distilled and stored under inert atm)
- **Reaction setup:** Degas by sparging the entire reaction mixture with nitrogen for 10 minutes.
- **Irradiation:** Kessil blue LED lamps (6 cm distance between lamp and reaction vial), ambient temperature (with fan cooling).

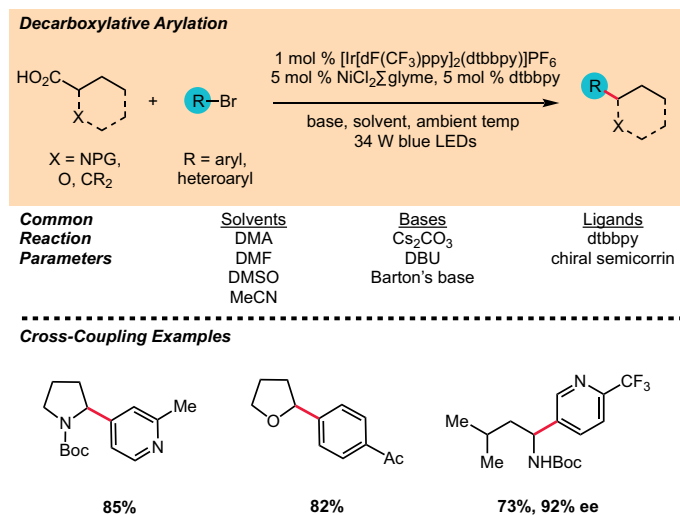


Figure 20. Metallaphotoredox Decarboxylative Arylation

Notes, Tips, and Troubleshooting

Identity of base: The optimal base is typically dependent on the nature of the aryl halide. For simple arenes, 3-halopyridines and 5-halopyrimidines, Cs₂CO₃ is typically the optimal base. For other heteroarenes, DBU is recommended. When using simple aliphatic carboxylic acids, Barton's base often gives the best results.

Identity of photocatalyst: For α -heteroatom carboxylic acids, [Ir[dF(CF₃)ppy]₂(dtbbpy)]PF₆ is optimal. For simple aliphatic carboxylic acids switching to [Ir[dF(Me)ppy]₂(dtbbpy)]PF₆ or [Ir[dF(F)ppy]₂(dtbbpy)]PF₆ can often prove beneficial.

Solvent: Typically, polar aprotic solvents provide the highest efficiencies and DMA is the optimal solvent for most substrates. For simple aliphatic carboxylic acids, DMSO can be a superior solvent.

Nickel catalyst: The nickel salt and ligand can be pre-ligated (stir or sonicate for 10 minutes) in the reaction solvent, and this solution is added directly to the reaction mixture. Other nickel(II) salts that were tested worked well, with the exception of Ni(OAc)₂ and Ni(acac)₂ which typically deliver large quantities of protodehalogenation byproducts and should be avoided.

Functional group tolerance: Under the published reaction conditions, broad functional group tolerance is observed. A wide range of aryl and heteroaryl bromides and iodides with differing electronic properties and substitution patterns are tolerated. Typically, iodides perform better than bromides for electron-rich arene partners. Electron-rich aryl chlorides and bromides are challenging substrates for this technology. Electron-deficient aryl chlorides are tolerated, however longer reaction times are required. Using DBU as base, a variety of heteroaromatic bromides can be coupled

using this protocol. In some cases, heteroaryl chlorides perform better than the corresponding bromides (*i.e.* for highly activated substrates). A diverse array of carboxylic acids couple efficiently under the reaction conditions. When using simple aliphatic acids, changing the photocatalyst, solvent and base can be beneficial (see above). Alcohols, protected amines, alkenes, strained ring systems, and orthogonal coupling handles such as aryl boronic acids are well tolerated.

Tips for Improving Low Yielding Reactions

- **Nickel loading:** Modulating the loading of nickel catalyst can improve reaction yields. If large amounts of protodehalogenation are observed, decreasing the nickel loading to 2.5 or 1 mol % can be beneficial. When large amounts of starting material are recovered, increasing the nickel loading to 7.5 or 10 mol % can lead to better levels of conversion.
- **Concentration:** Diluting the reaction to 0.02 M can be beneficial for reducing byproduct formation.

Decarboxylative Vinylation

In addition to decarboxylative arylation, the MacMillan laboratory has demonstrated that vinyl halides can be utilized in decarboxylative cross-couplings to give the C(sp²)-C(sp³) coupled products (**Figure 21**).¹⁰⁰

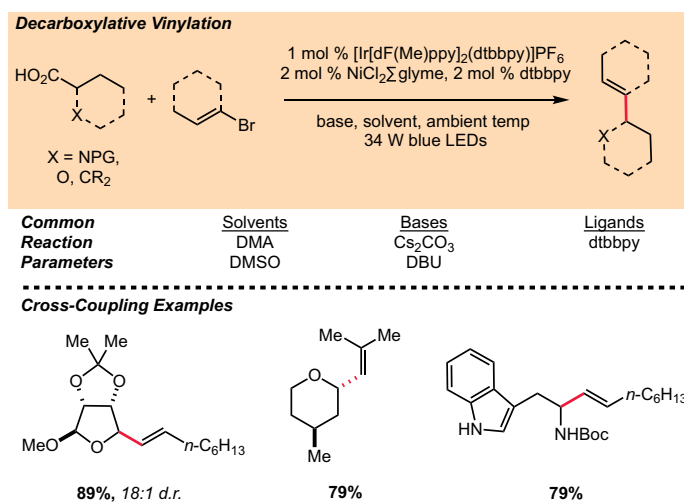


Figure 21. Metallaphotoredox Decarboxylative Vinylation

Common Conditions

- **Solvent:** DMSO (0.1 M), degassed and anhydrous.
- **Stoichiometry:** 1 equiv. vinyl halide and 1.6 equiv. carboxylic acid and base are typically employed. Comparable efficiency is observed when the stoichiometry is inverted.
- **Photoredox catalyst:** [Ir(dF(Me)ppy)₂(dtbbpy)]PF₆ (1 mol %).
- **Nickel catalyst:** NiCl₂·glyme (2 mol %)
- **Ligand:** dtbbpy (2 mol %)
- **Base:** DBU (1.6 equiv., distilled and stored under inert atm) or Cs₂CO₃ (1.6 equiv., stored in glovebox)
- **Reaction setup:** Degas by sparging the entire reaction mixture with nitrogen for 10 minutes.
- **Irradiation:** Kessil blue LED lamps (6 cm distance between lamp and reaction vial), ambient temperature (with fan cooling).

Notes, Tips, and Troubleshooting

Nickel catalyst: The nickel catalyst and ligand should be pre-ligated in the reaction solvent by sonicating a stock solution until homogenous. The stock solution of nickel complex was added immediately before sparging the entire reaction mixture.

Functional group tolerance: Vinyl iodides and bromides can both be employed. For more sterically encumbered substrates iodides generally deliver higher yields. A wide range of carboxylic acids performed well in this transformation. Under the published conditions, protected amines and alcohols are tolerated and coupling of an unprotected indole-containing substrate has been demonstrated.

Tips for Improving Low Yielding Reactions

- **Concentration:** Diluting the reaction to 0.02 M can be beneficial and reduce byproduct formation.
- **N-H amino acids:** When using amino acids with a free N-H group, it is often advantageous to switch the base to Cs₂CO₃, and the solvent to DMA.
- **Aliphatic acids:** For carboxylic acids lacking an α -heteroatom substituent, changing the base to Cs₂CO₃ can be beneficial. It was also found that diluting the reaction to 0.025 M can also be a helpful modification.
- **Acyclic α -oxy acids:** When coupling sterically hindered vinyl halides and acyclic α -oxy acids, the vinyl bromide should be used (*vs.* iodide). In addition, using DMA as solvent (0.1 M), Cs₂CO₃ as base, and adding 0.06 equiv. of *N*-Boc-benzylamine as an additive can enhance reaction efficiency.

Decarboxylative Alkylation

MacMillan and co-workers have demonstrated that the aforementioned decarboxylative functionalization strategy can be harnessed to address the long-standing challenge of C(sp³)-C(sp³) coupling by demonstrating cross-coupling with alkyl halides (Figure 22).⁹²

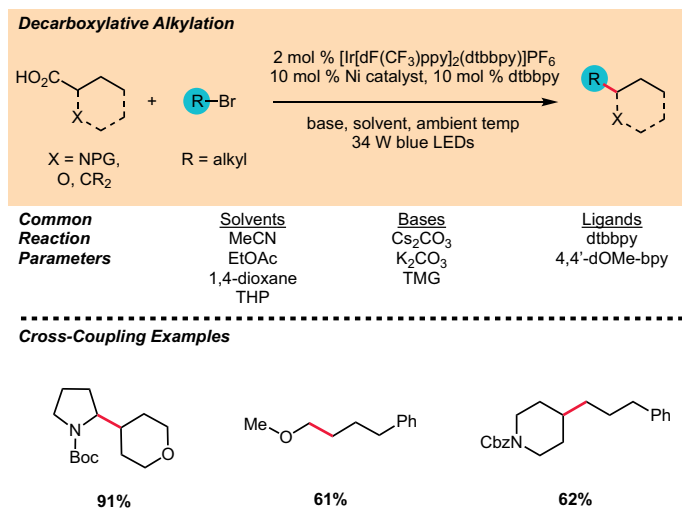


Figure 22. Metallaphotoredox Decarboxylative Alkylation

Common Conditions

- **Solvent:** MeCN (0.05-0.1 M), degassed. Alternatively: MeCN/EtOAc (1:1, 0.02 M), degassed.
- **Stoichiometry:** 1 equiv. alkyl halide, 1.5 equiv. carboxylic acid and 2 equiv. base are typically employed.
- **Photoredox catalyst:** [Ir[dF(CF₃)ppy]₂(dtbbpy)]PF₆ (2 mol %) or [Ir[dF(F)ppy]₂(dtbbpy)]PF₆ (2 mol %).
- **Nickel catalyst:** NiCl₂•glyme (10 mol %)
- **Ligand:** 4,4'-dOMe-bpy (4,4'-dimethoxy-2,2'-bipyridine) or dtbbpy (10 mol %)
- **Base:** K₂CO₃ (2 equiv., stored in desiccator) or Cs₂CO₃ (2 equiv., stored in glovebox). Preliminary studies showed that organic bases such as TMG (tetramethylguanidine, distilled and stored under inert atm) can also be used, providing a homogenous reaction mixture that enables conversion to a flow setup.
- **Reaction setup:** Degas by sparging the entire reaction mixture with nitrogen for ten minutes.

- **Irradiation:** Kessil blue LED lamps (6 cm distance between lamp and reaction vial), ambient temperature (cooling by placing the reaction vessel in a water bath with fan cooling – see temperature control section).
- **Addition of water:** Water can be an important additive in this transformation, with 15–20 equiv. providing a good starting point for optimization.

Notes, Tips, and Troubleshooting

Nickel pre-catalyst: The nickel catalyst and ligand should be pre-ligated in MeCN by sonicating a stock solution for 10 minutes prior to addition.

Reaction vessel: When running the alkylation reaction on larger scale (>5 mL solvent), it can be beneficial to perform these reactions in a 40 mL vial with large cross-shaped stir bars. Here, vortexing the reaction mixture provides a larger surface area and increases light exposure.

Sonication: It is often advantageous to sonicate the reaction mixture for 2 minutes under nitrogen after degassing to ensure formation of a homogeneous suspension.

Functional group tolerance: A diverse array of primary and secondary carboxylic acids couple with primary alkyl halides utilizing the published procedure. Coupling of secondary acids with secondary bromides can be challenging (with the exception of proline), a common feature of Ni-catalyzed C(sp³)-C(sp³) cross-couplings. Alkyl bromides are competent electrophiles in this procedure, alkyl chlorides do not undergo coupling, and alkyl iodides lead predominantly to competing esterification. Alkyl tosylates can be used if converted to the alkyl bromide *in situ* via the addition of CsBr (5–7 equiv.). Alcohols, protected amines, alkyl chlorides, aldehydes, and epoxides are all tolerated under these mild reaction conditions.

Tips for Improving Low Yielding Reactions

- **Solvent mixtures:** The identity of the solvent and the amount of water added can have a drastic effect on this reaction. Addition of water can help to accelerate the reaction rate when low conversion is observed. When esterification of the alkyl bromide is observed as a major byproduct, addition of a non-polar cosolvent such as EtOAc, 1,4-dioxane or THP (tetrahydropyran) can be highly beneficial.
- **Sequential photocatalyst addition:** If incomplete conversion of the starting material is observed after 24 hours, it can be advantageous to add a second batch of photocatalyst in a minimal quantity of degassed MeCN and continue irradiation.

- **Methylation:** When running the decarboxylative methylation, it is best to invert the stoichiometry and use a stock solution of MeBr in MeCN (1.5 equiv. MeBr). Alternatively, MeOTf can be used in the presence of a large excess of CsBr (5-7 equiv.).

Product Description	Product Number
[Ir[dF(CF ₃)ppy] ₂ (dtbbpy)]PF ₆	747793
[Ir[dF(Me)ppy] ₂ (dtbbpy)]PF ₆	901409
NiCl ₂ •glyme	696668
4,4'-Di- <i>tert</i> -butyl-2,2'-bipyridine	515477
4,4'-Dimethoxy-2,2'-bipyridine	245739
Cs ₂ CO ₃	441902
K ₂ CO ₃	209619
1,8-Diazabicyclo[5.4.0]undec-7-ene (DBU)	139009
2- <i>tert</i> -Butyl-1,1,3,3-tetramethylguanidine (Barton's base, BTMG)	20615
1,1,3,3-Tetramethylguanidine (TMG)	241768

Alcohols as Latent Nucleophiles in Cross-Coupling

The MacMillan group has also shown that alcohols can be employed as precursors to carbon-centered radicals. Here, the corresponding oxalate half esters can undergo photoredox-mediated double decarboxylation to deliver a radical coupling partner (**Figure 23**). The merger of this activation mode with Ni catalysis has enabled the development of a protocol for C(sp³)-C(sp²) cross-coupling of alcohols and aryl halides.³⁰ The oxalate half esters are readily prepared and can be used directly in the cross-coupling reaction without purification.

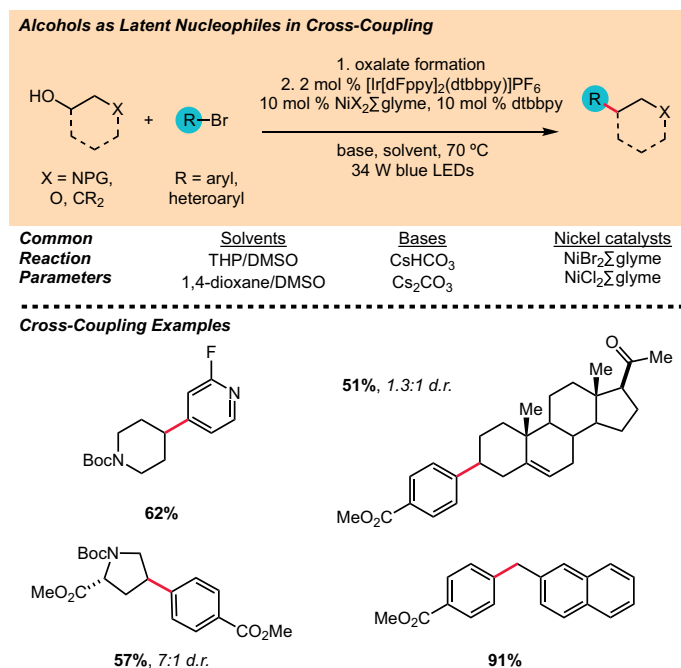


Figure 23. Double Decarboxylative Cross-Coupling of Oxalates

Common Conditions

- **Solvent:** THP/DMSO (10:1, 0.02–0.1 M), degassed and anhydrous. Yields are typically higher when the reaction is run at lower concentrations.
- **Stoichiometry:** 1 equiv. alkyl halide, 1.3 equiv. oxalate and 1.5 equiv. base are typically employed.
- **Photoredox catalyst:** [Ir[dFppy]₂(dtbbpy)]PF₆ (1 mol %)
- **Nickel catalyst:** NiBr₂•glyme or NiCl₂•glyme (5 mol %).
- **Ligand:** dtbbpy (5 mol %)
- **Base:** CsHCO₃ (1.5 equiv., dried at 100 °C and stored in desiccator) or Cs₂CO₃ (1.5 equiv., stored in glovebox).
- **Reaction setup:** Degas by sparging the entire reaction mixture with nitrogen for 10 minutes.
- **Irradiation:** Kessil blue LED lamps. The reactions should be preheated to 70 °C prior to irradiation. The reaction temperature can be maintained at 70 °C by placing the reaction vessel between two 34 W Kessil lamps (2 cm distance between the vial and each lamp) and enclosing the setup within a box lined with aluminium foil.

Notes, Tips, and Troubleshooting

Oxalate preparation: The oxalate half esters can be prepared in a single step and used without purification. A solution of the alcohol in Et₂O/DCM (1:1) at 0 °C can be treated with two equivalents of oxalyl chloride. After stirring for 18 hours, the mixture is quenched by the addition of water. The oxalate can then be partitioned into Et₂O and isolated by concentrating the combined organic layers. Rigorous drying of the oxalate is required to avoid hydrolysis during the reaction. If placing under high vacuum is not sufficient to remove all residual water, these substrates can be azeotropically dried from toluene.

Nickel pre-catalyst: The nickel catalyst and ligand should be pre-ligated in the reaction solvent and added as a stock solution. In some instances a suspension can form, however addition of the catalyst stock solution as a suspension typically does not diminish the yield.

Functional group tolerance: Under the published reaction conditions, a broad array of alcohol and (hetero)aryl bromide coupling partners perform competently. Primary alcohols may require the reaction to be heated to 85 °C for high efficiency. Protected amines and alcohols, aldehydes, esters, aryl chlorides, sulfonamides, pyridines and alkenes are all well tolerated.

Tips for Improving Low Yielding Reactions

- Increasing temperature:** If conversion is slow or a large amount of aryl ester product (originating from mono-decarboxylation) is observed, the reaction can be heated to 80–85 °C to accelerate the second decarboxylation. This can be particularly helpful when a less stable radical coupling partner is being formed (e.g. from primary alcohols).
- Solvent mixtures:** Changing from THF to 1,4-dioxane, and modifying the DMSO:ethereal solvent ratio can be beneficial. When large amounts of protodehalogenation are observed, increasing the ratio of DMSO is often helpful.
- Nickel loading:** Adjusting the nickel loading can often impact the reaction yield. When large amounts of protodeoxygenation are observed, increasing the nickel loading can lead to more effective trapping of the radical intermediate. Conversely, when protodehalogenation is a major problem decreasing the nickel loading can serve to retard this unproductive nickel-mediated pathway.

Product Description	Product Number
[Ir[dFppy] ₂ (dtbbpy)]PF ₆	901368
NiBr ₂ •glyme	406341
NiCl ₂ •glyme	696668
4,4'-Di- <i>tert</i> -butyl-2,2'-bipyridine	515477
Cs ₂ CO ₃	441902
CsHCO ₃	218227
Oxalyl chloride	221015

Metallaphotoredox Cross-Coupling of Trifluoroborate Salts

Photoredox nickel dual catalysis is broadly useful for the cross-coupling of alkyltrifluoroborates with aryl bromides (Figure 24). These transformations are generally robust and tolerant of a vast majority of common functional groups. Numerous protocols have been developed for use with various individual classes of organoboron reagents.^{10,25,93,103–105} These protocols differ with respect to the optimal nickel source, ligand, solvent, and additives. For the cross-coupling of trifluoroborates for which specific conditions have been reported, it is advisable for practitioners to first make use of the optimized reaction conditions. In the event that these conditions fail to achieve the desired transformation, optimization studies are likely to be most effective if focused on identification of the optimal base/additive and solvent.

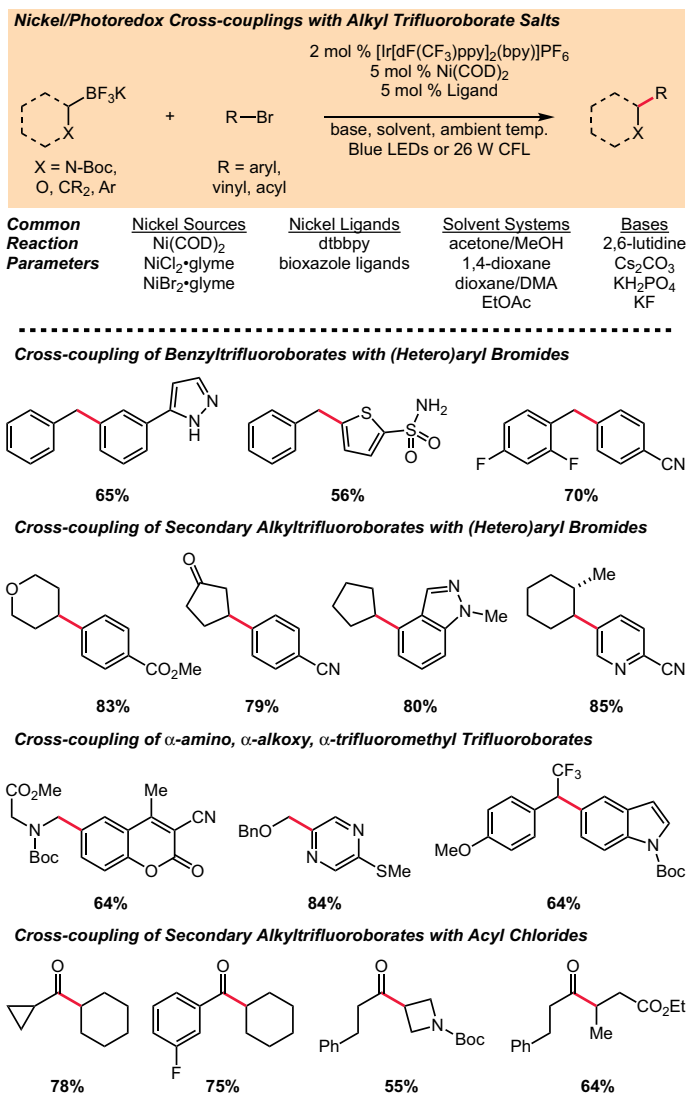


Figure 24. Coupling with Trifluoroborate Salts

Base. Although the precise role of the base in these reactions is not fully understood, they have consistently been observed to improve conversion of starting material to product, while suppressing undesired side reactions such as protodehalogenation. Cesium carbonate and K₂HPO₄ have generally been the most ubiquitous bases, although KF and 2,6-lutidine have also been effective in specific circumstances. Tertiary amine bases typically interfere with reactivity due to competitive oxidation and should be avoided.

Solvent. 1,4-Dioxane is one of the most generally effective solvents for trifluoroborate cross-couplings, and, as such, is typically a good starting point for optimization studies. Polar aprotic solvents, such as acetone and DMA, have also been used successfully. DMSO and DMF are usually less effective than DMA, often completely shutting down reactivity, and should

not be viewed as surrogates for the performance of DMA. Non-polar solvents, such as toluene and dichloromethane, are sometimes suitable, but are rarely optimal. Alcohols typically perform poorly as solvents, but can sometimes be beneficial as cosolvents.

Nickel source. Nickel source can slightly influence the efficiency of the reaction and the prevalence of various side products, but productive reactivity is usually observed with most sources of nickel. Nickel(II) sources are most convenient, due to their air and moisture stability. NiCl₂•glyme is usually effective, and is convenient for its solubility, stability, and commercial availability. Other nickel(II) sources, such as NiBr₂•glyme or Ni(NO₃)₂•6H₂O sometimes outperform NiCl₂•glyme by 5-20%. Nickel precatalysts such as [(TMEDA)Ni(*o*-tolyl)Cl] can also sometimes be effective. Ni(COD)₂, undesirable because of its high cost and instability, can be considered a reagent of last resort if all other nickel sources prove insufficient to achieve the desired reactivity. Ni(OTf)₂ and NiI₂ are usually ineffective. An important consideration in the use of nickel(II) catalysts is the necessity to preform the Ni/ligand complex, usually by dissolving them in THF with heating, then removing residual solvent.⁸² Reactions executed without preformation of the nickel catalyst will almost always fail to give the desired product. The Ni(II)dtbbpy complex can be prepared in bulk as its tetrahydrate and is stable to storage for extended periods of time.⁹⁶

Ligand. 4,4'-Di-*tert*-butyl-2,2'-bipyridine (dtbbpy) is almost invariably an effective ligand for a variety of cross-couplings. Some dtbbpy variants, including bpy (2,2'-bipyridine), 4,4'-dOMe-bpy, bathophenanthroline, phen (1,10-phenanthroline), and neocuproine, can sometimes outperform dtbbpy. Certain classes of substrates perform better with the 2,2'-bioxazoline and pyridine-oxazoline (PyrOx) ligand classes. A variety of monodentate and bidentate phosphines have never been observed to serve as effective ligands.

Photoredox catalyst. Previous studies have demonstrated that photocatalysts [Ir[dF(CF₃)ppy]₂(bpy)]PF₆,^{25,93} [Ir[dF(CF₃)ppy]₂(dtbbpy)]PF₆, and 1,2,3,5-tetrakis(carbazol-9-yl)-4,6-dicyanobenzene (4-CzIPN)^{96,106} are often similarly effective in promoting the dual catalytic cross-coupling of alkyltrifluoroborates with aryl bromides. Typically, [Ir[dF(CF₃)ppy]₂(bpy)]PF₆ affords slightly faster reaction times than the less strongly oxidizing [Ir[dF(CF₃)ppy]₂(dtbbpy)]PF₆. Nevertheless, productive reactivity is usually observed with all three, so this variable is unlikely to rescue a recalcitrant reaction.

Functional group compatibility. Although substrate functional group compatibility has been demonstrated to be high, tertiary amines and nitro groups are rarely tolerated because of competing electron transfer. Electron-rich 5-membered ring heterocycles, including pyrazole, furan, pyrrole, and imidazole, are typically inert. However, their benzoannulated analogs are often tolerated. Oddly, aryl iodides have rarely been observed to couple productively with alkyltrifluoroborates. Electron-poor aryl chlorides, such as 4-chlorobenzonitrile, usually can be coupled with moderate yields and extended reaction times. Highly activated heteroaryl chlorides, such as 2-chloropyridine derivatives, can be rather effective coupling partners. Alkenyl halides have generally been recalcitrant to coupling with trifluoroborates, but can couple effectively with alkylbis(catecholato)silicates.¹⁰⁷

Light source and reaction setup. Both blue LEDs and white fluorescent lights are competent to promote these cross-couplings. Faster reaction rates are often observed with the more efficient blue LED illumination, and reaction rate is usually photon limited, so care should be taken to maximize illuminated surface area. Tall vials are the preferred reaction vessels, but round-bottomed flasks are also acceptable. Reactions should be cooled with a fan to prevent the temperature from rising significantly due to heat from the lamp. Hot reactions often suffer from side reactions resulting from reaction of the radical intermediates with solvent, leading to protodeboronation and arylated solvent molecules. Most reactions can be scaled up to produce large quantities of material (ca. 1 g), but typically require longer reaction times due to inefficient illumination. Continuous flow procedures have been developed to address this limitation.^{108,109}

See the recent *Nature Protocols* article published by Molander and co-workers for detailed instructions and additional troubleshooting tips for the photoredox nickel-catalyzed cross-couplings of trifluoroborate and silicate salts with aryl halides.⁸²

Product Description	Product Number
NiCl ₂ •glyme	696668
NiBr ₂ •glyme	406341
Ni(NO ₃) ₂ •6H ₂ O	72252
4,4'-Di- <i>tert</i> -butyl-2,2'-bipyridine	515477
[Ir[dF(CF ₃)ppy] ₂ (bpy)]PF ₆	804215
[Ir[dF(CF ₃)ppy] ₂ (dtbbpy)]PF ₆	747793
1,2,3,5-tetrakis(carbazol-9-yl)-4,6-dicyanobenzene (4-CzIPN)	901817
Cs ₂ CO ₃	441902
2,6-Lutidine	336106
K ₂ HPO ₄	P3786
KF	402931

Cross-Electrophile Coupling

Recently, a mild and general protocol was developed for cross-electrophile coupling through the merger of nickel and photoredox catalysis (**Figure 25**).⁹⁷ Here, the combination of a dtbbpy-ligated Ni catalyst, Ir[dF(CF₃)ppy]₂(dtbbpy)]PF₆ and tris(trimethylsilyl)silane (TTMSS) enables efficient cross-coupling of alkyl and aryl bromides. Silyl radical formation enables the generation of carbon-centered radicals from alkyl bromides via halogen abstraction and these radical coupling partners can undergo arylation with a wide variety of (hetero)aromatic coupling partners. This cross-coupling protocol exhibits wide functional group tolerance, allowing coupling of typically challenging reaction partners such as tertiary alkyl radicals, ortho-substituted arenes and 5-membered heterocycles.

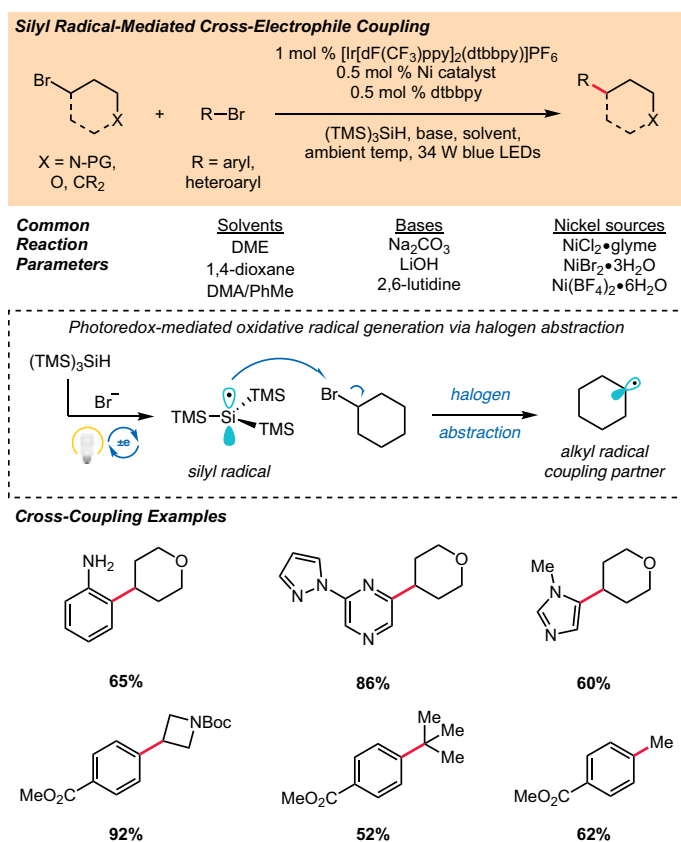


Figure 25. Cross-Electrophile Coupling

Common Conditions

- **Solvent:** DME, 1,4-dioxane, MeCN, 1:1 DMA/toluene (0.1 M), degassed and anhydrous.
- **Stoichiometry:** 1.5 equiv. alkyl bromide and 1 equiv. aryl bromide are typically employed. The stoichiometry can be inverted and employing a 1:1 ratio of coupling partners does not significantly reduce reaction efficiency.
- **Photoredox catalyst:** [Ir[dF(CF₃)ppy]₂(dtbbpy)]PF₆ (1 mol %)
- **Nickel catalyst:** NiCl₂•glyme (0.5 mol %)
- **Ligand:** dtbbpy (0.5 mol %)
- **Silane:** tris(trimethylsilyl)silane (1 equiv.)
- **Base:** Na₂CO₃ (2 equiv., stored in desiccator), LiOH (2 equiv., dried (see below) and stored in desiccator), 2,6-lutidine (2-5 equiv., distilled and stored under inert atm)
- **Reaction setup:** Degas by sparging the entire reaction mixture with nitrogen for 10 minutes.
- **Irradiation:** Kessil blue LED lamps (6 cm distance between lamp and reaction vial), ambient temperature (with fan cooling), 6-24 h or Photoreactor m1 for comparable yields and increased reaction rates.

Notes, Tips, and Troubleshooting

Identity of base: *Inorganic bases:* Both Na₂CO₃ and LiOH can be used but LiOH performs better when employing heteroaromatic bromide coupling partners. LiOH•H₂O is dried by heating to 100 °C at <100 mTorr prior to use. *Organic bases:* The use of 2,6-lutidine as base provides homogenous reaction conditions and similar levels of reaction efficiency are observed. For heteroaromatic bromides, 5 equivalents of 2,6-lutidine is recommended. An organic base (*i.e.* 2,6-lutidine) is recommended when conducting cross-electrophile couplings in the Photoreactor m1 at 100% light intensity.

Solvent: DME or 1,4-dioxane as solvent typically provides the highest reaction efficiencies. For challenging substrates, significant quantities of solvent-coupled products (arylation of DME/1,4-dioxane) can be observed and, in these cases, it is sometimes preferable to switch to MeCN or DMA/toluene (1:1).

Nickel catalyst: A wide variety of nickel(II) pre-catalysts can be employed and the only nickel source tested which did not provide the desired product was Ni(OH)₂. The bipyridine ligand, dtbbpy, is broadly applicable to the cross-electrophile coupling of aryl and alkyl bromides. Pre-complexation of the ligand and nickel catalyst can be accomplished by sonicating or stirring a stock solution of the two components in the specified reaction solvent for 5 minutes, the pre-complexed catalyst is then syringed directly into the reaction vessel prior to degassing.

Functional group compatibility: Under the published reaction conditions, broad functional group tolerance is observed. A wide range of aryl bromides with differing electronic properties and substitution patterns are tolerated, including unprotected anilines and ortho-substituted arenes. Electron-deficient aryl chlorides are tolerated, however longer reaction times are required. Aryl iodides and electron-rich aryl chlorides are challenging substrates for this technology. Using LiOH or 2,6-lutidine as base, a variety of heteroaromatic bromides can be coupled using this protocol. In some cases, heteroaryl chlorides perform better than the corresponding bromides (*i.e.* for highly activated substrates). A range of cyclic and acyclic primary, secondary, and tertiary alkyl bromides couple efficiently under the published reaction conditions. Higher Ni catalyst loadings are required for tertiary alkyl bromides. Methylation of arenes can be achieved by generating methyl bromide *in situ* from methyl tosylate and a bromide source (*i.e.* LiBr, NaBr, NBu₄Br).

Tips for Improving Low Yielding Reactions

- **Silane equivalents:** Increasing to two equivalents of TTMSS.
- **Adjusting loading of the nickel catalyst:** Increasing the Ni loading can improve the yields when coupling heteroaromatic halides or tertiary alkyl bromides.
- **Base equivalents:** Increasing the equivalents of base can be beneficial (particularly for organic bases such as lutidine).
- **Stoichiometry:** Increasing the equivalency of the alkyl bromide coupling partner can improve the yield for challenging substrates.

Product Description	Product Number
NiCl ₂ •glyme	696668
4,4'-Di- <i>tert</i> -butyl-2,2'-bipyridine	515477
[Ir[dF(CF ₃)ppy] ₂ (dtbbpy)]PF ₆	747793
Tris(trimethylsilyl)silane	360716
Na ₂ CO ₃	223484
2,6-Lutidine	336106
LiOH	545856

C–H Functionalization via HAT, Photoredox, and Nickel Catalysis

The merger of photoredox and nickel catalysis has delivered a general catalytic manifold wherein the generation of carbon-centered radical coupling partners via oxidative single electron transfer-mediated pathways enables the development of new cross-coupling protocols. Recently, MacMillan and co-workers demonstrated that carbon-centered radicals could be generated from aliphatic C–H nucleophiles via photoredox-mediated hydrogen-atom transfer (HAT) with amine radical cations (**Figure 26**).¹¹⁰ Incorporation of this activation mode into the outlined dual nickel photoredox catalysis platform enables direct functionalization of α -amino and α -oxy C–H bonds with aromatic substituents.⁴⁸ More specifically, the combination of a nickel catalyst (NiBr₂•4,7-dOMe-phen), a photocatalyst ([Ir[dF(CF₃)ppy]₂(dtbbpy)]PF₆) and a hydrogen atom transfer catalyst (3-acetoxyquinuclidine) mediates arylation of a wide variety of α -heteroatom C–H bonds. Following this report, MacMillan and co-workers demonstrated that this mechanistic paradigm could be utilized to achieve C(sp³)-C(sp³) cross-coupling between α -heteroatom C–H nucleophiles and alkyl bromides.¹¹¹ Further details regarding these C–H functionalization protocols are outlined below. The Doyle and Molander laboratories have recently demonstrated that the combination of nickel and photocatalysis can enable direct arylation of α -oxy and benzylic C–H bonds through halogen radical-mediated HAT.^{112,113} It should be noted that, while involving the merger of nickel catalysis and photocatalysis, these transformations are proposed to proceed via mechanistically distinct pathways.

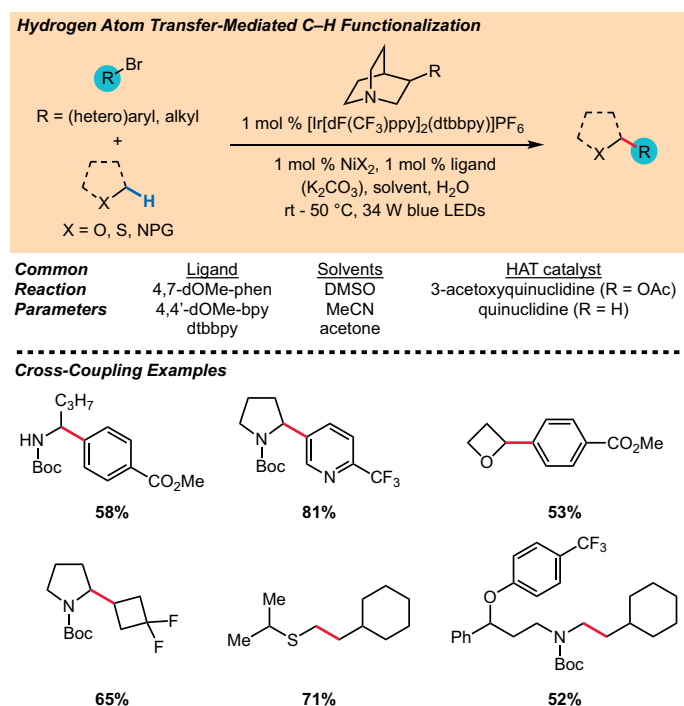


Figure 26. C–H Arylation/Alkylation via HAT, Photoredox and Nickel Catalysis

Common Conditions for C–H Arylation

- **Solvent:** DMSO (0.25 M), degassed. Alternative solvents that provide moderate yields: MeCN, acetone.
- **Stoichiometry:** 2 equiv. C–H nucleophile and 1 equiv. aryl halide are typically used. Reverse stoichiometry can result in the formation of difunctionalized products – 1:1 ratio provides higher yields than with excess aryl halide.
- **Photoredox catalyst:** [Ir[dF(CF₃)ppy]₂(dtbbpy)]PF₆ (1 mol %)
- **Nickel catalyst:** NiBr₂•3H₂O (1 mol %)
- **Ligand:** 4,7-dOMe-phen (4,7-dimethoxy-1,10-phenanthroline, 1 mol %)
- **HAT reagent:** 3-Acetoxyquinuclidine (1.1 equiv.)
- **Water cosolvent:** 30-50 equivalents is usually optimal with DMSO as solvent.
- **Reaction setup:** Degas by sparging the entire reaction mixture with nitrogen for 20 minutes or through two cycles of freeze-pump-backfill-thaw.
- **Irradiation:** Kessil blue LED lamps (6 cm distance between lamp and reaction vial), ambient temperature (with fan cooling), 6-48 h or Photoreactor m1 for comparable yields and increased reaction rates.

Common Conditions for C–H Alkylation

- **Solvent:** H₂O/MeCN (0.125 M), degassed.
- **Stoichiometry:** 2–5 equiv. C–H nucleophile and 1 equiv. alkyl halide are typically used. Reverse stoichiometry can result in the formation of difunctionalized products – 1:1 ratio provides higher yields than with excess alkyl halide.
- **Photoredox catalyst:** [Ir[dF(CF₃)ppy]₂(dtbbpy)]PF₆ (1 mol %)
- **Nickel catalyst:** Ni(BF₄)₂•6H₂O (2–10 mol %)
- **Ligand:** 4,4'-dOMe-bpy, 4,4'-dMe-bpy (4,4'-dimethyl-2,2'-bipyridine), dtbbpy, phen (2–10 mol %)
- **HAT reagent:** Quinuclidine (5-20 mol %)
- **Base:** K₂CO₃, Li₂CO₃ (1–1.5 equiv., stored in desiccator)
- **Water:MeCN ratio:** From 9:1 to 1:1 MeCN:H₂O.
- **Reaction setup:** Degas by sparging the entire reaction mixture with nitrogen at 0 °C for 15 minutes
- **Irradiation:** Kessil blue LED lamps (5 cm distance between lamp and reaction vial), ambient temperature - 50 °C (with or without fan cooling), 24 h.

Notes, Tips, and Troubleshooting

Nickel catalyst: A wide variety of nickel(II) pre-catalysts can be employed in the C–H functionalization protocols. The phenanthroline ligand, 4,7-dOMe-phen, is generally the optimal ligand for the C–H arylation protocol. However, in both the C–H arylation and alkylation methodologies, a range of bipyridine and phenanthroline ligands bearing electron-donating substituents perform comparably (*I.e.* dtbbpy, 3,4,7,8-tetramethyl-1,10-phenanthroline, 4,4'-dOMe-bpy, 4,4'-dMe-bpy). Pre-complexation of the ligand to the Ni catalyst is accomplished either by (i) sonicating a stock solution of the two components in the reaction solvent for 5 minutes (*arylation protocol*) or (ii) stirring the two components in the specified reaction solvent for 15 minutes (*alkylation protocol*). The pre-complexed catalyst can then be syringed directly into the reaction vessel prior to degassing.

HAT catalyst: *Arylation:* Significantly higher reaction efficiencies and broader substrate scope are observed when 3-Acetoxyquinuclidine (1.1 equiv) is employed as the HAT catalyst (vs. unsubstituted quinuclidine). 3-acetoxyquinuclidine can be synthesized in one step from commercial starting materials through acetylation of 3-quinuclidinol. Stoichiometric quantities of 3-acetoxyquinuclidine are employed as this reagent functions as both the HAT catalyst and base. *Alkylation:* Sub-stoichiometric quantities of HAT catalyst (5-20 mol % quinuclidine) with stoichiometric inorganic base (1 –1.5 equiv.) provides the highest reaction efficiencies. Carbonate bases afford the highest reaction yields, with comparable results achieved with various counter-ions (K₂CO₃, Na₂CO₃, Cs₂CO₃, Li₂CO₃).

Solvent/water loading: *Arylation:* DMSO (0.25 M) is generally the optimal solvent for the C–H arylation protocol. Addition of water as a cosolvent is vital for achieving high reaction efficiencies and typically the addition of 30-50 equivalents of water is optimal. For some heteroaromatic chloride coupling partners (*i.e.* highly activated heteroarenes with electron-withdrawing groups), water-free conditions provide the highest yield. For low yielding reactions, decreasing the reaction concentration to 0.125 M (while maintaining the optimal DMSO:H₂O ratio) can sometimes provide enhanced efficiencies. When changing reaction solvent, the ratio of solvent:H₂O often has to be adjusted. *Alkylation:* MeCN as solvent provides the highest reaction yields. The use of a water cosolvent is extremely important and typically 9:1 v/v MeCN:H₂O provides a good starting point for optimization, with increased quantities of H₂O (up to 1:1 v/v) preferable for some substrate combinations.

Functional group compatibility: Under the published reaction conditions, a wide range of aryl bromides with differing electronic properties and substitution patterns (arenes with bulky ortho-substituents are challenging substrates) are tolerated. Aryl iodide and electron-rich aryl chloride coupling partners react with low efficiency. However, electron-deficient aryl chlorides are tolerated (with extended reaction times) and, in some cases, heteroaryl chlorides provide higher yields than the corresponding bromides. In the alkylation, a range of cyclic and acyclic, primary and secondary alkyl bromides were well tolerated. Selective cross-coupling of alkyl bromides in the presence of alkyl chlorides can be achieved. For both the arylation and alkylation methodologies, the optimized reaction conditions enable coupling of a wide range of cyclic and acyclic Boc-protected amines. Both primary and secondary α -amino C–H bonds undergo functionalization, with a preference for arylation/alkylation at the primary position when both types of C–H bond are present. Tertiary and benzylic α -amino C–H bonds cannot be functionalized using the outlined protocols. However, both urea and amide α -amino C–H bonds and dialkylether α -oxy C–H bonds can be engaged using these cross-coupling technologies. Moreover, for the C–H alkylation, direct functionalization of thioethers was demonstrated.

Tips for Improving Low Yielding Reactions

- **Stoichiometry:** Increasing the equivalents of C–H nucleophile generally improves the reaction yields.
- **Varying water loading:** The ratio of solvent:H₂O can have a dramatic impact on reaction efficiency.
- **Sequential addition of HAT reagent:** For sluggish reactions, addition of the HAT reagent in two portions (0.55 equiv. at 0 h and 0.55 equiv. at ~8 h for arylation, 0.1 equiv. at 0 h and 0.1 equiv. at ~12 h for alkylation) often improves the rate of reaction and provides a small increase in reaction yield (5-15%).

- **Adjusting Ni loading:** *Arylation:* If significant quantities of protodehalogenated or phenol byproducts are observed, try decreasing the nickel catalyst loading.

Tip: For challenging amine substrates (*i.e.* sterically hindered acyclic amines), use of a Bac-protecting group (-CONH*t*-Bu) on nitrogen in place of a Boc-protecting group often improved reaction efficiency in the C–H arylation.

Tip: Pyridine HCl salts can be utilized directly in the arylation by increasing the quantity of 3-acetoxyquinuclidine to 2.1 equivalents.

Tip: Modified reaction conditions are required for arylation with 2-halopyridines: 1.1 equiv. quinuclidine (instead of 3-acetoxyquinuclidine), MeCN as solvent (instead of DMSO) and 100 equiv. H₂O (instead of 40 equiv. H₂O).

Product Description	Product Number
[Ir[dF(CF ₃)ppy] ₂ (dtbbpy)]PF ₆	747793
NiBr ₂ •3H ₂ O	72243
4,7-Dimethoxy-1,10-phenanthroline	678023
4,4'-Dimethoxy-2,2'-bipyridine	536040
4,4'-Di(<i>tert</i> -butyl)-2,2'-bipyridine	515477
4,4'-Dimethyl-2,2'-bipyridine	245739
1,10-Phenanthroline	131377
3-Quinuclidinol	253340
Quinuclidine	197602
K ₂ CO ₃	209619
Li ₂ CO ₃	255823

C–Heteroatom Bond Formation via the Merger of Nickel and Photoredox Catalysis

In addition to C–C bond-forming reactions, the combination of nickel and photoredox catalysis has been demonstrated as a powerful platform for C–X (O, N, S) bond-forming reactions (**Figure 27**). Reports from MacMillan, Jamison, Molander, and others have demonstrated that Ni-mediated C–O,¹¹⁴ C–N,^{49,115,116} and C–S^{117,118} cross-couplings are promoted by the addition of a photocatalyst and visible light when using alcohol, amine, and thiol nucleophiles, respectively. In many cases, this strategy enables elusive Ni-mediated cross-couplings that previously would only have been possible by employing alternate metals and specific ligand classes. Two key strategies have been employed in metallaphotoredox-catalyzed C–X bond formations and these rely on generation of a high-valent nickel species to promote productive bond formation. Firstly, the excited-state photocatalyst has been implicated in direct modulation of the oxidation state of the Ni-catalyst via single-electron transfer oxidation of an intermediate Ni(II)-aryl complex. Here, generation of a high valent Ni(III)-aryl complex is postulated to promote reductive elimination and stoichiometric studies have provided support for this mechanistic pathway.^{49,114,115} Alternatively, photoredox-mediated formation of heteroatom-centered radicals can facilitate C–X bond formation, in a mechanistically analogous manner to the C–C bond-forming protocols outlined in **Figure 19**.^{116–118} A related metallaphotocatalysis strategy for aryl ester C–O bond formation demonstrated by MacMillan and co-workers relies on generation of an excited-state Ni complex, however this mechanistically distinct process lies beyond the scope of this guide.¹¹⁹

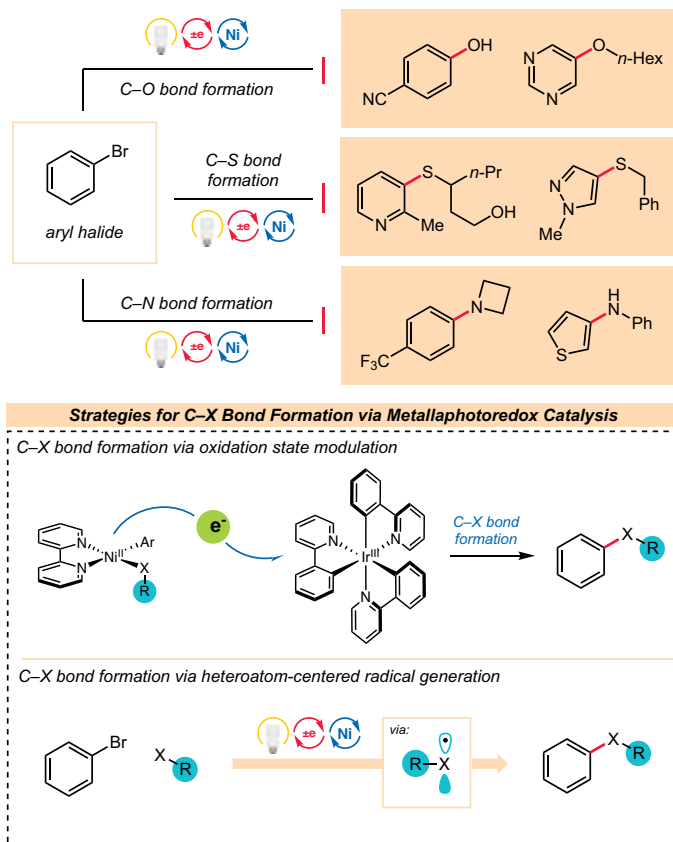


Figure 27. Metallaphotoredox C–Heteroatom Couplings

C–O Bond Formation via Nickel Photoredox Catalysis

MacMillan and co-workers have developed a general procedure for the synthesis of aryl ethers using a combination of Ir[dF(CF₃)ppy]₂(dtbbpy)]PF₆ and a dtbbpy-ligated Ni(II) salt (**Figure 28**).¹¹⁴ In the proposed mechanism, the highly oxidizing excited state of the iridium photocatalyst oxidizes an *in-situ* formed nickel(II)-aryl-alkoxide complex and subsequent reductive elimination from the high valent metal center affords the C–O linkage. A broad array of primary and secondary alcohols can be coupled with a wide variety of (hetero)aryl halides.

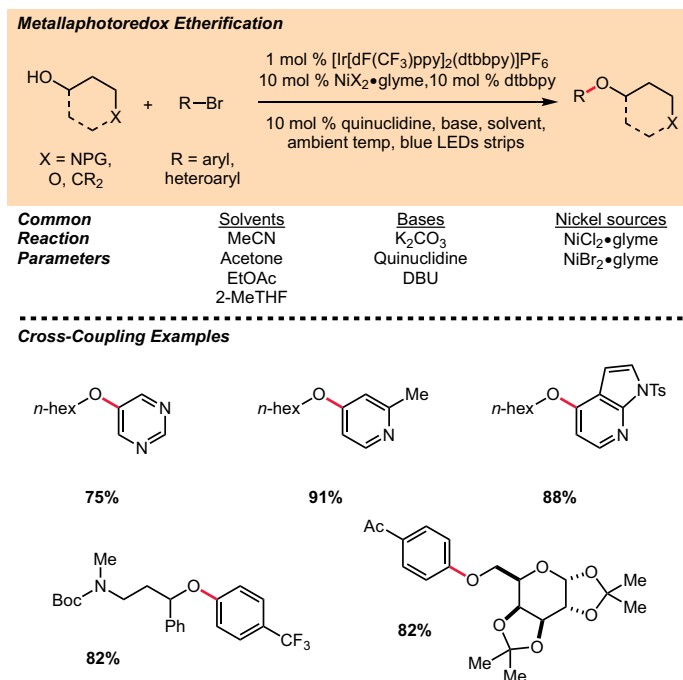


Figure 28. Metallaphotoredox Etherification

Common Conditions

- **Solvent:** MeCN (0.25 M), degassed and anhydrous.
- **Stoichiometry:** 1 equiv. aryl bromide and 1.5 equiv. alcohol are typically employed. When using secondary alcohols, an excess of 3 equivalents is preferable for high reaction efficiency. Comparable efficiency is observed when the stoichiometry is inverted.
- **Photoredox catalyst:** [Ir[dF(CF₃)ppy]₂(dtbbpy)]PF₆ (1 mol %)
- **Nickel catalyst:** NiCl₂•glyme (10 mol %)
- **Ligand:** dtbbpy (10 mol %)
- **Sacrificial reductant:** quinuclidine
- **Base:** K₂CO₃ (1 equiv., stored in desiccator).
- **Reaction setup:** Degas via three cycles of freeze-pump-backfill-thaw. Alternatively - degas by sparging the entire reaction mixture with nitrogen for 10 minutes at 0 °C.
- **Irradiation:** Three double density sapphire blue LED strips wrapped inside a recrystallization dish (1 cm between vial and LEDs), ambient temperature (with fan cooling). CFL lamps provide comparable results but slightly reduced efficiency has been observed when using high power 34 or 40 W Kessil blue LED lamps.

Notes, Tips, and Troubleshooting

Identity of base: Granular K₂CO₃ is the optimal base for this reaction. If you plan to scale the reaction up using flow, stoichiometric quinuclidine provides a homogenous reaction mixture.

Identity of sacrificial reductant: When using aryl bromides and electron-deficient heteroaryl chlorides, quinuclidine is optimal. When employing aryl iodides, DBU should be used.

Solvent: Acetone and EtOAc can be used in place of MeCN, albeit with slightly diminished efficiency.

Nickel catalyst: The nickel salt and ligand can be pre-ligated (stir or sonicate for 10 minutes) in MeCN, and this solution added directly to the reaction mixture. A range of nickel(II) salts perform comparably, with the exception of NiI₂, Ni(OAc)₂ and Ni(acac)₂ which typically deliver large quantities of protodehalogenation byproducts and should be avoided.

Functional group tolerance: A diverse array of electronically differentiated aryl and heteroaryl halides couple under the published conditions. Primary and secondary alcohols, including non-nucleophilic alcohols such as trifluoroethanol, are well tolerated. Tertiary alcohols do not couple under the reported reaction conditions. When using a diol containing both a primary and secondary alcohol, the primary alcohol couples preferentially. Esters, sugar derivatives, and protected amines are well tolerated.

Tips for Improving Low Yielding Reactions

- **Alcohol equivalents:** Increasing to 2 or 3 equivalents of alcohol substrate can accelerate the reaction and improve efficiencies.
- **Reaction temperature:** Electron-rich aromatics and heteroaromatics often require heating in order to obtain high efficiencies. This is readily achieved by conducting the reaction without fan cooling.
- **Water coupling:** When using water as the nucleophile (10 equiv. required), the reaction solvent should be changed to 2-MeTHF.

Product Description	Product Number
[Ir[dF(CF ₃)ppy] ₂ (dtbbpy)]PF ₆	747793
NiCl ₂ •glyme	696668
NiBr ₂ •glyme	406341
4,4'-Di(<i>tert</i> -butyl)-2,2'-bipyridine	515477
Quinuclidine	197602
K ₂ CO ₃	209619
1,8-Diazabicyclo[5.4.0]undec-7-ene (DBU)	139009

C–N Bond Formation via Nickel Photoredox Catalysis

The cross-coupling of amines and aryl halides, to generate medicinally relevant aniline motifs, is one of the most broadly employed catalytic transformations in the pharmaceutical industry.¹²⁰ This prevalence results, in part, from the development of highly general, robust methodologies by the laboratories of Buchwald and Hartwig. Here, efficient Pd-catalyzed C–N coupling technologies have been established through the elegant design and development of complex ligand architectures.¹²¹ While Ni-catalyzed C–N cross-couplings traditionally require forcing conditions and exhibit comparatively limited substrate scope due to the difficulty of reductive elimination from Ni(II)-amido complexes,^{122,123} the combination of nickel and photoredox catalysis has recently been shown to facilitate recalcitrant amination reactions and enable development of mild protocols for C–N bond formation (**Figure 29**).

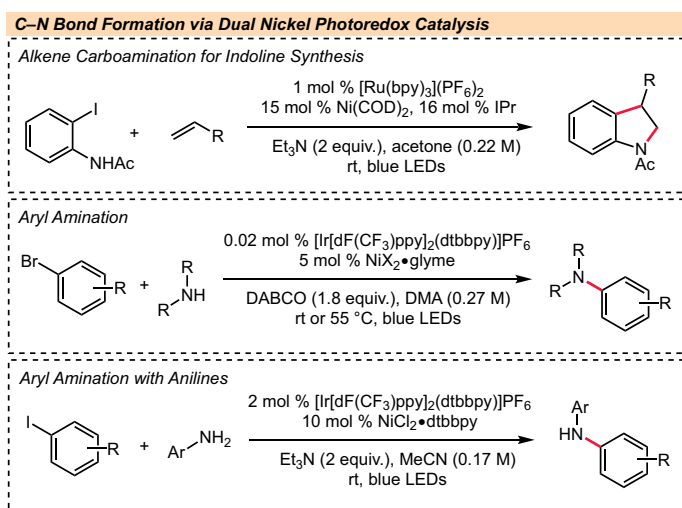


Figure 29. Metallaphotoredox C–N Bond Formation

Jamison and co-workers demonstrated that the merger of nickel and photoredox catalysis provides access to indolines from 2-iodoacetanilides and terminal alkenes.¹¹⁵ Stoichiometric studies lent support to the proposed mechanism wherein C(sp³)–N bond formation is facilitated by photoredox-mediated oxidation of the Ni(II)-amido complex to a high valent Ni(III)-amido complex. Through the combination of Ni(COD)₂, a carbene ligand (IPr) and [Ru(bpy)₃](PF₆)₂, highly selective generation of 3-substituted indoline products was observed and, while limited to mono-substituted terminal alkenes, a range of sterically and electronically differentiated alkenes participated in good yields.

A general Ni-catalyzed amination protocol was recently developed through a collaboration between the MacMillan group, Buchwald group, and scientists at MSD. (**Figure 30**).⁴⁹ Upon exposure to the

photoredox catalyst [Ir[dF(CF₃)ppy]₂(dtbbpy)]PF₆ and visible light, simple Ni(II)-halide pre-catalysts were found to mediate highly efficient cross-coupling of aryl halides and amines without the requirement of exogenous ligand. The use of a mild organic base, DABCO, enables coupling of a wide array of primary and secondary amines and extremely low photocatalyst loadings are required. Further details regarding this Ni-mediated amination protocol are outlined below.

Following this report, Oderinde and Johannes demonstrated that cross-coupling of anilines and aryl iodides could be achieved through the combination of nickel and photoredox catalysis.¹¹⁶ Employing a similar catalyst system to that described by MacMillan and co-workers, with inclusion of dtbbpy as ligand, a variety of electronically and sterically differentiated aryl iodides and anilines coupled in moderate to excellent yields. Here, the amination reaction is proposed to proceed via a mechanistically distinct aminyl radical generation/trapping reaction pathway.

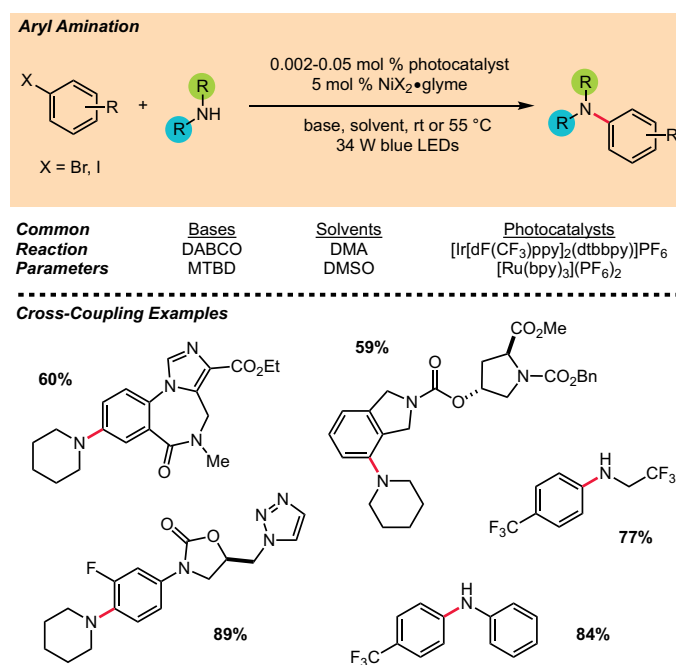


Figure 30. MacMillan/Buchwald Photoredox Aryl Amination

Aryl Amination Common Conditions

- **Solvent:** DMA or DMSO (0.27 M), degassed and anhydrous.
- **Stoichiometry:** 1.5 equiv. amine (distilled and stored under inert atm) and 1 equiv. aryl halide.
- **Photoredox catalyst:** [Ir[dF(CF₃)ppy]₂(dtbbpy)]PF₆ or [Ru(bpy)₃](PF₆)₂ (0.002 mol % for reactions with MTBD, 0.02 mol % for reactions with DABCO)
- **Nickel catalyst:** NiBr₂•glyme or NiCl₂•glyme (5 mol %)

- **Ligand:** no exogenous ligand required
- **Base:** DABCO (1.8 equiv.) or MTBD (1 equiv.)
- **Reaction setup:** Degas by sparging the entire reaction mixture for 20 minutes with nitrogen at 0 °C or through three cycles of freeze-pump-backfill-thaw.
- **Irradiation:** Kessil blue LED lamps (6 cm distance between lamp and reaction vial), ambient temperature (with fan cooling) or 55 °C (no fan, enclosed setup), 3-48 h or Photoreactor m1 for comparable yields and increased reaction rates.

Notes, Tips, and Troubleshooting

Photocatalyst: Both $[\text{Ir}[\text{dF}(\text{CF}_3)\text{ppy}]_2(\text{dtbbpy})]\text{PF}_6$ and $[\text{Ru}(\text{bpy})_3](\text{PF}_6)_2$ have been demonstrated as competent photocatalysts. Generally, low photocatalyst loadings (0.002-0.05 mol %) provide optimal yields as this reduces formation of protodehalogenation byproducts. Lower photocatalyst loadings should be used when MTBD is employed as the base (0.002 mol % photocatalyst) compared with DABCO as base (0.02 mol % photocatalyst). During reaction setup, accurate measurement of these small quantities of photocatalyst is achieved by microliter syringe addition of a stock solution of the required photocatalyst in DMA or DMSO.

Base: The bases that provide the highest yields in the aryl amination protocol are DABCO, MTBD, and quinuclidine. DABCO (1.8 equiv.), a cheap, mild organic base, provides a useful starting point for reaction optimization. Increasing the equivalents of DABCO and amine coupling partners can improve the reaction yields for challenging substrates. For electron-neutral/rich arenes and primary amines, MTBD (1 equiv.) as base often results in higher reaction efficiency.

Temperature: For relatively nucleophilic amines and electron-deficient aryl halides, cross-couplings proceed with high efficiency at ambient temperature (exposure to a 34 W blue LED lamp with fan cooling). Electron-neutral and electron-rich aryl halides, and less nucleophilic amines (e.g. anilines, fluorinated amines) couple slowly at ambient temperature and require heating to 55 °C (exposure to a 34 W blue LED lamp without fan cooling).

Functional group compatibility: A wide variety of electron-poor and electron-neutral (hetero)aryl bromides and iodides couple with high efficiency under the published reaction conditions. Electron-rich aryl bromides and aryl chlorides are challenging coupling partners that require elevated temperature and extended reaction times. The outlined amination protocol is applicable to both primary and secondary amines, with complete selectivity for C–N coupling in the presence of unprotected alcohols. Amines without α -hydrogens require slightly modified conditions (see below). The published protocol enables coupling of challenging fluorinated amines and is tolerant of moderately sterically encumbered amine coupling partners.

Tips for Improving Low Yielding Reactions

- **Nickel loading:** Electron-neutral and electron-rich arenes generally require higher Ni catalyst loadings.
- **Reaction stoichiometry:** Increasing the equivalents of amine coupling partner and base can improve the reaction yield.
- **Photocatalyst loading/light intensity:** If significant quantities of aryl halide protodehalogenation is observed, decreasing the photocatalyst loading and/or reducing the light intensity can help reduce formation of this byproduct.

Tip: Under the published reaction conditions, cross-coupling of amines without α -hydrogens (e.g. anilines, sulfonamides) requires addition of sub-stoichiometric quantities of a sacrificial amine (i.e. 10 mol % pyrrolidine) to facilitate generation of an active Ni catalyst. Here, lower Ni loadings are required to achieve high yields (0.5 mol % Ni catalyst). Small quantities of the pyrrolidine-coupled arene are generated under these reaction conditions (~5% pyrrolidine-coupled byproduct).

Tip: The HCl salt of amines can be used directly by employing 2 equiv. of MTBD as base and heating the reaction to 55 °C (no fan cooling).

Product Description	Product Number
$[\text{Ir}[\text{dF}(\text{CF}_3)\text{ppy}]_2(\text{dtbbpy})]\text{PF}_6$	747793
$[\text{Ru}(\text{bpy})_3](\text{PF}_6)_2$	754730
NiBr ₂ •glyme	406341
NiCl ₂ •glyme	696668
Ni(COD) ₂	244988
1,3-Bis(2,6-diisopropylphenyl)-1,3-dihydro-2H-imidazol-2-ylidene (IPr)	696196
1,4-Diazabicyclo[2.2.2]octane (DABCO)	D27802
7-Methyl-1,5,7-triazabicyclo[4.4.0]dec-5-ene (MTBD)	359505

C–S Bond Formation via Nickel Photoredox Catalysis

The combination of photoredox and nickel catalysis has also been shown to facilitate thioetherification of aryl halides. In these protocols, a distinct mechanistic pathway involving generation and trapping of a thiyl radical coupling partner is proposed (**Figure 31**). Notably, broad substrate scope and functional group tolerance is observed in the outlined C–S bond-forming protocols due to the mild reaction conditions developed.

Oderinde and Johannes reported C–S cross-coupling of aryl iodides and thiols through the combination of a nickel catalyst, $\text{NiCl}_2 \cdot \text{dtbbpy}$, and a photoredox catalyst, $\text{Ir}[\text{dF}(\text{CF}_3)\text{ppy}]_2(\text{dtbbpy})\text{PF}_6$, in the presence of pyridine as base and visible light (**Figure 31A**).¹¹⁷ Here, generation of a thiyl radical is postulated to occur via an oxidation-deprotonation sequence and this ultimately enables formation of a Ni(III)-aryl-sulfide complex that can readily undergo reductive elimination to generate the thioether product. While the protocol is limited to aryl iodides, a variety of differentially substituted arenes containing orthogonal functional handles, such as aryl bromide and boronic ester groups, can be coupled in good yields. A range of thiophenols and alkyl thiols coupled efficiently under the optimized conditions, with complete selectivity for C–S bond formation in the presence of other reactive functionality, such as free alcohols and carboxylic acids.

Thioetherification of aryl bromides has also been accomplished using a hydrogen atom transfer-mediated thiyl radical generation strategy. As previously discussed (**Figure 19B**), alkylbis(catecholato)silicates deliver alkyl radicals via an oxidative SET pathway upon exposure to visible light and a photoredox catalyst. Molander and co-workers used this activation mode to generate 1° alkyl radicals, which then engaged in a HAT event with the thiol substrate to deliver the desired thiyl radical coupling partners (**Figure 31B**).¹¹⁸ Here, the combination of $[\text{Ru}(\text{bpy})_3](\text{PF}_6)_2$, $\text{NiCl}_2 \cdot \text{dtbbpy}$ and an isobutylsilicate salt enables efficient coupling of a range of electron-deficient and electron-neutral (hetero)arenes. Notably, tertiary thiols underwent coupling in excellent yield and protic functionality, such as unprotected primary amines and alcohols, was well tolerated under the base-free reactions conditions, with complete selectivity for C–S bond formation observed.

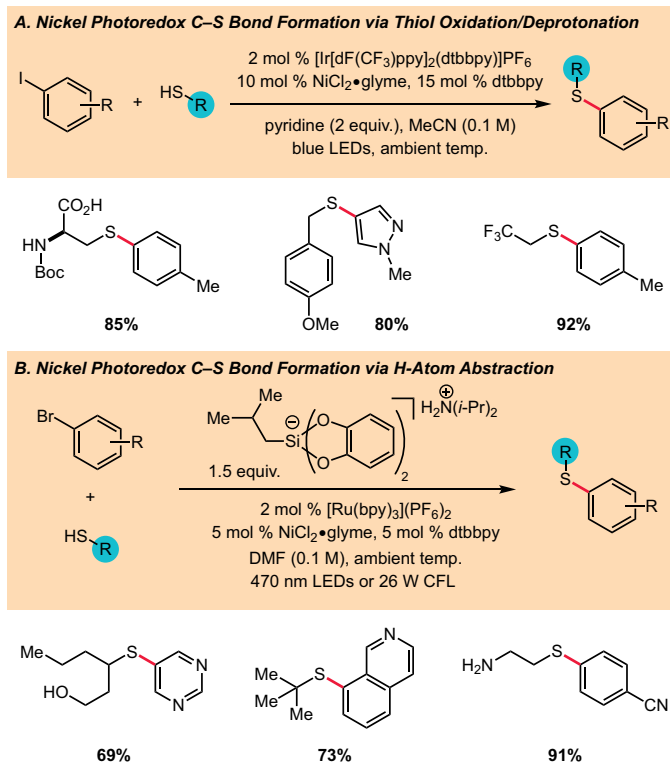


Figure 31. Metallaphotoredox C–S Bond Formation

VII. Late-Stage Functionalization and Trifluoromethylation

Late-Stage C–H Functionalization: Photoredox Minisci Chemistry

Another field that has been recently impacted by photoredox catalysis is late-stage functionalization of heterocyclic systems. In part this is due to the potentially beneficial effects that incorporation of groups such as methyl,¹²⁴ hydroxymethyl,¹²⁵ and fluorine¹²⁶ can have on relevant properties of a biologically active molecule. A common strategy deployed by MacMillan,^{127,128} DiRocco,⁶⁰ and Krska⁶¹ for late-stage C–H functionalization of heteroaromatic substrates was the Minisci reaction and the use of photoredox catalysis to access key alkyl radical species. As shown in **Figure 32**, one can achieve C–H alkylation, hydroxymethylation, and α -oxyalkylation using this approach. Furthermore, many of the methods highlighted in this section share a common photocatalyst, $[\text{Ir}[\text{dF}(\text{CF}_3)\text{ppy}]_2(\text{dtbbpy})]\text{PF}_6$, and radical formation strategy. Alkyl radicals are produced from perester precursors by perester protonation and reduction (by $^*\text{Ir}^{\text{III}}$), followed by decomposition to, and β -scission of, an intermediate O-centered radical to form an alkyl radical and acetone. Similarly, for hydroxymethylation, electron transfer (from $^*\text{Ir}^{\text{III}}$) to benzoyl peroxide produces $\bullet\text{Ph}$ after decomposition. Hydrogen atom transfer with methanol produces benzene and the hydroxymethyl radical, which then engages the heterocyclic substrate. Finally, α -oxy radical species are accessible from ether precursors through a HAT pathway. Persulfate reduction (by $^*\text{Ir}^{\text{III}}$) forms the sulfate anion radical, which is then used to generate the α -oxy alkyl radical via HAT. Two key factors govern selectivity in the latter two HAT pathways. Firstly, the lower bond dissociation enthalpies (BDEs) of the α -heteroatom CH bonds, relative to other unactivated C–H or O–H bonds present in the molecule, renders HAT with these C–H bonds more thermodynamically favorable. Secondly, electrophilic heteroatom-centered radicals, such as the sulfate radical anion, show a strong kinetic preference for abstraction of the most electron-rich C–H bond, likely due to favorable electrostatic interactions in the transition state.¹²⁹ As a result, in the Minisci protocol outlined by MacMillan and co-workers (using sulfate radical anions as the HAT catalyst), the authors observe selective functionalization of stronger, electron-rich α -oxy C–H bonds over weaker, acidic C–H bonds (e.g. α -carbonyl C–H bonds) present in the same molecule.

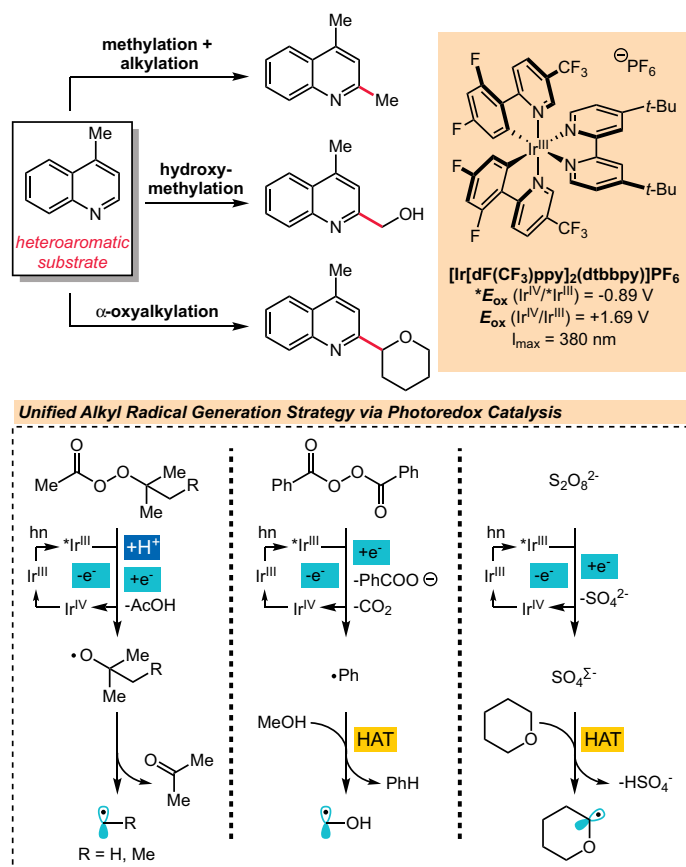


Figure 32. Photoredox Minisci Chemistry: Unified Approach

DiRocco and co-workers reported the late-stage methylation and alkylation of heterocyclic drug-like compounds using a perester (e.g. *t*-butylperacetate) and $[\text{Ir}[\text{dF}(\text{CF}_3)\text{ppy}]_2(\text{dtbbpy})]\text{PF}_6$ under acidic conditions (**Figure 33A**).⁶⁰ The alkylated products were isolated in good yields, occasionally alongside a separable bisalkylated product. The use of drug-like substrates with this system highlighted the utility and functional group tolerance of this transformation.

MacMillan and co-workers showed alkylation of *N*-heterocycles could be accomplished using alcohols as alkylating agents through a spin-center shift process (**Figure 33B**).¹²⁸ This elegant system utilizes a thiol HAT cocatalyst, $[\text{Ir}(\text{ppy})_2(\text{dtbbpy})]\text{PF}_6$ catalyst, acidic conditions, and produces water as a byproduct. The scope of the transformation with respect to the heteroaromatic substrate and alcohol alkylating agent was broad, and yields were generally high.

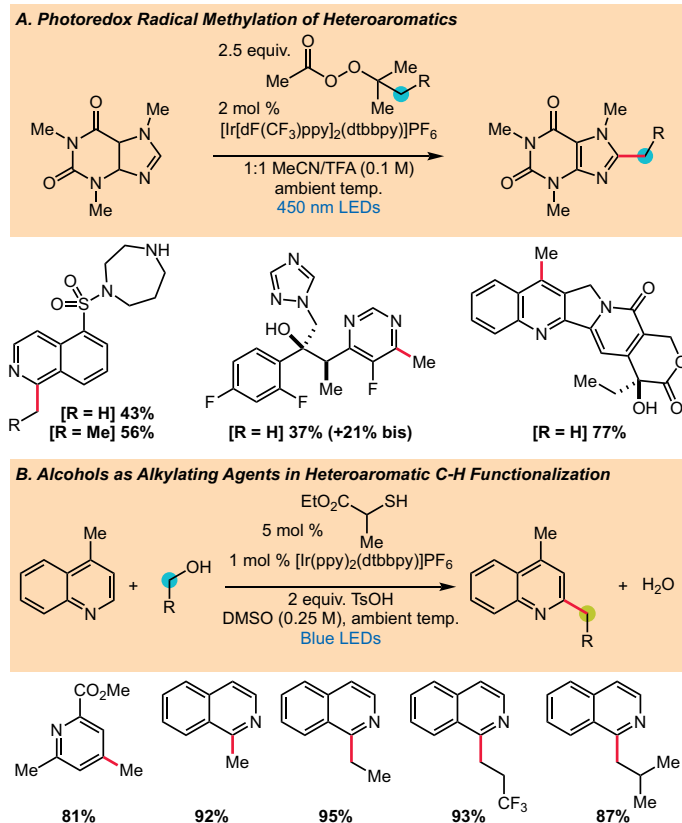


Figure 33. Alkylation of Heteroaromatic Substrates

Common Conditions for Heteroaromatic C-H Alkylation with Alcohols

- **Solvent:** DMSO (0.25 M), degassed and anhydrous. Alternative competent solvents: MeCN, DMF, DMA.
- **Stoichiometry:** For methylation, a large excess of methanol is preferable (50-100 equiv.). For other alcohol substrates, 10 equiv. of alcohol are typically employed although lower quantities (2-5 equiv.) can be used by extending the reaction time.
- **Photoredox catalyst:** [Ir](ppy)2(dtbbpy)PF6 (1 mol %)
- **Thiol catalyst:** ethyl 2-mercaptopropionate, methyl thioglycolate or 2,2,2-trifluoroethanethiol (5 mol %).
- **Acid:** TsOH (2 equiv.) usually provides the highest reaction efficiency. Alternative competent acids: conc. H2SO4, HBF4 (48 wt% in H2O).
- **Reaction setup:** Degas by sparging the reaction mixture with nitrogen for 10 minutes. Thiol catalyst and volatile alcohols should be added after degassing.
- **Irradiation:** Three double density sapphire blue LED strips wrapped inside a recrystallization dish (2 cm between vial and LEDs), ambient temperature (fan cooling), 20 to 48 h

Notes, Tips, and Troubleshooting

Low conversion: The identity of the best thiol catalyst varies with substrate and evaluation of a range of catalysts can aid reaction optimization.

- **Ethyl 2-mercaptopropionate:** best for methylation of a range of heteroaromatics.
- **Methyl thioglycolate:** best for reactions that employ a lower excess of the alcohol component (5-10 equiv.).

Tips for Improving Low Yielding Reactions

- **Thiol catalyst:** For challenging substrates, increased quantities of thiol catalyst (10-20 mol %) can improve the reaction yield.
- **Acid equivalents:** Increasing the equivalents of acid (3 equiv.) can improve the yield of alkylation for challenging substrates.
- **Reaction concentration:** Dilution of the reaction conditions is often beneficial for reaction efficiency.
- **Alcohol equivalency:** Increasing the number of equivalents of the alcohol component typically improves the yield.

Tip: If formation of the hydroxymethylated product is observed (*i.e.* wherein spin-center shift has not occurred), reduction to the alkylated product can be achieved by treating the hydroxymethylated product with [Ir](ppy)2(dtbbpy)PF6, TsOH (2 equiv.), and Bu3N-HCO2H (2 equiv.) in DMSO under irradiation with blue light.

Product Description	Product Number
<i>tert</i> -Butyl peracetate	388076 (solution, 50% wt)
<chem>[Ir](dF(CF3)ppy)2(dtbbpy)PF6</chem>	747793
Ethyl 2-mercaptopropionate	W327905
Methyl thioglycolate	108995
2,2,2-Trifluoroethanethiol	374008
<chem>[Ir](ppy)2(dtbbpy)PF6</chem>	747769

The late-stage hydroxymethylation of complex drug-like heteroaromatic systems was achieved by Krska and co-workers using benzoyl peroxide, [Ir](dF(CF3)ppy)2(dtbbpy)PF6, and methanol under acidic conditions (**Figure 34A**).⁶¹ The hydroxymethylated products were generally isolated in good yields, again occasionally alongside a separable bisalkylated product. Functional group tolerance was high, as exhibited by the use and successful functionalization of complex substrates with this system.

MacMillan and co-workers also showed general α -oxyalkylation of heterocyclic substrates, using alkyl ethers as radical precursors (**Figure 34B**).¹²⁷ Acidic conditions, the photoredox catalyst [Ir](dF(CF3)ppy)2(dtbbpy)PF6, sodium persulfate, and a 26 W CFL were used to effect the transformation shown. Structurally diverse ethers were coupled to substituted heterocyclic substrates in high yields. Volatile ether building blocks such as oxetane, diethyl ether, tetrahydrofuran, and dioxolane were tolerated in this ambient temperature coupling.

Radical Trifluoromethylation Protocols Enabled by Photoredox Catalysis

The strategic installation of fluorine or fluorine-containing groups, such as the trifluoromethyl group, is a tactic deployed in the pharmaceutical and agrochemical sectors to tune relevant properties of biologically active molecules. Properties that fluorination can impact include pK_a , metabolic stability, and lipophilicity.¹²⁶ As such, synthetic methods that enable the late-stage incorporation of fluorine-containing groups are beneficial for the design of biologically active species. Towards this end, many groups have stepped up to develop novel trifluoromethylation protocols, including (but not limited to) aryl trifluoromethylation,^{130,131} vinyl trifluoromethylation,^{132,133} and heterocycle trifluoromethylation.¹³⁴ Photoredox catalysis has impacted the field through the development of redox neutral radical trifluoromethylation strategies. The diversity of possible products is shown below in **Figure 35A** while **Figure 35B** shows how these methods are united through the intermediacy of the trifluoromethyl radical ($\bullet\text{CF}_3$). Trifluoroiodomethane, trifluoromethanesulfonyl chloride, Umemoto's reagent, Togni's reagent, and the shown trifluoroacetoxy pyridinium salt accept an electron and fragment to $\bullet\text{CF}_3$ and SO_2 and $\bullet\text{CF}_3$ (**Figure 36B**). Methods such as innate arene trifluoromethylation,^{69,135,136} trifluoromethylation of boronic acids,¹³⁷ alkene hydrotrifluoromethylation,^{136,138,139} alkene oxytrifluoromethylation,¹⁴⁰ hydrotrifluoromethylation of alkynes,^{136,138} vinyl trifluoromethylation,¹⁴¹ and aldehyde α -trifluoromethylation¹⁴² have been developed to complement existent systems. Again, it is advisable for practitioners to first make use of the reported conditions for the reaction of interest. Consult the referenced articles for optimized conditions for each trifluoromethylation protocol.

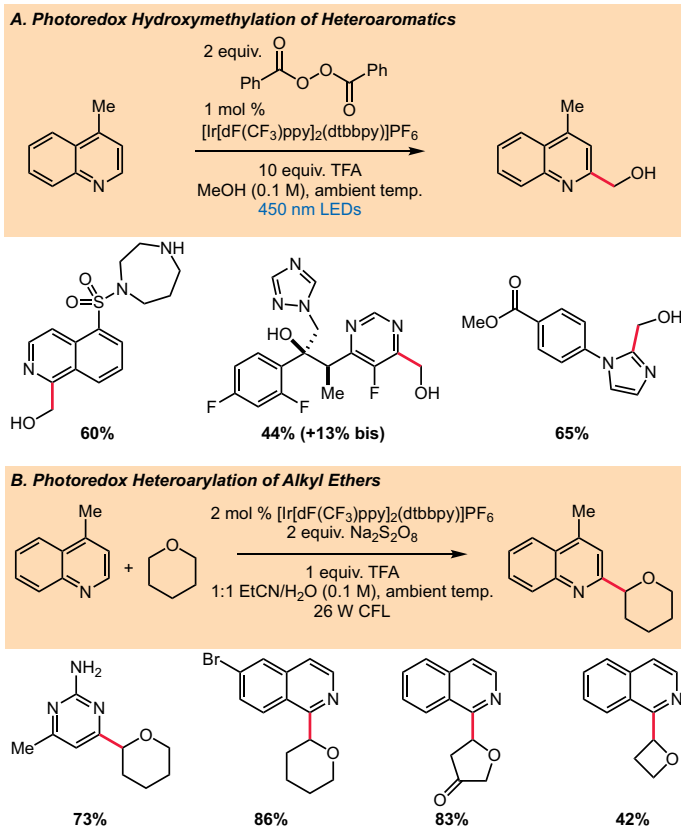
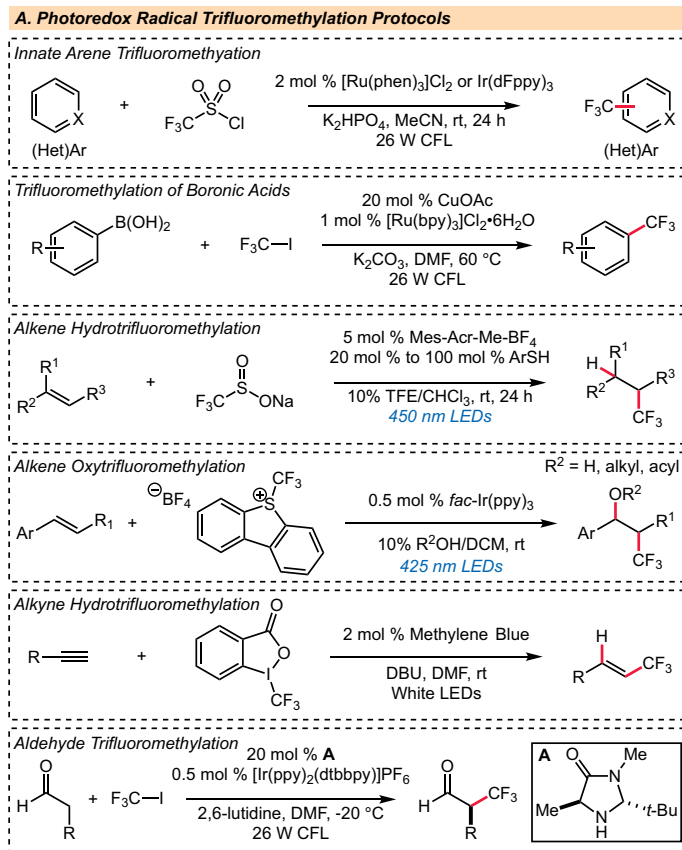


Figure 34. Expanded Scope of Photoredox Minisci Chemistry: Alcohol and Ether Radical Precursors^a

Product Description	Product Number
$[\text{Ir}[\text{d}(\text{CF}_3)\text{ppy}]_2(\text{dtbbpy})]\text{PF}_6$	747793
Dibenzoyl peroxide	179981
Sodium persulfate	216232



B. Photochemical Generation of Trifluoromethyl Radical

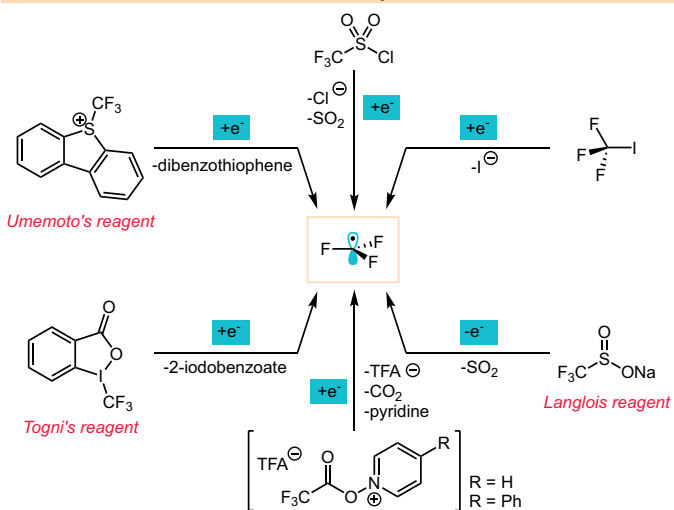
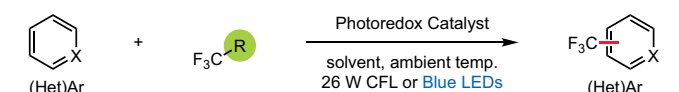


Figure 35. Radical Trifluoromethylation Strategies

A strategy to access trifluoromethylated arenes that obviates the need for substrate prefunctionalization is the innate C–H trifluoromethylation of aromatic compounds. This late-stage radical trifluoromethylation strategy was separately disclosed by MacMillan¹³⁵ and Stephenson,^{69,70} each using unique •CF₃ precursors (Figure 36). MacMillan utilized trifluoromethanesulfonyl chloride (Conditions A and B, below), while Stephenson used a trifluoroacetoxypyridinium salt generated *in situ* from pyridine *N*-oxide (or 4-phenylpyridine *N*-oxide) and trifluoroacetic anhydride (Conditions C, below). Both precursors generate •CF₃ upon reduction by the

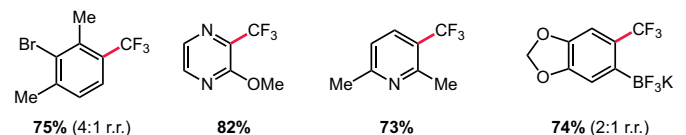
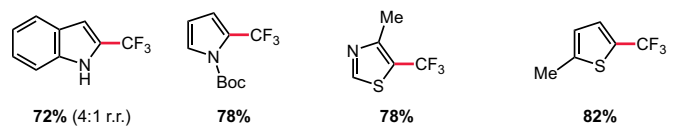
photoredox catalyst and fragmentation (Figure 36B). The MacMillan protocols were found to be effective for arenes as well as electron-rich or electron-deficient heteroarenes and the Stephenson protocols were found to be effective for the trifluoromethylation of electron-rich or electron-neutral arenes or heteroarenes, as shown in Figure 37B. Functional groups such as esters, carbamates, bromides, potassium trifluoroborates (BF₃K), and *N*-methyliminodiacetic acid boronates (MIDA) were retained over the course of these transformations and, in some cases, bis-alkylation was observed. Additionally, the method developed by Stephenson and co-workers (Conditions C) allows one to investigate other perfluoroalkyl groups by replacing trifluoroacetic anhydride with alternative fluorine-containing anhydrides, such as with pentafluoropropionic anhydride for pentafluoroethylation. The development of multiple complimentary aryl C–H trifluoromethylation methods allows one to access an extensive range of products, as each method has its strengths (e.g. using Condition B for pyridine derivatives rather than A or C).

A. Innate Arene Trifluoromethylation



Conditions A	Conditions B	Conditions C
electron-rich heteroarenes	electron-deficient heteroarenes and arenes	electron-rich and neutral arenes or heteroarenes
2 equiv.	2–4 equiv.	1–4 equiv. [R = H or Ph]
2 mol % [Ru(phen) ₃]Cl ₂	1–2 mol % Ir(dFppy) ₃	0.1–1 mol % [Ru(bpy) ₃]Cl ₂
K ₂ HPO ₄ , MeCN, rt 26 W CFL	K ₂ HPO ₄ , MeCN, rt 26 W CFL	MeCN, rt 13 W Blue LEDs

B. Examples - Conditions A



Examples - Conditions C

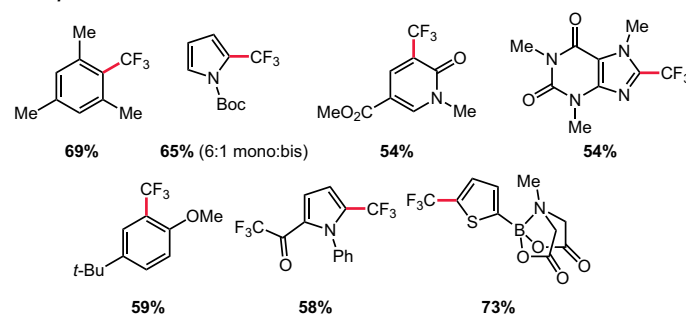


Figure 36. Innate Trifluoromethylation of Arenes and Heteroarenes

Common Conditions for Trifluoromethylation with Triflyl Chloride

- **Solvent:** MeCN (0.125 M), degassed and anhydrous.
- **Stoichiometry:** 2 equiv. triflyl chloride should be employed for electron-rich heteroaromatics and non-heteroarenes. When using electron-deficient heteroarenes, 4 equiv. triflyl chloride is required. Using a larger excess of triflyl chloride can result in bis-trifluoromethylation of certain substrates.
- **Photoredox catalyst:** For electron-rich heteroaromatics, [Ru(phen)₃]Cl₂ is the optimal catalyst. For other arenes and electron-deficient heteroarenes, Ir(Fppy)₃ is optimal.
- **Reaction setup:** Degas via three cycles of freeze-pump-backfill-thaw. Triflyl chloride should be added after degassing.
- **Irradiation:** 26 W CFL lamp (2 cm distance between lamp and the reaction vessel). Comparable efficiency has been observed using higher power Kessil blue LED lamps.

Regioselectivity: The site of trifluoromethylation is typically the most electron-rich position in the molecule. When both ortho- and para- functionalization is possible a mixture of products favoring ortho-substitution is typically obtained (2:1 to 5:1 *o:p*). When multiple electronically similar aryl C-H bonds are present in the molecule, it is likely a mixture of products will be obtained.

Functional group tolerance: Alkyl amines must be protected *in situ* through the addition of 1.2 equiv. of HCl (no drastic variation in yield is typically seen between different sources of HCl). Highly Lewis basic pyridines can be problematic, often necessitating the use of a large excess of triflyl chloride (8 equiv.). Carboxylic acids, alcohols, protected amines, amides, aldehydes, esters, aryl halides and BF₃K salts are all well tolerated.

Product Description	Product Number
[Ru(phen) ₃]Cl ₂	343714
<i>fac</i> -Ir(dFppy) ₃	900540
[Ru(bpy) ₃](PF ₆) ₂	754730
Trifluoromethanesulfonyl chloride	164798
Trifluoroacetic anhydride	106232
Pentafluoropropionic anhydride	252387
Pyridine- <i>N</i> -oxide	131652
4-Phenylpyridine- <i>N</i> -oxide	183490
K ₂ HPO ₄	P3786

A strategy for accessing trifluoromethylated alkanes is through alkene hydrotrifluoromethylation. Mild and operationally simple photoredox alkene hydrotrifluoromethylation methods were separately disclosed by Gouverneur (**Figure 37A**)¹³⁸ and Nicewicz (**Figure 37B**)¹³⁹ in 2013. The Gouverneur protocol was shown to be effective for aliphatic alkene and alkyne substrates, while the Nicewicz method was shown to be effective for aliphatic alkene and styrene substrates. Alkene hydrotrifluoromethylation was achieved by Nicewicz and co-workers using sodium trifluoromethanesulfinate (Langlois reagent) and an organic photoredox system comprised of an acridinium photoredox catalyst (Mes-Acr-Me-BF₄) and a thiol H-atom donor in TFE/CHCl₃ (**Figure 37B**).¹³⁹ Mono-, di-, and trisubstituted aliphatic alkenes bearing a variety of functional groups afforded the desired trifluoromethylated products in high yields and regioselectivity (**Figure 37C**). Additionally, styrenyl alkenes participated in the transformation, as shown in **Figure 38C**, albeit under modified reaction conditions. The addition of 20 mol % methyl thiosalicylate was sufficient to achieve high yields with aliphatic alkenes in TFE/CHCl₃, while 100 mol % thiophenol was required for styrenyl substrates in order to suppress oligomerization pathways and achieve good yields.

Hydrotrifluoromethylation Common Conditions

- **Solvent:** 10 % TFE (v/v) in CHCl_3 (0.2 M, degassed and anhydrous). TFE is required to obtain high yields, this is because TFE may participate as a H-atom donor or in H-atom donor regeneration.¹³⁹

- **Langlois Reagent:** 1.5 equiv. to 3 equiv.

- **Photoredox catalyst:** Mes-Acr-Me- BF_4 (5 mol %)

- **Hydrogen atom donor:**

- Methyl thiosalicylate (20 mol %) for aliphatic alkene substrates.

- Thiophenol (100 mol %) for styrenyl substrates.

- Probe thiol electronic effects and loading if a reaction is unproductive (e.g. undesired competitive processes).

- **Irradiation:** 450 nm blue LED lamps, ambient temperature, 24 h.

Functional group tolerance: Functional groups such as free alcohols, esters, tosylates, silyl ethers, carbamates, and phthalamides were retained during the transformation and products were obtained in good to high yields.

Regioselectivity: Alkene hydrotrifluoromethylation often delivers products with high regioselectivity. Trifluoromethyl radical addition typically occurs at the site resulting in the formation of the most stable intermediate carbon-centered radical (preceding H-atom transfer). When substrate positional differences are minimal (such as in some 1,2-disubstituted aliphatic alkenes) product mixtures are possible.

Low yield or incomplete conversion of substrate:

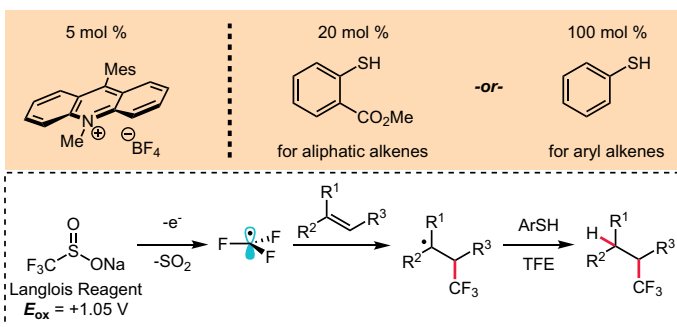
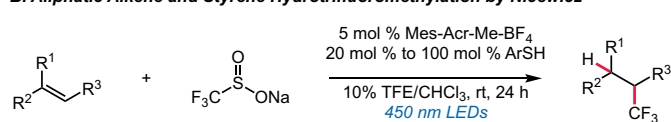
Low yielding reactions may benefit from increased reaction times, manipulating thiol H-atom donor loading, tuning thiol H-atom donor properties/electronics (for example, the beneficial effects observed moving from methyl thiosalicylate to thiophenol for styrenyl substrates), or altering the sodium trifluoromethanesulfinate loading.

Product Description	Product Number
Mes-Acr-Me- BF_4	794171
Methyl thiosalicylate	357758
Thiophenol	240249
2,2,2-Trifluoroethanol	T63002
Sodium trifluoromethanesulfinate	367907

A. Alkene and Alkyne Hydrotrifluoromethylation by Gouverneur



B. Aliphatic Alkene and Styrene Hydrotrifluoromethylation by Nicewicz



C. Hydrotrifluoromethylation Examples

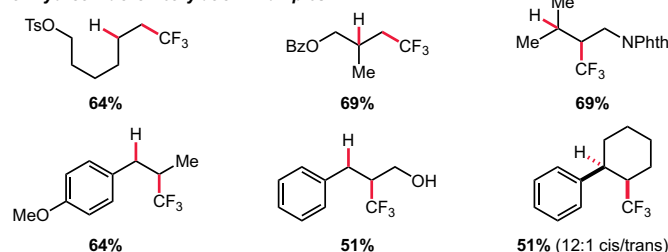


Figure 37. Hydrotrifluoromethylation of Alkenes and Styrenes

VIII. Alkene and Arene Functionalization Using Organic Photoredox Systems

A core focus of research in the Nicewicz laboratory is synthetic method development through organic photoredox catalysis. Reactive radical ion intermediates such as alkene and arene cation radicals can be accessed from alkene and arene substrates, respectively using strong photooxidants, such as acridinium and pyrylium photoredox catalysts. Leveraging the reactivity of radical ion intermediates, a suite of methods for the direct functionalization of alkenes and arenes, as well as other challenging bond constructions, have been published and are highlighted below.

Anti-Markovnikov Hydrofunctionalization of Alkenes

Photoredox catalysis has emerged as a powerful tool for alkene hydrofunctionalization. Single electron oxidation of an electron-rich alkene substrate renders the substrate reactive towards nucleophiles and results in umpolung reactivity (**Figure 38**).^{9,143} Furthermore, this pathway generates hydrofunctionalization products with anti-Markovnikov selectivity, complimentary to established Markovnikov-selective acid-catalyzed processes (**Figure 1B**).

Photoredox anti-Markovnikov hydrofunctionalization systems contain an oxidizable alkene substrate, a heteroatom nucleophile (intra- or intermolecular), and a dual catalytic system comprised of an acridinium photooxidant and a redox-active hydrogen atom donor cocatalyst (**Figure 38**).^{143,144} The reaction proceeds by excitation of the acridinium catalyst, followed by electron transfer with the olefin donor to generate the key cation radical intermediate. The nucleophile then engages the cation radical intermediate, with regioselectivity governed by distonic cation radical stability,^{143,145} and finally the desired product is furnished by hydrogen atom transfer from the hydrogen atom donor (HAD, thiophenol shown). A redox event between the persistent acridine radical and the transient thiyl radical ($\Delta E = +0.73$ V) regenerates the ground state acridinium catalyst and concomitant thiolate protonation regenerates the HAD.¹⁴⁴ Thiophenol

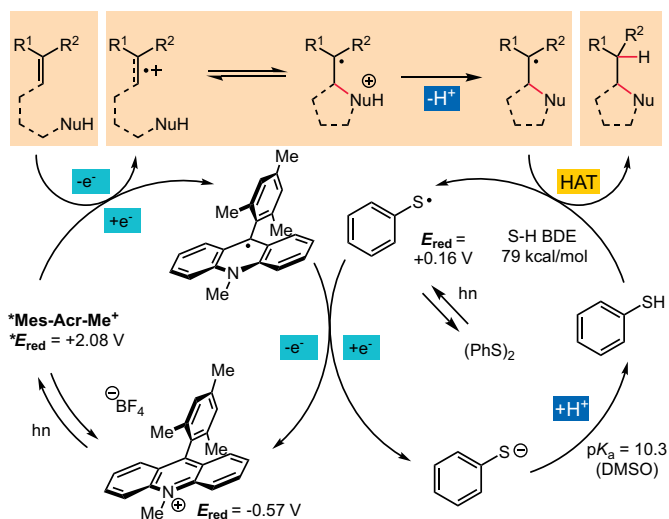
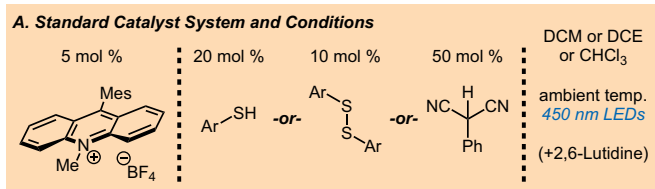


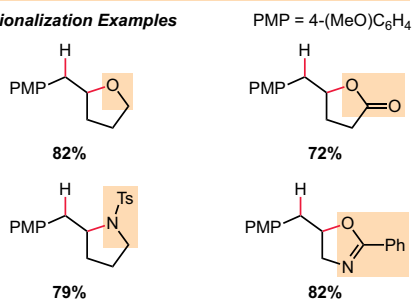
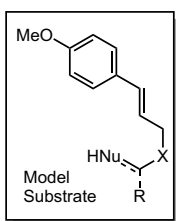
Figure 38. Catalytic Photoredox anti-Markovnikov Alkene Hydrofunctionalization

derivatives were found to be highly effective HAD cocatalysts (high yields, low catalyst loadings, lower reaction times),^{146,75} however aryl disulfides (which cleave upon irradiation),^{144,147} and 2-phenylmalononitrile (2-PMN)⁹ have also been used.

Common conditions are shown in **Figure 39A**, namely; catalytic loadings of an acridinium photocatalyst and HAD cocatalyst, use of a chlorinated solvent, and irradiation at ambient temperature with blue LED lamps. Hydroetherification,⁹ hydrolactonization,⁹ hydroamination,¹⁴⁶ and oxazoline synthesis¹⁴⁸ have been studied for intramolecular systems (**Figure 39B**). For intermolecular hydrofunctionalization, diverse nucleophile scope has been shown (**Figure 39C**): alcohols,⁹ carboxylic acids,⁷⁵ sulfonamides,¹⁴⁷ *N*-heterocycles/azoles,¹⁴⁷ sulfonic acids,⁴⁵ phosphoric acids,⁴⁵ chloride,⁴⁵ and fluoride⁴⁵ all furnish products in high yields and regioselectivity. See the referenced reports to view the optimization studies, and final conditions, that enabled each of these transformations as well as investigations into nucleophile and alkene scope.



B. Intramolecular Hydrofunctionalization Examples



C. Intermolecular Hydrofunctionalization Examples

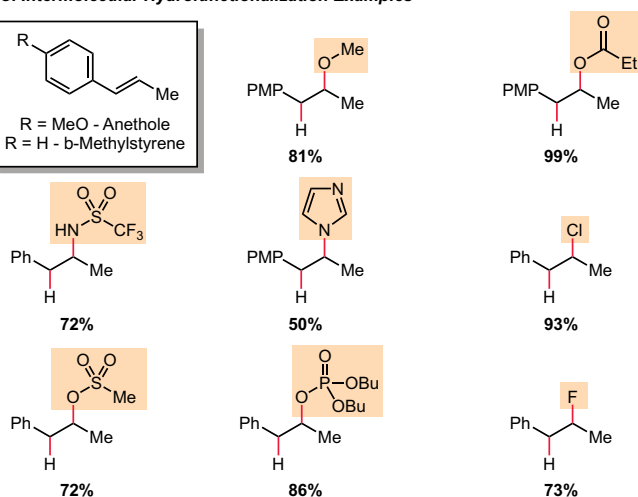
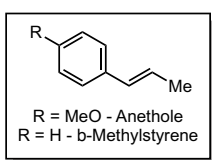


Figure 39. Examples of Photoredox Alkene Hydrofunctionalization

Common Conditions

- **Solvent:** DCM, DCE, or CHCl_3 (0.25 M to 0.5 M), degassed and anhydrous. 2.5:1 CHCl_3/TFE for hydrochlorination with lutidinium•HCl.
- **Intermolecular nucleophiles:** in excess, from 1.5 equiv. to 10 equiv. relative to alkene substrate.
 - Hydroetherification: 10 equiv. alcohol
 - Hydroacetoxylation: 10 equiv. carboxylic acid
 - Hydroamination: 1.5 equiv. sulfonamide or azole heterocycle
 - Hydrochlorination: 2 equiv. lutidinium•HCl or HCl generated *in situ* from TFE and pivaloyl chloride
 - Hydrooxysulfonylation: 2 equiv. lutidinium sulfonate salt
 - Hydroxyphosphorylation: 2 equiv. phosphoric acid or 2 equiv. lutidinium phosphate salt
 - Hydrofluorination: 1-2 equiv. $\text{Et}_3\text{N}\cdot 3\text{HF}$

- **Photoredox catalyst:** Mes-Acr-Me- BF_4 (2.5 mol % to 5 mol %)
- **Hydrogen atom donor:** thiophenol (20 mol %), phenyl disulfide (10 mol %) or a derivative thereof. 2-phenylmalononitrile (50 mol %) or a thiol HAD when using alkenols/alcohol nucleophiles.
- **Base:** 10 mol % to 25 mol % 2,6-lutidine (distilled and stored under inert atmosphere) for acidic nucleophiles such as carboxylic acids, phosphoric acids, or HCl. Preformed lutidinium salts can also be used (see **Tip**).
- **Irradiation:** 450 nm blue LED lamps, ambient temperature, 4 to 24 h.

The above conditions represent good, general, starting points for anti-Markovnikov alkene hydrofunctionalization. Practitioners are ultimately advised to begin with the optimized conditions for the transformations of interest (from the published reports) and make necessary changes from there.

Notes, Tips, and Troubleshooting

No reaction: Ensure that the oxidation potential of the olefin substrate lies within the acridinium redox window.

Low conversion: Ensure complete irradiation of the reaction(s).

Low conversion: If one suspects photocatalyst decomposition by means of nucleophilic or radical deactivation, use a more robust catalyst with substitution on the acridinium core such as Mes- $\text{Me}_2\text{Acr-Ph-BF}_4$ or Mes-(*t*- Bu_2)Acr- Ph-BF_4 .^{14,45,149} For example, deactivation was observed in alkene hydrofluorination optimization. Yields were rescued by using Mes- $\text{Me}_2\text{Acr-Ph-BF}_4$ in place of Mes-Acr-Me- BF_4 . See Supplementary Table 1 for examples of alternative acridinium photocatalysts.

No reaction or low conversion: The nature of the hydrogen atom donor cocatalyst can have a profound effect on reaction efficiency. Thiophenol substitution can impact S-H BDE, $\text{p}K_a$, and redox properties. As such, screening electronically (or sterically) diverse HAD derivatives can lead to improved reaction conditions.

- **PhSH (or Ph_2S_2):** best for hydroacetoxylation, hydroamination (using azoles and sulfonamides).
- **4-methoxythiophenol:** best for hydrochlorination and sulfonic acid addition.
- **4-nitrophenyl disulfide:** best for hydrofluorination using $\text{Et}_3\text{N}\cdot 3\text{HF}$.

Tip: Aryl disulfides can be used as HAD precursors in place of thiophenol derivatives. Aryl disulfides cleave to thiyl radicals upon irradiation (assuming sufficient spectral overlap with the light source) and may be attractive as they are more easily handled.

Tip: Strongly acidic species such as HCl, sulfonic acids, and phosphoric acids can be prepared and used as lutidinium salts.⁴⁵

Product Description	Product Number
Mes-Acr-Me-Bf ₄	794171
Mes-Me ₂ Acr-Ph-Bf ₄	793876
Thiophenol	240249
Phenyl disulfide	169021
4-Methoxythiophenol	109525
4-Nitrophenyl disulfide	N21022
2,6-Lutidine	336106

Complementary heteroatom-centered radical mediated anti-Markovnikov alkene hydrofunctionalization methods have also been developed (Figure 40). These methods proceed through thiol/amine oxidation to a heteroatom-centered radical rather than alkene oxidation to the alkene cation radical. Knowles and co-workers disclosed an alkene hydroamination system utilizing secondary amines, an iridium photocatalyst ([Ir(dF(Me)ppy)₂(dtbbpy)]PF₆), and a thiol HAD cocatalyst (Figure 40A).¹⁵⁰ This system relies on oxidation of the secondary amine to an aminium radical cation, which then goes on to intercept the alkene substrate. HAT from the thiol cocatalyst (trapping an intermediate carbon-centered radical) then forms the product. The Yoon and Stephenson laboratories separately described the photoredox anti-Markovnikov hydrothiolation of alkenes leveraging *in situ*-generated thiyl radicals (the radical thiol-ene reaction, Figure 40B).¹⁵¹⁻¹⁵³ The two strategies differ mechanistically with regard to thiyl radical formation, but ultimately converge on thiyl radical addition to the alkene substrate and propagation via H-atom abstraction from another thiol equivalent. Substrate scope was broad for all systems, consult the referenced articles for detailed protocols.

A. C-N Bond Formation Via Aminium Radical Cation Generation



B. C-S Bond Formation Via Thiyl Radical Generation



Figure 40. Heteroatom-Centered Radical Mediated Alkene Hydrofunctionalization

Aryl C-H Amination Using an Acridinium/TEMPO Photoredox System and Aryl C-H Cyanation

The direct C-H amination of electron-rich arenes was achieved through the use of an acridinium photooxidant/TEMPO catalyst system.¹⁴ This azole coupling technology enables the facile construction of complex heterocyclic frameworks and represents another example of photoredox late-stage functionalization (Figure 41). The intermediacy of an arene cation radical is invoked via direct substrate oxidation with excited state acridinium photooxidant *Mes-(*t*-Bu)₂Acr-Ph-BF₄.¹³ After SET the ground state catalyst is regenerated by O₂ reduction, forming superoxide (Figure 41). The *N*-nucleophile then engages the arene cation radical, which forms the depicted delocalized radical intermediate after deprotonation. While product is formed in the absence of TEMPO (presumably through the intervention of O₂ as this process is net oxidative, shown), yields are higher when TEMPO is included in catalytic quantities (20 mol %). The reason for this improvement may be twofold: TEMPO may play a role in product rearomatization via H-atom abstraction and TEMPO-H may scavenge reactive oxygen-centered radicals produced over the course of the reaction (such as superoxide and hydroperoxyl radical).¹⁴

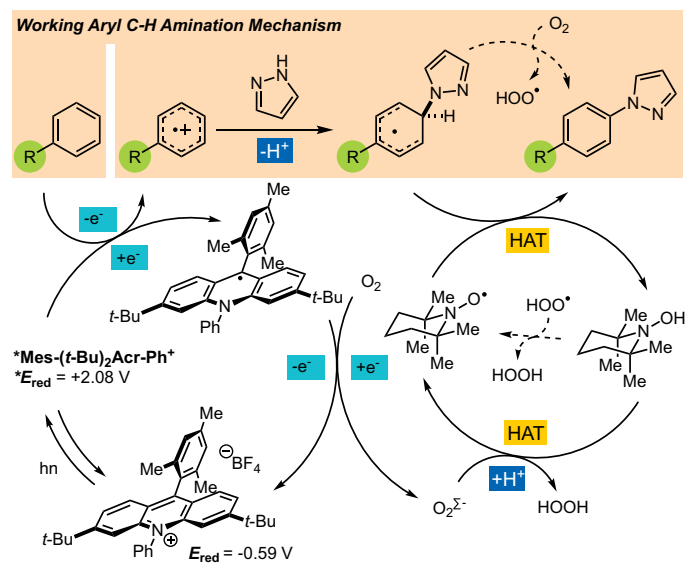


Figure 41. Working Mechanism for the Organic Photoredox C-H Amination of Arenes

Arene amination reactions are run under an O₂ atmosphere and standard conditions are displayed in **Figure 42A**. The shown substituted acridinium catalyst (see **Figure 41**) was found to be more stable under the reaction conditions, resulting in higher yields. With respect to the arene and amine nucleophile, the scope of the reaction is broad (**Figure 42B**). Substitution was tolerated at all positions of the arene substrate and complex heterocyclic substrates participated cleanly in the reaction. The arene oxidation potential should not exceed the catalyst excited state reduction potential, so electron-rich arenes work best. Azole nucleophiles including imidazole, pyrazole, benzimidazole, and triazole species participated in the transformation. Additionally, direct aniline synthesis from arene substrates was accomplished using ammonium carbamate (4 equiv.) in place of an azole nucleophile. This approach enabled the synthesis of aniline building blocks in good yields and shows that these transformations could potentially open new areas of chemical space. Practitioners are again advised to first utilize the published optimized conditions for the transformation of interest and then make any relevant changes.

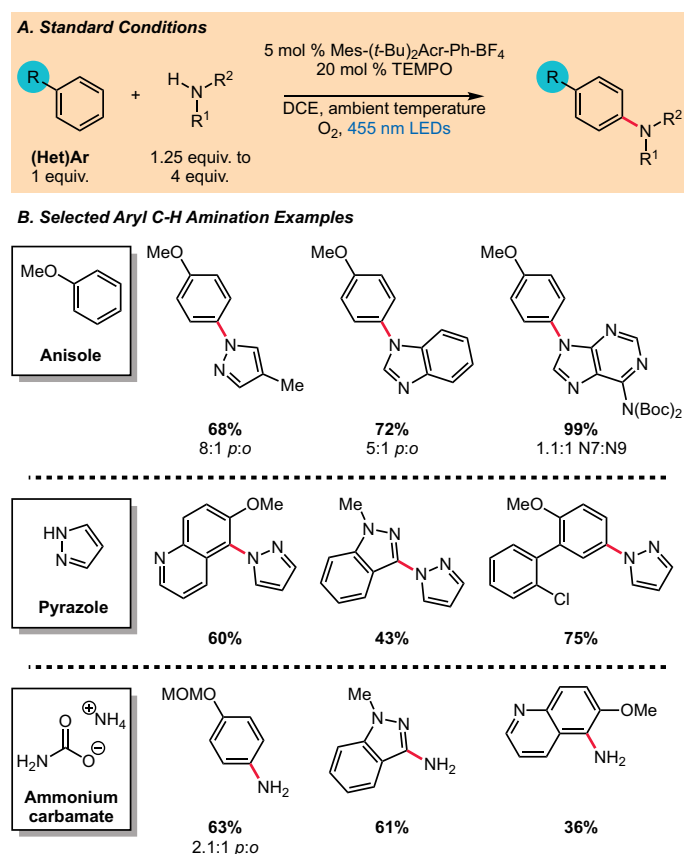


Figure 42. Standard Conditions and Selected Scope for Aryl C–H Amination Chemistry

Common Conditions

- **Solvent:** DCE or DCM (0.1 M, anhydrous). 10:1 DCE/H₂O when using ammonium carbamate.
- **Nucleophiles:** 1.25 equiv. to 2 equiv. for azoles, 4 equiv. for ammonium carbamate. In some systems inverted stoichiometry resulted in higher yields (e.g. with mesitylene, see **Note** below).
- **Catalyst:** Mes-(*t*-Bu)₂Acr-Ph-BF₄ (5 mol %)
- **Cocatalyst:** 20 mol % TEMPO. Immobilized TEMPO (20 mol %) can also be used.
- **Atmosphere:** Reactions sparged for 5 minutes with O₂ before irradiation. O₂ balloon retained during the reaction to maintain 1 atm O₂ in the headspace.
- **Irradiation:** 450 nm blue LED lamps, ambient temperature, 20 to 72 h.

Notes, Tips, and Troubleshooting

Aryl C–H functionalization site selectivity: Nicewicz and coworkers conducted a thorough investigation of the site selectivity for this reaction paradigm, studying a range of nucleophiles and (hetero)aryl substrates. The resulting data was used to develop a predictive model for site selectivity. Consult the referenced article for more details.¹⁵⁴

No reaction or low conversion: Make sure that the oxidation potential of the arene substrate lies within the acridinium catalyst redox window if no product is formed. Also ensure complete irradiation of the reaction(s).

Tip: An atmosphere of air can be used in place of O₂ at the expense of reaction time.

Tip: Commercially available acridinium photooxidants Mes-Acr-Me-BF₄ and Mes-Me₂Acr-Ph-BF₄ catalyze this transformation but may result in lower yields. This is due to diminished catalyst stability under the reaction conditions. Use of Mes-Me₂Acr-Ph-BF₄ was demonstrated with dihydrocoumarin and mesitylene.

Alternative conditions for challenging substrates: Alkyl-substituted arenes (e.g. mesitylene, *m*-xylene) and imidazole nucleophiles are prone to oxidative degradation under the standard conditions. Oxygen-free conditions were developed for use when one of the coupling partners is susceptible to decomposition pathways: 1 equiv. TEMPO (or TEMPONium-BF₄), 1 atm. N₂, and excess arene (2 equiv.) relative to the azole nucleophile.

Product Description	Product Number
Mes-(<i>t</i> -Bu) ₂ Acr-Ph-BF ₄	900421
Mes-Me ₂ Acr-Ph-BF ₄	793876
TEMPO	214000

Aryl C–H Cyanation Using an Acridinium Photooxidant

The arene C–H functionalization manifold was extended to C–H cyanation through the use of Me_3SiCN as the latent cyanide source and an MeCN/phosphate buffer solvent system (**Figure 43A**).¹⁵⁵ An atmosphere of oxygen is required and significant solvent/cosolvent effects were observed (with 10% v/v pH 9 aqueous phosphate buffer/MeCN resulting in the highest yields). Protected alcohols, halides, alkenes, and esters are tolerated in this transformation, along with substituted aryl or heteroaryl substrates (**Figure 43B**). Product formation is proposed to arise from cyanide addition into an arene cation radical, analogous to the proposed C–H amination mechanism (**Figure 41**).

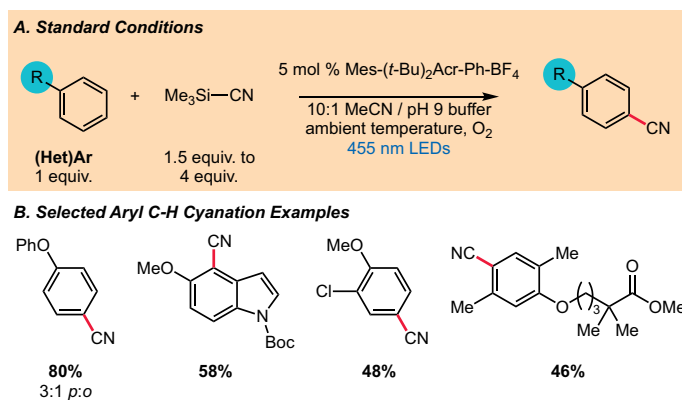


Figure 43. Aryl C–H Cyanation

Common Conditions

- **Solvent system:** MeCN (0.1 M), 10% v/v 4 M pH 9 aqueous phosphate buffer.
- **Nucleophile:** 1.5 equiv. to 4.0 equiv. Me_3SiCN .
- **Catalyst:** $\text{Mes-(}t\text{-Bu)}_2\text{Acr-Ph-BF}_4$ (5 mol %)
- **Atmosphere:** Reaction sparged for 5 minutes with O_2 before irradiation. O_2 balloon retained during reaction.
- **Irradiation:** 450 nm blue LED lamps, ambient temperature, 24 h.

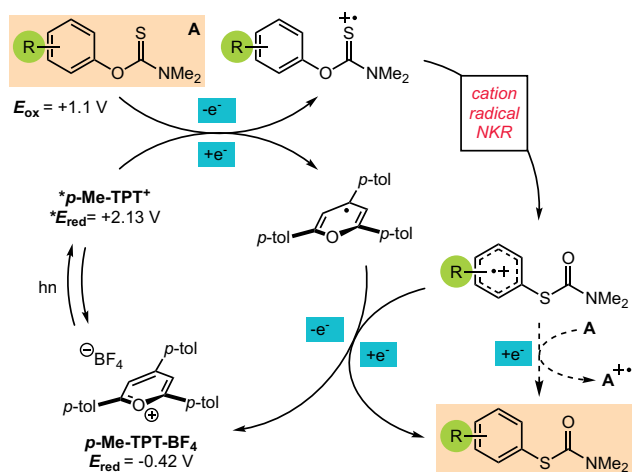
Aryl C–H functionalization site selectivity: Nicewicz and coworkers studied C–H cyanation along with C–H amination in the development of a C–H functionalization site selectivity predictive model. Consult the referenced article for more details on the model and (hetero)aryl substrates studied.¹⁵⁴

Product Description	Product Number
$\text{Mes-(}t\text{-Bu)}_2\text{Acr-Ph-BF}_4$	900421
Trimethylsilyl cyanide	212849

Pyrylium-Catalyzed Ambient-Temperature Newman-Kwart Rearrangement

The Newman-Kwart rearrangement (NKR) is an established strategy for the preparation of thiophenols from the corresponding phenol by means of an *O*-aryl carbamothioate intermediate.^{156,157} The thermal NKR proceeds via *ipso* nucleophilic attack of the thiocarbonyl moiety onto the arene at elevated temperatures, producing a strained spirocyclic intermediate. This ultimately gives way to *O* to *S* aryl migration, forming the product. The thermal rearrangement is most effective for electron-deficient arenes, however photoredox catalysis presented an opportunity to develop a complementary ambient temperature NKR method effective for electron-rich and neutral arenes (**Figure 44**).²⁹ This cation radical-accelerated NKR requires a pyrylium photoredox catalyst (*p*-Me-TPT⁺) and proceeds via oxidation of the thiocarbonyl moiety ($E_{\text{ox}} = +1.1$ V, $\Delta E = +1.03$ V, $\Delta G = -23.75$ kcal/mol) to the corresponding cation radical. From here, cation radical NKR furnishes an arene cation radical intermediate (**Figure 44A**) and single electron reduction of this species (either by the pyranil radical or via oxidation of another substrate equivalent) produces the rearrangement product.

A. Working Mechanism for Cation Radical-Accelerated NKR



B. Standard Conditions and Selected Examples

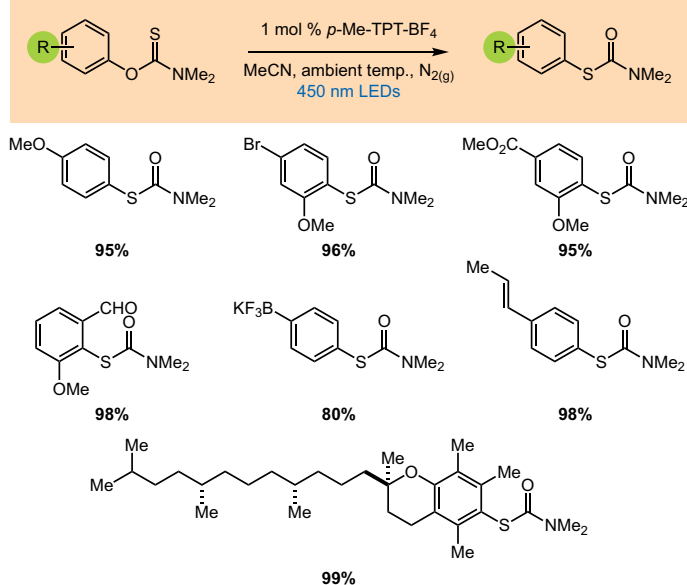


Figure 44. Cation Radical Accelerated Newman-Kwart Rearrangement

Standard reaction conditions are shown in **Figure 44B** and are listed below. The scope of the cation radical accelerated NKR was broad with respect to functional group tolerance as well as substitution on the arene. Cross-coupling functional handles (bromide and BF_3K groups) were retained over the course of the transformation, as well as other functional groups such as esters, aldehydes, and alkenes. Substitution at the *ortho*, *meta*, and *para* positions was studied and tolerated. This complimentary strategy for thiophenol synthesis enabled the synthesis of structurally diverse thiol HAD catalysts and aryl thiol building blocks useful for mapping new areas of chemical space.

Common Conditions

- **Solvent:** MeCN, degassed and anhydrous.
- **Concentration:** 0.5 M standard, 0.12 M or 0.06 M for slow substrates.
- **Photoredox catalyst:** *p*-Me-TPT- BF_4 (1 mol %)
- **Reaction setup:** Degas by sparging the entire reaction mixture with nitrogen for 15 minutes prior to irradiation.
- **Irradiation:** 450 nm blue LED lamps, ambient temperature, 2 to 24 h.

Notes, Tips, and Troubleshooting

Low conversion and tip: Dramatic NKR rate increases were observed for some recalcitrant substrates when adopting more dilute reaction conditions (0.12 M or 0.06 M).

Low conversion or no reaction: Some substitution patterns were not tolerated, such as *ortho* alkenyl, *ortho* *t*-butyl, or monosubstituted haloarenes. Consult the referenced communication for a more detailed discussion on successful substrates, unsuccessful substrates, and the electronic requirements of this transformation.

Tip: Commercially available triphenylpyrylium tetrafluoroborate (TPT- BF_4 , 1 mol %) also catalyzes this rearrangement.

Tip: Preparation of multi-gram quantities of rearrangement products was demonstrated in flow. No precautions were taken to exclude water or oxygen and deleterious effects were not observed.

Product Description	Product Number
<i>p</i> -Me-TPT- BF_4	900685
TPT- BF_4	272345
Dimethylthiocarbamoyl chloride	135895

IX. Recent Cyclization Strategies Enabled by Photoredox Catalysis

Lewis Acid/Photoredox-Catalyzed [2+2] and [3+2] Cycloadditions to Construct Substituted Cyclobutanes and Cyclopentanes

The Yoon group has made photoredox and photochemical cycloaddition methodology a core research focus. They have explored photoredox [2+2], [3+2], and [4+2] cycloaddition strategies operating through oxidative and reductive quenching cycles (see **Figure 17** for two intramolecular examples). Recently disclosed was the group's dual catalytic strategy for the enantioselective synthesis of substituted cyclobutanes and cyclopentanes via [2+2]¹⁵ and [3+2]⁵⁰ cycloadditions, respectively (**Figure 45**). Each system utilizes a photoredox catalyst ($\text{Ru}(\text{bpy})_3^{2+}$), a reductive quencher (*i*-Pr₂NEt), and a chiral Lewis acid. Enantioselective intermolecular [2+2] cycloadditions of enones were achieved using a chiral europium Lewis acid and relies on single electron reduction of a Lewis acid-activated aryl enone (**Figure 17B**, **Figure 45A**). Enantioselective [3+2] cycloadditions of aryl cyclopropyl ketones and styrenes/dienes were achieved using a chiral gadolinium Lewis acid and relies on single electron reduction of the Lewis acid-activated ketone and concomitant cyclopropane ring opening (**Figure 45B**). Both cycloaddition strategies are flexible with respect to functional groups and substitution, with products typically formed in good yield, d.r., and ee. Operationally these transformations are straightforward (requiring a CFL for irradiation and stirring at ambient temperature in degassed acetonitrile) and represent elegant approaches to the synthesis of substituted carbocycles.

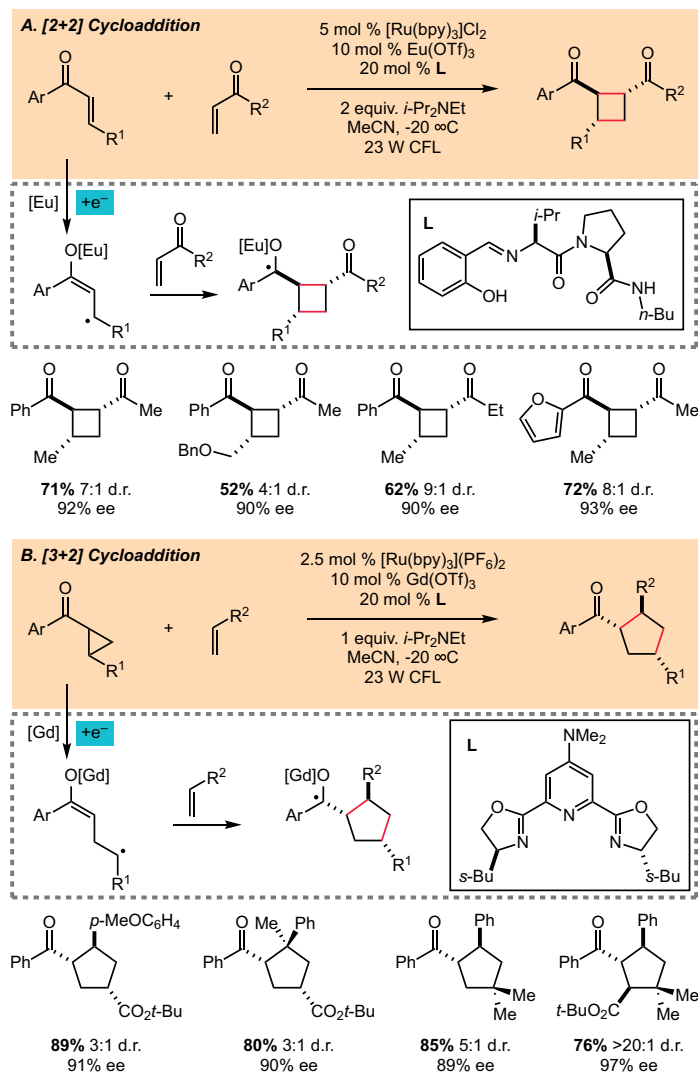


Figure 45. Dual-Catalytic [2+2] and [3+2] Cycloaddition Reactions

Product Description	Product Number
$[\text{Ru}(\text{bpy})_3](\text{PF}_6)_2$	754730
$\text{Eu}(\text{OTf})_3$	425680
(<i>S</i>)- <i>N</i> -Butyl-1-[(<i>S</i>)-2-((<i>E</i>)-2-hydroxybenzylideneamino)-3-methylbutanoyl]pyrrolidine-2-carboxamide	798819
$\text{Gd}(\text{OTf})_3$	425176
2,6-Bis[4(<i>S</i>)-4,5-dihydro-4[(1 <i>S</i>)-1-methylpropyl]-2-oxazolyl]- <i>N,N</i> -dimethyl-4-pyridinamine	NA
<i>N,N</i> -Diisopropylethylamine	D125806

Intermolecular Synthesis of Saturated N- and O-Heterocycles from Oxidizable Alkenes

In addition to hydrofunctionalization products, saturated heterocyclic species can be produced directly from alkene cation radical intermediates by way of a polar radical crossover cyclization (**PRCC, Figure 46**).⁷⁴ Here, products are constructed from an oxidizable alkene substrate and an unsaturated heteroatom nucleophile such as an allylic alcohol, allylic amine, or α,β -unsaturated carboxylic acid. Again, a dual catalytic acridinium/H-atom donor system is active (**Figure 46A-B**).^{28,74} The reaction proceeds by excitation of the acridinium catalyst and single electron oxidation of the olefin substrate. The unsaturated nucleophile engages the cation radical and 5-exo-trig radical cyclization produces the exocyclic radical species shown (**Figure 46A**). Finally, H-atom transfer from the HAD cocatalyst furnishes the product.

Common reaction conditions along with examples (using *trans*- β -methylstyrene as the model substrate) are shown in **Figure 46B**. Substituted tetrahydrofurans were constructed from allylic alcohol nucleophiles.⁷⁴ α -Alkyl- γ -butyrolactones and α -benzyloxyamino- γ -butyrolactones were constructed from unsaturated carboxylic acids and *O*-benzyloxime acids, respectively.^{158,159} Finally, direct pyrrolidine synthesis was accomplished using *N*-Boc allylic amine nucleophiles and γ -lactam synthesis was achieved employing *N*-Tf unsaturated amide nucleophiles (sulfonimides).²⁸ Broad scope was demonstrated for all transformations and functional groups such as esters, protected amines, silyl ethers, and free alcohols were retained during the transformations.

Common Conditions

- **Solvent:** DCM or CHCl_3 (0.08 M to 0.5 M), degassed and anhydrous.
- **Nucleophiles:**
 - Lactone synthesis: 1.1 equiv. α,β -unsaturated acid when using a monoester fumarate nucleophile.
 - Lactone synthesis: 1 equiv. α,β -unsaturated acid when using a cinnamic acid or propiolic acid derived nucleophile (3 equiv. alkene).
 - α -Benzyloxyamino lactone synthesis: 1 equiv. *O*-benzyloxime acid (1.5 equiv. alkene substrate).
 - Lactam synthesis: 1.5 equiv. *N*-Tf α,β -unsaturated amide.
 - Tetrahydrofuran synthesis: 5 equiv. substituted allylic alcohol.
 - Pyrrolidine synthesis: 1 equiv. *N*-Boc allylic amine (3 equiv. alkene).

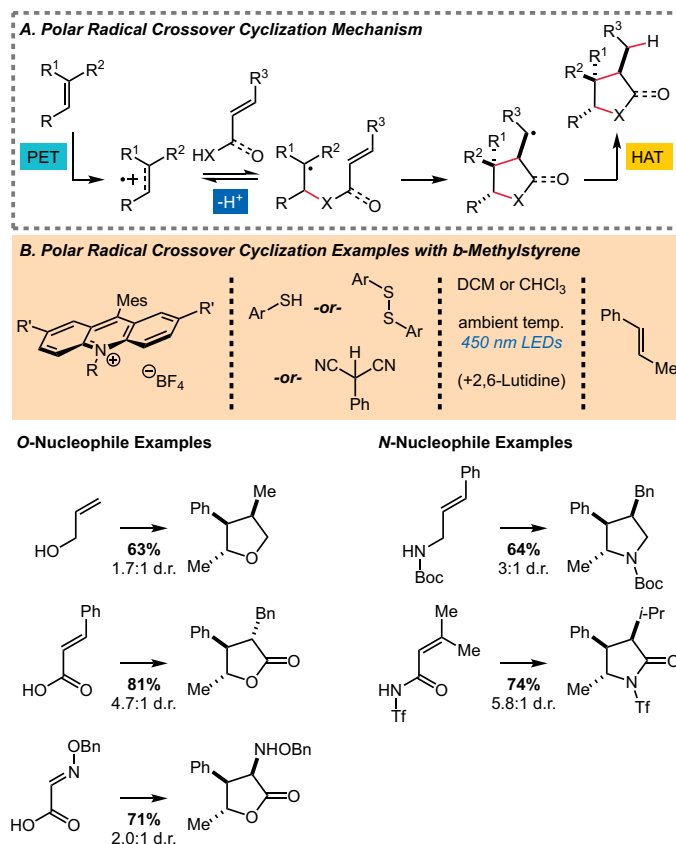


Figure 46. Intermolecular Heterocycle Synthesis by Polar Radical Crossover Cyclization

- **Photoredox catalyst:** Mes-Acr-Me- BF_4 (2.5 mol % to 5 mol %) is a good starting point. Derivatives such as Mes-Acr-Ph- BF_4 (5 mol %, for *N*-Tf amides) and Mes-Me₂Acr-Ph- BF_4 (5 mol %, for *N*-Boc allylic amines) also work well.
- **Hydrogen atom donor:** Thiophenol (20 mol %), phenyl disulfide (15 mol %) or a derivative thereof.
 - 2-Phenylmalononitrile (100 mol %) rather than a thiol for tetrahydrofuran synthesis with alkenols.
 - 4-Methoxythiophenol (20 mol %) for lactam synthesis with *N*-Tf unsaturated amides.
- **Base:** 10 mol % to 20 mol % 2,6-lutidine (distilled and stored under inert atmosphere) for acidic nucleophiles such as carboxylic acids and *N*-Tf amides.
- **Irradiation:** 450 nm blue LED lamps, ambient temperature, 24 to 48 h.

As this reaction is proposed to be mechanistically similar to the alkene hydrofunctionalization chemistry (**Figure 38**) many of the same considerations also apply to this system. Practitioners are advised to start with the optimized conditions indicated in this section and in the referenced publications.

Notes, Tips, and Troubleshooting

No reaction or low conversion: If no product is formed, ensure that the substrate oxidation potential lies within the acridinium catalyst redox window. Also ensure complete and consistent irradiation of the reaction(s).

Low conversion: Change to robust acridinium derivatives, such as Mes-Me₂Acr-Ph-BF₄ or Mes-Acr-Ph-BF₄, if one suspects catalyst deactivation is occurring (Supplementary Table 1).

No reaction, low conversion, or low cyclized product yield: The properties of the hydrogen atom donor can influence the reaction outcome. Screening electronically and sterically diverse H-atom donors may lead to a better “match” for the system and improved conditions, so scan HAD space. For example, in lactam synthesis PhSH and 4-(MeO)PhSH resulted in higher yields (56% and 63%, respectively) compared to 2-phenylmalononitrile (20%), 9-cyanofluorene (12%), or methyl thiosalicylate (19%).

Also, H-atom transfer before the radical cyclization can lead to uncyclized hydrofunctionalization products. HAD properties can influence cyclized/uncyclized product selectivity, as observed for tetrahydrofuran synthesis (**Figure 47**) and lactone synthesis.¹⁵⁸ Additionally, radical-stabilizing groups (e.g. arene or ester) at the β-position of the unsaturated nucleophile helped favor the radical cyclization in some systems (lactone synthesis, **Figure 47**).¹⁵⁸

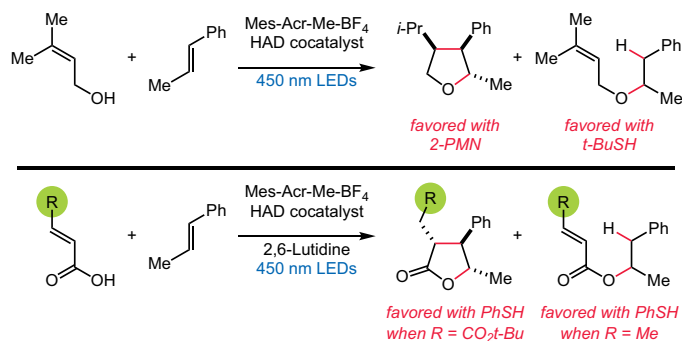


Figure 47. Uncyclized Products in PRCC

Tip: Inverting the standard reaction stoichiometry described above helped rescue yields for some challenging cyclization examples.

Product Description	Product Number
Mes-Acr-Me-BF ₄	794171
Mes-Acr-Ph-BF ₄	793221
Mes-Me ₂ Acr-Ph-BF ₄	793876
Phenyl disulfide	169021
4-Methoxythiophenol	109525
2-Phenylmalononitrile	NA
2,6-Lutidine	336106

X. Conclusion

The principles of photoredox catalysis and photoinduced electron transfer were presented, along with literature examples to help strengthen one's understanding of the field. Redox potentials were presented as a means of predicting the thermodynamic feasibility of electron transfer and the accompanying tables were designed as a reference tool for both catalysts and potential substrates. Finally, recent advances in photoredox catalysis were highlighted and the troubleshooting tips included should enable one to effectively set up and troubleshoot key reactions.

We hope this introductory photoredox catalysis guide will serve as a useful reference tool and aid synthetic and medicinal chemists when they look to use photoredox catalysis. Finally, we hope this reference tool is useful to those who are optimizing transformations, looking to develop new synthetic methods, or those looking to learn more about the growing field of photoredox catalysis.

XI. Abbreviations and Symbols

1,4-DCB	1,4-Dicyanobenzene	HPLC	High performance liquid chromatography
2-PMN	2-Phenylmalononitrile	HTE	High-Throughput Experimentation
4-CzIPN	1,2,3,5-tetrakis(carbazol-9-yl)-4,6-dicyanobenzene	$h\nu$	Energy (Planck's constant \times frequency)
Ac	Acetyl	<i>i</i> -Pr	<i>iso</i> -Propyl
acac	Acetylacetonate	IPr	1,3-Bis(2,6-diisopropylphenyl)-1,3-dihydro-2 <i>H</i> -imidazol-2-ylidene
Acr	Acridinium	ISC	Intersystem crossing
A ⁿ	Generic Electron acceptor	L	Ligand
Ar	Aryl substituent	LC-MS	Liquid-chromatography-mass spectrometry
atm	Atmosphere	LED	Light emitting diode
Bac	<i>tert</i> -Butylaminocarbonyl	LSF	Late-stage functionalization
Barton's base	2- <i>tert</i> -Butyl-1,1,3,3-tetramethylguanidine	M	Molar concentration
BDE	Bond dissociation energy	Me	Methyl
BET	Back electron transfer	Mes	Mesityl
Bn	Benzyl	MLCT	Metal-to-ligand charge transfer
Boc	<i>tert</i> -Butyloxycarbonyl	mm	Millimeter
bpy	2,2'-Bipyridine	MTBD	7-Methyl-1,5,7-triazabicyclo[4.4.0]dec-5-ene
bpz	2,2'-Bipyrazine	MTS	Methyl thiosalicylate
Bu	Butyl	NKR	Newman-Kwart rearrangement
cat or [cat]	Photoredox catalyst	nm	Nanometer
CFL	Compact fluorescent lamp	NMR	Nuclear magnetic resonance spectroscopy
cm	centimeter	PCET	Proton coupled electron transfer
COD	1,5-Cyclooctadiene	PET	Photoinduced electron transfer
d.r.	Diastereomeric ratio	PG	Protecting group
D ^m	Generic Electron donor	Ph	Phenyl
DABCO	1,4-Diazabicyclo[2.2.2]octane	phen	1,10-Phenanthroline
DBU	1,8-Diazabicyclo[5.4.0]undec-7-ene	ppy	2-Phenylpyridine
dF(CF ₃)ppy	2-(2,4-Difluorophenyl)-5-(trifluoromethyl)pyridine	PRCC	Polar radical crossover cyclization
dF(F)ppy	2-(2,4-Difluorophenyl)-5-fluoropyridine	PTFE	Polytetrafluoroethylene
dF(Me)ppy	2-(2,4-Difluorophenyl)-5-methylpyridine	r.r.	Regiomer ratio
dFppy	2-(2,4-Difluorophenyl)-pyridine	rt	Room temperature
DMA	<i>N,N</i> -Dimethylacetamide	S ₀	Singlet ground state
DME	1,2-Dimethoxyethane	S ₁	First singlet excited state
DMF	<i>N,N</i> -Dimethylformamide	SCE	Saturated calomel electrode
DMSO	Dimethyl sulfoxide	SET	Single electron transfer
4,4'-dMe-bpy	4,4'-Dimethyl-2,2'-bipyridine	T ₁	First triplet excited state
4,4'-dOMe-bpy	4,4'-Dimethoxy-2,2'-bipyridine	<i>t</i> -Bu	<i>tert</i> -Butyl
4,7-dOMe-phen	4,7-Dimethoxy-1,10-phenanthroline	TEMPO	(2,2,6,6-Tetramethylpiperidin-1-yl)oxyl
dtbbpy	4,4'-Di- <i>tert</i> -butyl-2,2'-bipyridine	Tf	Trifluoromethanesulfonyl
EDG	Electron donating group	TFA	Trifluoroacetic acid
ee	Enantiometric excess	TFE	2,2,2-trifluoroethanol
E_{ox} (D ⁺ /D)	Donor oxidation potential	THP	Tetrahydropyran
E_{red} (A/A ⁻)	Acceptor reduction potential	TMEDA	<i>N,N,N',N'</i> -Tetramethylethylenediamine
Et	Ethyl	TMG	1,1,3,3-Tetramethylguanidine
EWG	Electron withdrawing group	TPT	2,4,6-Triphenylpyrylium tetrafluoroborate
<i>F</i>	Faraday constant	Ts	Tosyl, 4-Toluenesulfonyl
<i>fac</i>	Facial isomer	TTMSS	Tris(trimethylsilyl)silane
FG	Generic functional group	UV	Ultraviolet
GC-MS	Gas chromatography-mass spectrometry	V	Volt
glyme	1,2-Dimethoxyethane	v/v	Volume/volume percent
HAD	Hydrogen atom donor	W	Watt
HAT	Hydrogen-atom transfer	ΔG	Gibbs free energy
		λ	Wavelength

XII. References

1. Prier, C. K.; Rankic, D. A.; MacMillan, D. W. C. *Chem. Rev.* **2013**, *113* (7), 5322–5363.
2. Fukuzumi, S.; Ohkubo, K. *Org. Biomol. Chem.* **2014**, *12* (32), 6059–6071.
3. Shaw, M. H.; Twilton, J.; MacMillan, D. W. C. *J. Org. Chem.* **2016**, *81* (16), 6898–6926.
4. Romero, N. A.; Nicewicz, D. A. *Chem. Rev.* **2016**, *116* (17), 10075–10166.
5. Skubi, K. L.; Blum, T. R.; Yoon, T. P. *Chem. Rev.* **2016**, *116* (17), 10035–10074.
6. Poplata, S.; Tröster, A.; Zou, Y.-Q.; Bach, T. *Chem. Rev.* **2016**, *116* (17), 9748–9815.
7. Kärkäs, M. D.; Porco, J. A.; Stephenson, C. R. J. *Chem. Rev.* **2016**, *116* (17), 9683–9747.
8. Lin, S.; Ischay, M. A.; Fry, C. G.; Yoon, T. P. *J. Am. Chem. Soc.* **2011**, *133* (48), 19350–19353.
9. Hamilton, D. S.; Nicewicz, D. A. *J. Am. Chem. Soc.* **2012**, *134* (45), 18577–18580.
10. Yamashita, Y.; Tellis, J. C.; Molander, G. A. *Proc. Natl. Acad. Sci.* **2015**, *112* (39), 12026–12029.
11. Amat, M.; Guignard, G.; Llor, N.; Bosch, J. *J. Org. Chem.* **2014**, *79* (6), 2792–2802.
12. Terrett, J. A.; Clift, M. D.; MacMillan, D. W. C. *J. Am. Chem. Soc.* **2014**, *136* (19), 6858–6861.
13. Ohkubo, K.; Mizushima, K.; Iwata, R.; Fukuzumi, S. *Chem. Sci.* **2011**, *2* (4), 715–722.
14. Romero, N. A.; Margrey, K. A.; Tay, N. E.; Nicewicz, D. A. *Science* **2015**, *349* (6254), 1326–1330.
15. Du, J.; Skubi, K. L.; Schultz, D. M.; Yoon, T. P. *Science* **2014**, *344* (6182), 392–396.
16. Cuthbertson, J. D.; MacMillan, D. W. C. *Nature* **2015**, *519* (7541), 74–77.
17. Chu, L.; Ohta, C.; Zuo, Z.; MacMillan, D. W. C. *J. Am. Chem. Soc.* **2014**, *136* (31), 10886–10889.
18. Zuo, Z.; Ahneman, D. T.; Chu, L.; Terrett, J. A.; Doyle, A. G.; MacMillan, D. W. C. *Science* **2014**, *345* (6195), 437–440.
19. Zhu, Q.; Gentry, E. C.; Knowles, R. R. *Angew. Chem. Int. Ed.* **2016**, *55* (34), 9969–9973.
20. Nicewicz, D. A.; MacMillan, D. W. C. *Science* **2008**, *322* (5898), 77–80.
21. Nguyen, J. D.; D’Amato, E. M.; Narayanam, J. M. R.; Stephenson, C. R. J. *Nat. Chem.* **2012**, *4* (10), 854–859.
22. Narayanam, J. M. R.; Tucker, J. W.; Stephenson, C. R. J. *J. Am. Chem. Soc.* **2009**, *131* (25), 8756–8757.
23. Choi, G. J.; Knowles, R. R. *J. Am. Chem. Soc.* **2015**, *137* (29), 9226–9229.
24. Tarantino, K. T.; Liu, P.; Knowles, R. R. *J. Am. Chem. Soc.* **2013**, *135* (27), 10022–10025.
25. Tellis, J. C.; Primer, D. N.; Molander, G. A. *Science* **2014**, *345* (6195), 433–436.
26. (Keshari, T.; Yadav, V. K.; Srivastava, V. P.; Yadav, L. D. S. *Green Chem.* **2014**, *16* (8), 3986–3992.
27. Meyer, A. U.; Jäger, S.; Prasad Hari, D.; König, B. *Adv. Synth. Catal.* **2015**, *357* (9), 2050–2054.
28. Gesmundo, N. J.; Grandjean, J.-M. M.; Nicewicz, D. A. *Org. Lett.* **2015**, *17* (5), 1316–1319.
29. Perkowski, A. J.; Cruz, C. L.; Nicewicz, D. A. *J. Am. Chem. Soc.* **2015**, *137* (50), 15684–15687.
30. Zhang, X.; MacMillan, D. W. C. *J. Am. Chem. Soc.* **2016**, *138* (42), 13862–13865.
31. Miller, D. C.; Choi, G. J.; Orbe, H. S.; Knowles, R. R. *J. Am. Chem. Soc.* **2015**, *137* (42), 13492–13495.
32. Le, C. “Chip”; Wismer, M. K.; Shi, Z.-C.; Zhang, R.; Conway, D. V.; Li, G.; Vachal, P.; Davies, I. W.; MacMillan, D. W. C. *ACS Cent. Sci.* **2017**, *3* (6), 647–653.
33. Tucker, J. W.; Zhang, Y.; Jamison, T. F.; Stephenson, C. R. J. *Angew. Chem. Int. Ed.* **2012**, *51* (17), 4144–4147.
34. Candish, L.; Freitag, M.; Gensch, T.; Glorius, F. *Chem. Sci.* **2017**, *8* (5), 3618–3622.
35. Stevenson, S. M.; Shores, M. P.; Ferreira, E. M. *Angew. Chem. Int. Ed.* **2015**, *54* (22), 6506–6510.
36. Oderinde, M. S.; Varela-Alvarez, A.; Aquila, B.; Robbins, D. W.; Johannes, J. W. *J. Org. Chem.* **2015**, *80* (15), 7642–7651.
37. Higgins, R. F.; Fatur, S. M.; Shepard, S. G.; Stevenson, S. M.; Boston, D. J.; Ferreira, E. M.; Damrauer, N. H.; Rappé, A. K.; Shores, M. P. *J. Am. Chem. Soc.* **2016**, *138* (16), 5451–5464.
38. Redmond, R. W.; Gamlin, J. N. *Photochem. Photobiol.* **1999**, *70* (4), 391–475.
39. Ono, K.; Nakagawa, M.; Nishida, A. *Angew. Chem. Int. Ed.* **2004**, *43* (15), 2020–2023.
40. Martiny, M.; Steckhan, E.; Esch, T. *Chem. Ber.* **1993**, *126* (7), 1671–1682.
41. Miranda, M. A.; Garcia, H. *Chem. Rev.* **1994**, *94* (4), 1063–1089.
42. Ohkubo, K.; Mizushima, K.; Iwata, R.; Souma, K.; Suzuki, N.; Fukuzumi, S. *Chem. Commun.* **2010**, *46* (4), 601–603.
43. Gesmundo, N. J.; Nicewicz, D. A. *Beilstein J. Org. Chem.* **2014**, *10* (1), 1272–1281.

44. Pangborn, A. B.; Giardello, M. A.; Grubbs, R. H.; Rosen, R. K.; Timmers, F. J. *Organometallics* **1996**, *15* (5), 1518–1520.
45. Wilger, D. J.; Grandjean, J.-M. M.; Lammert, T. R.; Nicewicz, D. A. *Nat. Chem.* **2014**, *6* (8), 720–726.
46. Griffin, J. D.; Zeller, M. A.; Nicewicz, D. A. *J. Am. Chem. Soc.* **2015**, *137* (35), 11340–11348.
47. Wilfred L. F. Armarego; Christina Li Lin Chai. *Purification of Laboratory Chemicals, Seventh Edition*; Butterworth-Heinemann: Oxford, UK, 2013.
48. Shaw, M. H.; Shurtleff, V. W.; Terrett, J. A.; Cuthbertson, J. D.; MacMillan, D. W. C. *Science* **2016**, *352* (6291), 1304–1308.
49. Corcoran, E. B.; Pirnot, M. T.; Lin, S.; Dreher, S. D.; DiRocco, D. A.; Davies, I. W.; Buchwald, S. L.; MacMillan, D. W. C. *Science* **2016**, *353* (6296), 279–283.
50. Amador, A. G.; Sherbrook, E. M.; Yoon, T. P. *J. Am. Chem. Soc.* **2016**, *138* (14), 4722–4725.
51. Zuo, Z.; Cong, H.; Li, W.; Choi, J.; Fu, G. C.; MacMillan, D. W. C. *J. Am. Chem. Soc.* **2016**, *138* (6), 1832–1835.
52. Dreher, S. D.; Dormer, P. G.; Sandrock, D. L.; Molander, G. A. *J. Am. Chem. Soc.* **2008**, *130* (29), 9257–9259.
53. Molander, G. A.; Argintaru, O. A.; Aron, I.; Dreher, S. D. *Org. Lett.* **2010**, *12* (24), 5783–5785.
54. Bellomo, A.; Celebi-Olcum, N.; Bu, X.; Rivera, N.; Ruck, R. T.; Welch, C. J.; Houk, K. N.; Dreher, S. D. *Angew. Chem. Int. Ed.* **2012**, *51* (28), 6912–6915.
55. Friedfeld, M. R.; Shevlin, M.; Hoyt, J. M.; Krska, S. W.; Tudge, M. T.; Chirik, P. J. *Science* **2013**, *342* (6162), 1076–1080.
56. Preshlock, S. M.; Ghaffari, B.; Maligres, P. E.; Krska, S. W.; Maleczka, R. E.; Smith, M. R. *J. Am. Chem. Soc.* **2013**, *135* (20), 7572–7582.
57. Buitrago Santanilla, A.; Christensen, M.; Campeau, L.-C.; Davies, I. W.; Dreher, S. D. *Org. Lett.* **2015**, *17* (13), 3370–3373.
58. Christensen, M.; Nolting, A.; Shevlin, M.; Weisel, M.; Maligres, P. E.; Lee, J.; Orr, R. K.; Plummer, C. W.; Tudge, M. T.; Campeau, L.-C.; Ruck, R. T. *J. Org. Chem.* **2016**, *81* (3), 824–830.
59. Cernak, T.; Gesmundo, N. J.; Dykstra, K.; Yu, Y.; Wu, Z.; Shi, Z.-C.; Vachal, P.; Sperbeck, D.; He, S.; Murphy, B. A.; Sonatore, L.; Williams, S.; Madeira, M.; Verras, A.; Reiter, M.; Lee, C. H.; Cuff, J.; Sherer, E. C.; Kuethe, J.; Goble, S.; Perrotto, N.; Pinto, S.; Shen, D.-M.; Nargund, R.; Balkovec, J.; DeVita, R. J.; Dreher, S. D. *J. Med. Chem.* **2017**, *60* (9), 3594–3605.
60. DiRocco, D. A.; Dykstra, K.; Krska, S.; Vachal, P.; Conway, D. V.; Tudge, M. *Angew. Chem. Int. Ed.* **2014**, *53* (19), 4802–4806.
61. Huff, C. A.; Cohen, R. D.; Dykstra, K. D.; Streckfuss, E.; DiRocco, D. A.; Krska, S. W. *J. Org. Chem.* **2016**, *81* (16), 6980–6987.
62. Halperin, S. D.; Kwon, D.; Holmes, M.; Regalado, E. L.; Campeau, L.-C.; DiRocco, D. A.; Britton, R. *Org. Lett.* **2015**, *17* (21), 5200–5203.
63. Jouffroy, M.; Primer, D. N.; Molander, G. A. *J. Am. Chem. Soc.* **2016**, *138* (2), 475–478.
64. Cambié, D.; Bottecchia, C.; Straathof, N. J. W.; Hessel, V.; Noël, T. *Chem. Rev.* **2016**, *116* (17), 10276–10341.
65. Morse, P. D.; Beingessner, R. L.; Jamison, T. F. *Isr. J. Chem.* **2017**, *57* (3–4), 218–227.
66. Su, Y.; Straathof, N. J. W.; Hessel, V.; Noël, T. *Chem. – Eur. J.* **2014**, *20* (34), 10562–10589.
67. Lévesque, F.; Seeberger, P. H. *Org. Lett.* **2011**, *13* (19), 5008–5011.
68. Su, Y.; Kuijpers, K.; Hessel, V.; Noël, T. *React. Chem. Eng.* **2016**, *1* (1), 73–81.
69. Beatty, J. W.; Douglas, J. J.; Cole, K. P.; Stephenson, C. R. J. *Nat. Commun.* **2015**, *6*, 7919.
70. Beatty, J. W.; Douglas, J. J.; Miller, R.; McAtee, R. C.; Cole, K. P.; Stephenson, C. R. J. *Chem* **2016**, *1* (3), 456–472.
71. Beatty, J. W.; Stephenson, C. R. J. *J. Am. Chem. Soc.* **2014**, *136* (29), 10270–10273.
72. Narayanam, J. M. R.; Stephenson, C. R. J. *Chem Soc Rev* **2010**, *40* (1), 102–113.
73. Roth, H.; Romero, N.; Nicewicz, D. *Synlett* **2015**, *27* (5), 714–723.
74. Grandjean, J.-M. M.; Nicewicz, D. A. *Angew. Chem. Int. Ed.* **2013**, *52* (14), 3967–3971.
75. Perkowski, A. J.; Nicewicz, D. A. *J. Am. Chem. Soc.* **2013**, *135* (28), 10334–10337.
76. Ischay, M. A.; Anzovino, M. E.; Du, J.; Yoon, T. P. *J. Am. Chem. Soc.* **2008**, *130* (39), 12886–12887.
77. Ischay, M. A.; Lu, Z.; Yoon, T. P. *J. Am. Chem. Soc.* **2010**, *132* (25), 8572–8574.
78. Alfonzo, E.; Alfonso, F. S.; Beeler, A. B. *Org. Lett.* **2017**, *19* (11), 2989–2992.
79. Joshi-Pangu, A.; Lévesque, F.; Roth, H. G.; Oliver, S. F.; Campeau, L.-C.; Nicewicz, D.; DiRocco, D. A. *J. Org. Chem.* **2016**, *81* (16), 7244–7249.
80. Rillema, D. P.; Allen, G.; Meyer, T. J.; Conrad, D. *Inorg. Chem.* **1983**, *22* (11), 1617–1622.
81. Schultz, D. M.; Sawicki, J. W.; Yoon, T. P. *Beilstein J. Org. Chem.* **2015**, *11* (1), 61–65.

82. Kelly, C. B.; Patel, N. R.; Primer, D. N.; Jouffroy, M.; Tellis, J. C.; Molander, G. A. *Nat. Protoc.* **2017**, *12* (3), 472–492.
83. Juris, A.; Balzani, V.; Barigelletti, F.; Campagna, S.; Belser, P.; von Zelewsky, A. *Coord. Chem. Rev.* **1988**, *84*, 85–277.
84. Lowry, M. S.; Goldsmith, J. I.; Slinker, J. D.; Rohl, R.; Pascal, R. A.; Malliaras, G. G.; Bernhard, S. *Chem. Mater.* **2005**, *17* (23), 5712–5719.
85. Goldsmith, J. I.; Hudson, W. R.; Lowry, M. S.; Anderson, T. H.; Bernhard, S. *J. Am. Chem. Soc.* **2005**, *127* (20), 7502–7510.
86. Ladouceur, S.; Swanick, K. N.; Gallagher-Duval, S.; Ding, Z.; Zysman-Colman, E. *Eur. J. Inorg. Chem.* **2013**, *2013* (30), 5329–5343.
87. Singh, A.; Teegardin, K.; Kelly, M.; Prasad, K. S.; Krishnan, S.; Weaver, J. D. *J. Organomet. Chem.* **2015**, *776*, 51–59.
88. Choi, G. J.; Zhu, Q.; Miller, D. C.; Gu, C. J.; Knowles, R. R. *Nature* **2016**, *539* (7628), 268–271.
89. Monos, T. M.; Sun, A. C.; McAtee, R. C.; Devery, J. J.; Stephenson, C. R. J. *J. Org. Chem.* **2016**, *81* (16), 6988–6994.
90. Tamayo, A. B.; Alleyne, B. D.; Djurovich, P. I.; Lamansky, S.; Tsyba, I.; Ho, N. N.; Bau, R.; Thompson, M. E. *J. Am. Chem. Soc.* **2003**, *125* (24), 7377–7387.
91. Gutierrez, O.; Tellis, J. C.; Primer, D. N.; Molander, G. A.; Kozlowski, M. C. *J. Am. Chem. Soc.* **2015**, *137* (15), 4896–4899.
92. Johnston, C. P.; Smith, R. T.; Allmendinger, S.; MacMillan, D. W. C. *Nature* **2016**, *536* (7616), 322–325.
93. Primer, D. N.; Karakaya, I.; Tellis, J. C.; Molander, G. A. *J. Am. Chem. Soc.* **2015**, *137* (6), 2195–2198.
94. Corcé, V.; Chamoreau, L.-M.; Derat, E.; Goddard, J.-P.; Ollivier, C.; Fensterbank, L. *Angew. Chem. Int. Ed.* **2015**, *54* (39), 11414–11418.
95. Nakajima, K.; Nojima, S.; Nishibayashi, Y. *Angew. Chem. Int. Ed.* **2016**, *55* (45), 14106–14110.
96. Gutiérrez-Bonet, Á.; Tellis, J. C.; Matsui, J. K.; Vara, B. A.; Molander, G. A. *ACS Catal.* **2016**, *6* (12), 8004–8008.
97. Zhang, P.; Le, C. “Chip”; MacMillan, D. W. C. *J. Am. Chem. Soc.* **2016**, *138* (26), 8084–8087.
98. Joe, C. L.; Doyle, A. G. *Angew. Chem. Int. Ed.* **2016**, *55* (12), 4040–4043.
99. Ahneman, D. T.; Doyle, A. G. *Chem. Sci.* **2016**, *7* (12), 7002–7006.
100. Noble, A.; McCarver, S. J.; MacMillan, D. W. C. *J. Am. Chem. Soc.* **2015**, *137* (2), 624–627.
101. Chu, L.; Lipshultz, J. M.; MacMillan, D. W. C. *Angew. Chem. Int. Ed.* **2015**, *54* (27), 7929–7933.
102. Le, C. “Chip”; MacMillan, D. W. C. *J. Am. Chem. Soc.* **2015**, *137* (37), 11938–11941.
103. Tellis, J. C.; Kelly, C. B.; Primer, D. N.; Jouffroy, M.; Patel, N. R.; Molander, G. A. *Acc. Chem. Res.* **2016**, *49* (7), 1429–1439.
104. Tellis, J. C.; Amani, J.; Molander, G. A. *Org. Lett.* **2016**, *18* (12), 2994–2997.
105. Matsui, J. K.; Molander, G. A. *Org. Lett.* **2017**, *19* (3), 436–439.
106. Luo, J.; Zhang, J. *ACS Catal.* **2016**, *6* (2), 873–877.
107. Patel, N. R.; Kelly, C. B.; Jouffroy, M.; Molander, G. A. *Org. Lett.* **2016**, *18* (4), 764–767.
108. Palaychuk, N.; DeLano, T. J.; Boyd, M. J.; Green, J.; Bandarage, U. K. *Org. Lett.* **2016**, *18* (23), 6180–6183.
109. DeLano, T. J.; Bandarage, U. K.; Palaychuk, N.; Green, J.; Boyd, M. J. *J. Org. Chem.* **2016**, *81* (24), 12525–12531.
110. Jeffrey, J. L.; Terrett, J. A.; MacMillan, D. W. C. *Science* **2015**, *349* (6255), 1532–1536.
111. Le, C.; Liang, Y.; Evans, R. W.; Li, X.; MacMillan, D. W. C. *Nature* **2017**, *547* (7661), 79–83.
112. Heitz, D. R.; Tellis, J. C.; Molander, G. A. *J. Am. Chem. Soc.* **2016**, *138* (39), 12715–12718.
113. Shields, B. J.; Doyle, A. G. *J. Am. Chem. Soc.* **2016**, *138* (39), 12719–12722.
114. Terrett, J. A.; Cuthbertson, J. D.; Shurtleff, V. W.; MacMillan, D. W. C. *Nature* **2015**, *524* (7565), 330–334.
115. Tasker, S. Z.; Jamison, T. F. *J. Am. Chem. Soc.* **2015**, *137* (30), 9531–9534.
116. Oderinde, M. S.; Jones, N. H.; Juneau, A.; Frenette, M.; Aquila, B.; Tentarelli, S.; Robbins, D. W.; Johannes, J. W. *Angew. Chem. Int. Ed.* **2016**, *55* (42), 13219–13223.
117. Oderinde, M. S.; Frenette, M.; Robbins, D. W.; Aquila, B.; Johannes, J. W. *J. Am. Chem. Soc.* **2016**, *138* (6), 1760–1763.
118. Jouffroy, M.; Kelly, C. B.; Molander, G. A. *Org. Lett.* **2016**, *18* (4), 876–879.
119. Welin, E. R.; Le, C.; Arias-Rotondo, D. M.; McCusker, J. K.; MacMillan, D. W. C. *Science* **2017**, *355* (6323), 380–385.
120. Corbet, J.-P.; Mignani, G. *Chem. Rev.* **2006**, *106* (7), 2651–2710.
121. Surry, D. S.; Buchwald, S. L. *Chem. Sci.* **2010**, *2* (1), 27–50.

122. Koo, K.; Hillhouse, G. L. *Organometallics* **1995**, *14* (9), 4421–4423.
123. Lin, B. L.; Clough, C. R.; Hillhouse, G. L. *J. Am. Chem. Soc.* **2002**, *124* (12), 2890–2891.
124. Schönherr, H.; Cernak, T. *Angew. Chem. Int. Ed.* **2013**, *52* (47), 12256–12267.
125. Sloan, K. B.; Bodor, N. *Int. J. Pharm.* **1982**, *12* (4), 299–313.
126. Liang, T.; Neumann, C. N.; Ritter, T. *Angew. Chem. Int. Ed.* **2013**, *52* (32), 8214–8264.
127. Jin, J.; MacMillan, D. W. C. *Angew. Chem. Int. Ed.* **2015**, *54* (5), 1565–1569.
128. Jin, J.; MacMillan, D. W. C. *Nature* **2015**, *525* (7567), 87–90.
129. Roberts, B. P. *Chem. Soc. Rev.* **1999**, *28* (1), 25–35.
130. Cho, E. J.; Senecal, T. D.; Kinzel, T.; Zhang, Y.; Watson, D. A.; Buchwald, S. L. *Science* **2010**, *328* (5986), 1679–1681.
131. Morimoto, H.; Tsubogo, T.; Litvinas, N. D.; Hartwig, J. F. *Angew. Chem. Int. Ed.* **2011**, *50* (16), 3793–3798.
132. Cho, E. J.; Buchwald, S. L. *Org. Lett.* **2011**, *13* (24), 6552–6555.
133. Parsons, A. T.; Senecal, T. D.; Buchwald, S. L. *Angew. Chem. Int. Ed.* **2012**, *51* (12), 2947–2950.
134. Ji, Y.; Brueckl, T.; Baxter, R. D.; Fujiwara, Y.; Seiple, I. B.; Su, S.; Blackmond, D. G.; Baran, P. S. *Proc. Natl. Acad. Sci.* **2011**, *108* (35), 14411–14415.
135. Nagib, D. A.; MacMillan, D. W. C. *Nature* **2011**, *480* (7376), 224–228.
136. Pitre, S. P.; McTiernan, C. D.; Ismaili, H.; Scaiano, J. C. *ACS Catal.* **2014**, *4* (8), 2530–2535.
137. Ye, Y.; Sanford, M. S. *J. Am. Chem. Soc.* **2012**, *134* (22), 9034–9037.
138. Mizuta, S.; Verhoog, S.; Engle, K. M.; Khotavivattana, T.; O’Duill, M.; Wheelhouse, K.; Rassias, G.; Médebielle, M.; Gouverneur, V. *J. Am. Chem. Soc.* **2013**, *135* (7), 2505–2508.
139. Wilger, D. J.; Gesmundo, N. J.; Nicewicz, D. A. *Chem. Sci.* **2013**, *4* (8), 3160–3165.
140. Yasu, Y.; Koike, T.; Akita, M. *Angew. Chem. Int. Ed.* **2012**, *51* (38), 9567–9571.
141. Iqbal, N.; Choi, S.; Kim, E.; Cho, E. J. *J. Org. Chem.* **2012**, *77* (24), 11383–11387.
142. Nagib, D. A.; Scott, M. E.; MacMillan, D. W. C. *J. Am. Chem. Soc.* **2009**, *131* (31), 10875–10877.
143. Margrey, K. A.; Nicewicz, D. A. *Acc. Chem. Res.* **2016**, *49* (9), 1997–2006.
144. Romero, N. A.; Nicewicz, D. A. *J. Am. Chem. Soc.* **2014**, *136* (49), 17024–17035.
145. Mangion, D.; Arnold, D. R. *Acc. Chem. Res.* **2002**, *35* (5), 297–304.
146. Nguyen, T. M.; Nicewicz, D. A. *J. Am. Chem. Soc.* **2013**, *135* (26), 9588–9591.
147. Nguyen, T. M.; Manohar, N.; Nicewicz, D. A. *Angew. Chem. Int. Ed.* **2014**, *53* (24), 6198–6201.
148. Morse, P. D.; Nicewicz, D. A. *Chem. Sci.* **2014**, *6* (1), 270–274.
149. Lin, Y.-C.; Chen, C.-T. *Org. Lett.* **2009**, *11* (21), 4858–4861.
150. Musacchio, A. J.; Lainhart, B. C.; Zhang, X.; Naguib, S. G.; Sherwood, T. C.; Knowles, R. R. *Science* **2017**, *355* (6326), 727–730.
151. Tyson, E. L.; Ament, M. S.; Yoon, T. P. *J. Org. Chem.* **2013**, *78* (5), 2046–2050.
152. (Tyson, E. L.; Niemeyer, Z. L.; Yoon, T. P. *J. Org. Chem.* **2014**, *79* (3), 1427–1436.
153. Keylor, M. H.; Park, J. E.; Wallentin, C.-J.; Stephenson, C. R. J. *Tetrahedron* **2014**, *70* (27–28), 4264–4269.
154. Margrey, K. A.; McManus, J. B.; Bonazzi, S.; Zecri, F.; Nicewicz, D. A. *J. Am. Chem. Soc.* **2017**, *139*, 11288–11299.
155. McManus, J. B.; Nicewicz, D. A. *J. Am. Chem. Soc.* **2017**, *139* (8), 2880–2883.
156. Newman, M. S.; Karnes, H. A. *J. Org. Chem.* **1966**, *31* (12), 3980–3984.
157. Kwart, H.; Evans, E. R. *J. Org. Chem.* **1966**, *31* (2), 410–413.
158. Zeller, M. A.; Riener, M.; Nicewicz, D. A. *Org. Lett.* **2014**, *16* (18), 4810–4813.
159. Cavanaugh, C. L.; Nicewicz, D. A. *Org. Lett.* **2015**, *17* (24), 6082–6085.

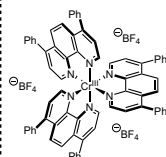
XIII. Appendix Table 1: Photoredox catalysts

Table 1. Photoredox catalysts

E_{red}^* = excited state reduction potential
 E_{red} = ground state reduction potential
 E_{ox}^* = excited state oxidation potential
 E_{ox} = ground state oxidation potential

Values are reported in volts (V) versus saturated calomel electrode (SCE)

Chromium photocatalyst

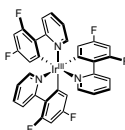


E_{red}^* (Cr^{III}/Cr^{II}) = +1.40 V
 E_{red} (Cr^{III}/Cr^{II}) = -0.27 V
 I_{max} = 300-400 nm

Homoleptic iridium photoredox catalysts

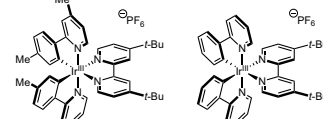


E_{red}^* (Ir^{III}/Ir^{II}) = +0.31 V
 E_{red} (Ir^{III}/Ir^{II}) = -2.19 V
 E_{ox}^* (Ir^{III}/Ir^{IV}) = -1.73 V
 E_{ox} (Ir^{III}/Ir^{IV}) = +0.77 V
 I_{max} = 375 nm

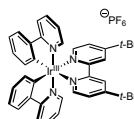


E_{red}^* (Ir^{III}/Ir^{II}) = +0.77 V
 E_{red} (Ir^{III}/Ir^{II}) = -2.00 V
 E_{ox}^* (Ir^{III}/Ir^{IV}) = -1.46 V
 E_{ox} (Ir^{III}/Ir^{IV}) = +1.29 V
 I_{max} = 346 nm

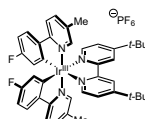
Heteroleptic iridium photoredox catalysts



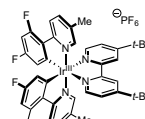
E_{red}^* (Ir^{III}/Ir^{II}) = +0.55 V
 E_{red} (Ir^{III}/Ir^{II}) = -1.52 V
 E_{ox}^* (Ir^{III}/Ir^{IV}) = -0.87 V
 E_{ox} (Ir^{III}/Ir^{IV}) = +1.21 V
 I_{max} = 380 nm



E_{red}^* (Ir^{III}/Ir^{II}) = +0.66 V
 E_{red} (Ir^{III}/Ir^{II}) = -1.51 V
 E_{ox}^* (Ir^{III}/Ir^{IV}) = -0.96 V
 E_{ox} (Ir^{III}/Ir^{IV}) = +1.21 V
 I_{max} = 380 nm

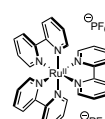


E_{red}^* (Ir^{III}/Ir^{II}) = +0.77 V
 E_{red} (Ir^{III}/Ir^{II}) = -1.50 V
 E_{ox}^* (Ir^{III}/Ir^{IV}) = -0.94 V
 E_{ox} (Ir^{III}/Ir^{IV}) = +1.33 V

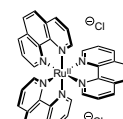


E_{red}^* (Ir^{III}/Ir^{II}) = +0.97 V
 E_{red} (Ir^{III}/Ir^{II}) = -1.44 V
 E_{ox}^* (Ir^{III}/Ir^{IV}) = -0.92 V
 E_{ox} (Ir^{III}/Ir^{IV}) = +1.49 V
 I_{max} = 360 nm

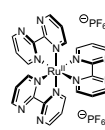
Ruthenium photoredox catalysts



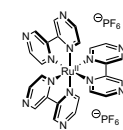
E_{red}^* (Ru^{II}/Ru^I) = +0.77 V
 E_{red} (Ru^{II}/Ru^I) = -1.33 V
 E_{ox}^* (Ru^{II}/Ru^{III}) = -0.81 V
 E_{ox} (Ru^{II}/Ru^{III}) = +1.29 V
 I_{max} = 452 nm



E_{red}^* (Ru^{II}/Ru^I) = +0.82 V
 E_{red} (Ru^{II}/Ru^I) = -1.36 V
 E_{ox}^* (Ru^{II}/Ru^{III}) = -0.87 V
 E_{ox} (Ru^{II}/Ru^{III}) = +1.26 V
 I_{max} = 422 nm



E_{red}^* (Ru^{II}/Ru^I) = +0.99 V
 E_{red} (Ru^{II}/Ru^I) = -0.91 V
 E_{ox}^* (Ru^{II}/Ru^{III}) = -0.21 V
 E_{ox} (Ru^{II}/Ru^{III}) = +1.69 V
 I_{max} = 454 nm

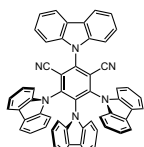


E_{red}^* (Ru^{II}/Ru^I) = +1.45 V
 E_{red} (Ru^{II}/Ru^I) = -0.80 V
 E_{ox}^* (Ru^{II}/Ru^{III}) = -0.26 V
 E_{ox} (Ru^{II}/Ru^{III}) = +1.86 V
 I_{max} = 443 nm

Cyanoarene photooxidants

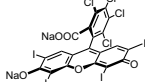


E_{red}^{S1} (DCA/DCA^{-•}) = +1.99 V
 E_{red} (DCA/DCA^{-•}) = -0.91 V
 I_{max} = 422 nm

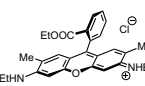


E_{red}^{S1} (4CzIPN/4CzIPN^{-•}) = +1.35 V
 E_{red} (4CzIPN/4CzIPN^{-•}) = -1.21 V
 E_{ox}^* (4CzIPN^{•+}/4CzIPN) = +1.04 V
 E_{ox} (4CzIPN^{•+}/4CzIPN) = +1.52 V
 I_{max} = 435 nm

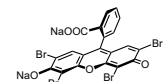
Fluorescein and Rhodamine dyes



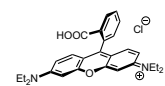
E_{red}^{S1} (RB²⁻/RB^{•-3-}) = +0.81 V
 E_{red} (RB²⁻/RB^{•-3-}) = -0.99 V
 E_{ox}^{S1} (RB²⁻/RB^{•-}) = +0.84 V
 I_{max} = 549 nm



E_{red}^{S1} (Rh6G⁺/Rh6G^{•2+}) = +1.18 V
 E_{red} (Rh6G⁺/Rh6G^{•2+}) = -1.14 V
 E_{ox}^{S1} (Rh6G^{•2+}/Rh6G⁺) = -1.09 V
 E_{ox} (Rh6G^{•2+}/Rh6G⁺) = +1.23 V
 I_{max} = 530 nm

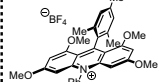


E_{red}^{S1} (EY²⁻/EY^{•-3-}) = +0.83 V
 E_{red} (EY²⁻/EY^{•-3-}) = -1.08 V
 E_{ox}^{S1} (EY²⁻/EY^{•-}) = -1.15 V
 E_{ox} (EY²⁻/EY^{•-}) = +0.76 V
 I_{max} = 520 nm

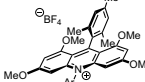


E_{red}^{S1} (RhB⁺/RhB^{•2+}) = +1.26 V
 E_{red} (RhB⁺/RhB^{•2+}) = -0.96 V
 E_{ox}^{S1} (RhB^{•2+}/RhB⁺) = -1.31 V
 E_{ox} (RhB^{•2+}/RhB⁺) = +0.91 V
 I_{max} = 550 nm

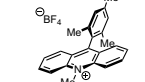
Acridinium dye photooxidants



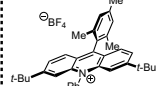
E_{red}^{S1} (Acr⁺/Acr^{•2+}) = +1.62 V
 E_{red} (Acr⁺/Acr^{•2+}) = -0.84 V
 I_{max} = 412 nm



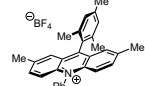
E_{red}^{S1} (Acr⁺/Acr^{•2+}) = +1.65 V
 E_{red} (Acr⁺/Acr^{•2+}) = -0.82 V
 I_{max} = 414 nm



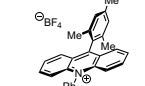
E_{red}^{S1} (Acr⁺/Acr^{•2+}) = +2.08 V
 E_{red} (Acr⁺/Acr^{•2+}) = -0.57 V
 I_{max} = 425 nm



E_{red}^{S1} (Acr⁺/Acr^{•2+}) = +2.08 V
 E_{red} (Acr⁺/Acr^{•2+}) = -0.59 V
 I_{max} = 420 nm

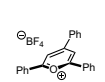


E_{red}^{S1} (Acr⁺/Acr^{•2+}) = +2.09 V
 E_{red} (Acr⁺/Acr^{•2+}) = -0.58 V
 I_{max} = 438 nm

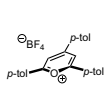


E_{red}^{S1} (Acr⁺/Acr^{•2+}) = +2.17 V
 E_{red} (Acr⁺/Acr^{•2+}) = -0.50 V
 I_{max} = 432 nm

Pyrylium dye photooxidants



E_{red}^{S1} (TPT⁺/TPT^{•2+}) = +2.39 V
 E_{red} (TPT⁺/TPT^{•2+}) = -0.27 V
 I_{max} = 416 nm



E_{red}^{S1} (TPT⁺/TPT^{•2+}) = +2.13 V
 E_{red} (TPT⁺/TPT^{•2+}) = -0.42 V
 I_{max} = 444 nm

Thiazine photoreductant



E_{ox}^{S1} (PTH²⁺/PTH^{•+}) = -2.10 V
 E_{ox} (PTH²⁺/PTH^{•+}) = +0.68 V
 I_{max} = <300 nm



E_{red}^{S1} (TPT⁺/TPT^{•2+}) = +1.84 V
 E_{red} (TPT⁺/TPT^{•2+}) = -0.50 V
 I_{max} = 470 nm

XIV. Appendix Table 2: Excited state photooxidants

Table 2. Excited state photooxidants

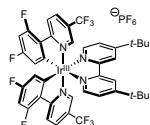
$DG_{PET} = -nF[E_{red}(cat) - E_{ox}(D^{n+}/D^n)]$

Compiled redox potentials reported in volts (V) versus Saturated Calomel Electrode (SCE)

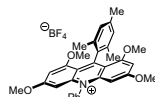
Compiled data represent measured $E_{1/2}$ (half-wave), E_p (peak potential), or $E_{p/2}$ (half-peak potential) values



[Ru(bpy)₃](PF₆)₂
 $E_{red}^{*}(Ru^{II}/Ru) = +0.77$ V
 $E_{red}(Ru^{II}/Ru) = -1.33$ V
 $E_{ox}(Ru^{II}/Ru^{III}) = -0.81$ V
 $E_{ox}(Ru^{III}/Ru^{II}) = +1.29$ V



[Ir(dFCF₃)ppy]₂(dtbbpy)PF₆
 $E_{red}^{*}(Ir^{III}/Ir^{II}) = +1.21$ V
 $E_{red}(Ir^{III}/Ir^{II}) = -1.37$ V
 $E_{ox}(Ir^{III}/Ir^{IV}) = -0.89$ V
 $E_{ox}(Ir^{IV}/Ir^{III}) = +1.69$ V



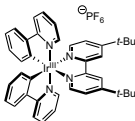
Mes-(MeO)₂Acr-Ph-BF₄
 $E_{red}^{*}(Acr^{+}/Acr^2) = +1.62$ V
 $E_{red}(Acr^{+}/Acr^2) = -0.84$ V



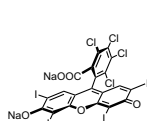
9,10-Dicyanoanthracene [DCA]
 $E_{red}^{*}(DCA/DCA^{\cdot-}) = +1.99$ V
 $E_{red}(DCA/DCA^{\cdot-}) = -0.91$ V



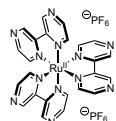
2,4,6-Triphenylpyrylium-BF₄ [TPT]
 $E_{red}^{*}(TPT^{+}/TPT^{\cdot+}) = +2.39$ V
 $E_{red}(TPT^{+}/TPT^{\cdot+}) = -0.27$ V



[Ir(ppy)₂(dtbbpy)]PF₆
 $E_{red}^{*}(Ir^{III}/Ir^{II}) = +0.66$ V
 $E_{red}(Ir^{III}/Ir^{II}) = -1.51$ V
 $E_{ox}(Ir^{III}/Ir^{IV}) = -0.96$ V
 $E_{ox}(Ir^{IV}/Ir^{III}) = +1.21$ V



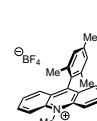
Rose Bengal [RB]
 $E_{red}^{*}(RB^{\cdot-}/RB^{2-\cdot}) = -0.81$ V
 $E_{red}(RB^{\cdot-}/RB^{2-\cdot}) = -0.99$ V
 $E_{ox}^{*}(RB^{\cdot-}/RB^{\cdot}) = -0.96$ V
 $E_{ox}(RB^{\cdot-}/RB^{\cdot}) = +0.84$ V



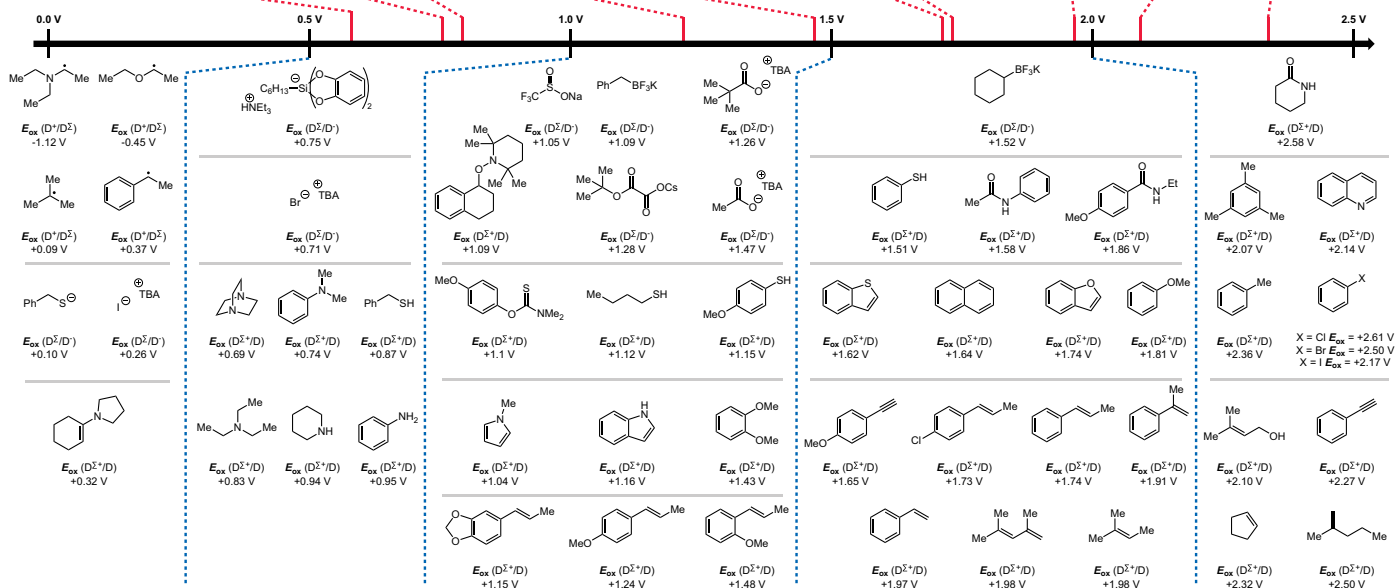
[Ru(tpz)₂](PF₆)₂
 $E_{red}^{*}(Ru^{II}/Ru) = +1.45$ V
 $E_{red}(Ru^{II}/Ru) = -0.80$ V
 $E_{ox}(Ru^{II}/Ru^{III}) = -0.26$ V
 $E_{ox}(Ru^{III}/Ru^{II}) = +1.86$ V



[Ir(dFCF₃)ppy]₂(5,5'-dCF₃-bpy)PF₆
 $E_{red}^{*}(Ir^{III}/Ir^{II}) = -1.68$ V
 $E_{red}(Ir^{III}/Ir^{II}) = -0.69$ V
 $E_{ox}(Ir^{III}/Ir^{IV}) = -0.43$ V
 $E_{ox}(Ir^{IV}/Ir^{III}) = +1.94$ V



Mes-Acr-Me-BF₄ [Ac]
 $E_{red}^{*}(Ac^{+}/Ac^2) = +2.08$ V
 $E_{red}(Ac^{+}/Ac^2) = -0.57$ V



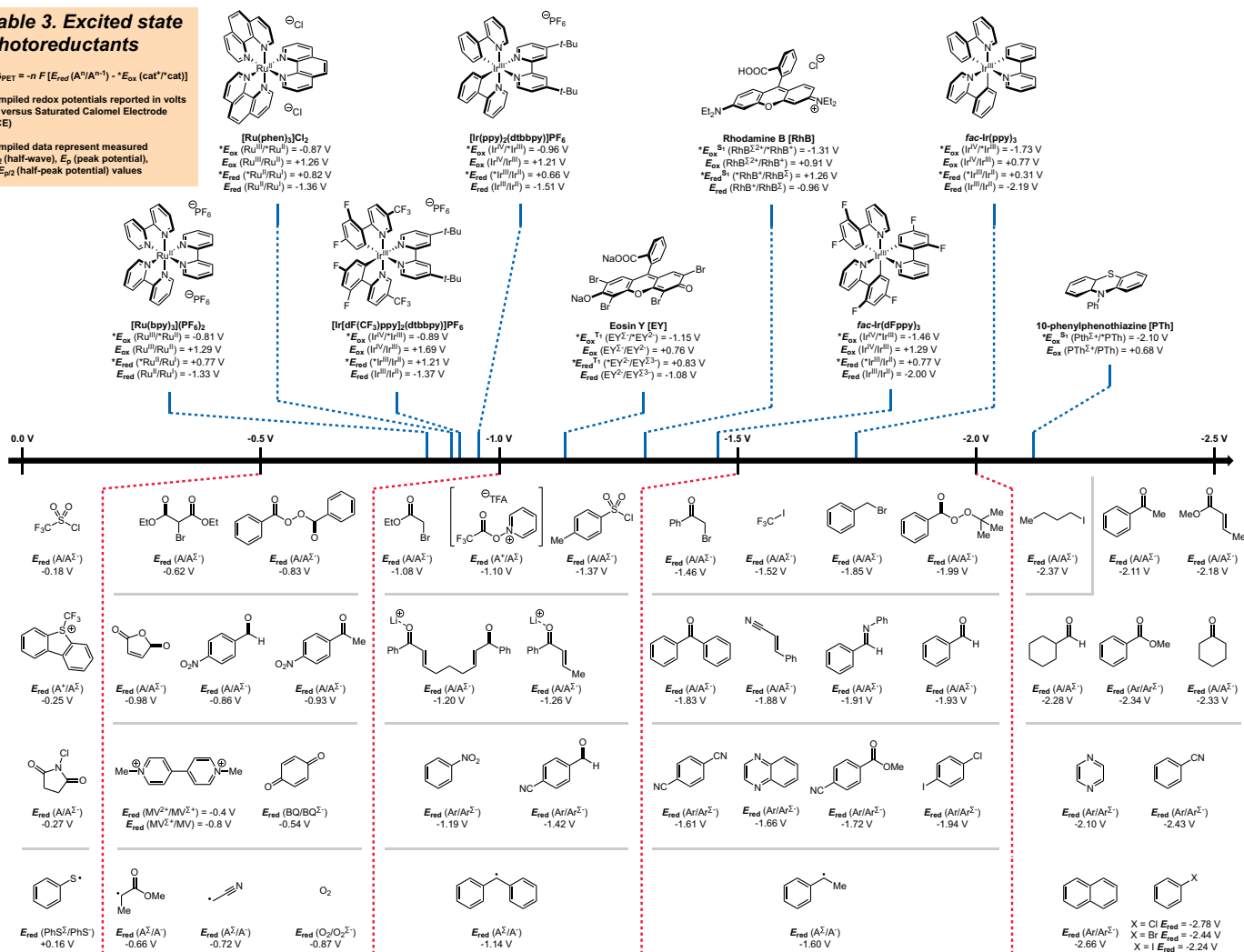
XV. Appendix Table 3: Excited state photoreductants

Table 3. Excited state photoreductants

$DG_{PET} = -n F [E_{red}(A^0/A^{n-1}) - E_{ox}(cat^+/cat)]$

Compiled redox potentials reported in volts (V) versus Saturated Calomel Electrode (SCE)

Compiled data represent measured $E_{1/2}$ (half-wave), E_p (peak potential), or $E_{p/2}$ (half-peak potential) values



XVI. Appendix Table 4: Catalyst references and properties

No.	Photoredox Catalyst	Local λ max (nm)	*Ered (V vs. SCE)	Ered (V vs. SCE)	*Eox (V vs. SCE)	Eox (V vs. SCE)	Product Number	Reference for catalyst properties	Reference for catalyst use
1	[Ru(bpy) ₃](PF ₆) ₂	452	0.77	-1.33	-0.81	1.29	754730	<i>Chem. Rev.</i> 2013 , 113, 5322	<i>Science</i> 2008 , 322, 77
2	[Ru(phen) ₃]Cl ₂ •H ₂ O	422	0.82	-1.36	-0.87	1.26	343714	<i>Chem. Rev.</i> 2013 , 113, 5322	<i>Nature</i> 2011 , 480, 224
3	[Ru(bpm) ₃]Cl ₂	454	0.99	-0.91	-0.21	1.69	747785	<i>Chem. Rev.</i> 2013 , 113, 5322	<i>Chem. Sci.</i> 2012 , 3, 2807
4	[Ru(bpz) ₃](PF ₆) ₂	443	1.45	-0.8	-0.26	1.86	747777	<i>Chem. Rev.</i> 2013 , 113, 5322	<i>J. Am. Chem. Soc.</i> 2011 , 133, 19350
5	fac-Ir(ppy) ₃	375	0.31	-2.19	-1.73	0.77	694924	<i>Chem. Rev.</i> 2013 , 113, 5322	<i>Nature Chem.</i> 2012 , 4, 85
6	fac-Ir(dFppy) ₃	346	0.77	-2	-1.46	1.29	900540	<i>Inorg. Chem. Front.</i> 2014 , 1, 562, <i>J. Am. Chem. Soc.</i> 2003 , 125, 7377	<i>Nature</i> 2011 , 480, 224
7	[Ir(dmppy) ₂ (dtbbpy)]PF ₆	--	0.55	-1.52	-0.87	1.21	N/A	<i>J. Am. Chem. Soc.</i> 2014 , 136, 6858	<i>J. Am. Chem. Soc.</i> 2014 , 136, 6858
8	[Ir(ppy) ₂ (dtbbpy)]PF ₆	380	0.66	-1.51	-0.96	1.21	747769	<i>Chem. Rev.</i> 2013 , 113, 5322	<i>J. Am. Chem. Soc.</i> 2013 , 135, 17735
9	[Ir[Fmppy] ₂ (dtbbpy)]PF ₆	--	0.77	-1.5	-0.94	1.33	N/A	<i>Chem. Mater.</i> 2005 , 17, 5712	<i>Chem. Mater.</i> 2005 , 17, 5712
10	[Ir[dF(Me)ppy] ₂ (dtbbpy)]PF ₆	360	0.97	-1.44	-0.92	1.49	901409	<i>Chem. Mater.</i> 2005 , 17, 5712, <i>Inorg. Chem.</i> 2011 , 50, 11514	<i>Science</i> 2017 , 355, 727
11	[Ir[dFppy] ₂ (dtbbpy)]PF ₆	365	1.14	-1.42	-0.96	1.6	901368	<i>J. Organo. Met. Chem.</i> 2015 , 776, 51, <i>J. Mater. Chem. C</i> 2016 , 4, 3726, <i>J. Am. Chem. Soc.</i> 2016 , 138, 13862	<i>J. Am. Chem. Soc.</i> 2016 , 138, 13862
12	[Ir[dF(Cf ₃)ppy] ₂ (dtbbpy)]PF ₆	380	1.21	-1.37	-0.89	1.69	747793	<i>Chem. Rev.</i> 2013 , 113, 5322 <i>Chem. Mater.</i> 2005 , 17, 5712	<i>Science</i> 2014 , 345, 437
13	[Ir[dF(Cf ₃)ppy] ₂ (bpy)]PF ₆	379	1.32	-1.37	-1	1.69	804215	<i>Inorg. Chem. Front.</i> 2014 , 1, 562	<i>Science</i> 2014 , 345, 433
14	[Ir[dF(Cf ₃)ppy] ₂ (5,5'-dCf ₃ -bpy)]PF ₆	--	1.68	-0.69	-0.43	1.94	N/A	<i>Nature</i> 2016 , 539, 268	<i>Nature</i> 2016 , 539, 268
15	[Cr(Ph ₂ phen) ₃](Bf ₄) ₃	300-400	1.4	-0.27	--	--	N/A	<i>Angew. Chem. Int. Ed.</i> 2015 , 54, 6506	<i>Angew. Chem. Int. Ed.</i> 2015 , 54, 6506
16	Rose Bengal [RB-Na ₂] (T1)	549	0.81	-0.99	-0.96	0.84	330000	<i>Chem. Rev.</i> 2016 , 116, 10075	<i>Green Chem.</i> 2012 , 14, 1293
17	Eosin Y [EY-Na ₂] (T1)	520	0.83	-1.08	-1.15	0.76	E4382	<i>Chem. Rev.</i> 2016 , 116, 10075	<i>Adv. Synth. Catal.</i> 2015 , 357, 2050
18	Rhodamine 6G [Rh6G] (S1)	530	1.18	-1.14	-1.09	1.23	252433	<i>Chem. Rev.</i> 2016 , 116, 10075	<i>J. Am. Chem. Soc. D</i> 1969 , 6, 251
19	Rhodamine B [RhB] (S1)	550	1.26	-0.96	-1.31	0.91	83689	<i>Chem. Rev.</i> 2016 , 116, 10075	<i>Synlett</i> 2015 , 26, 265
20	9,10-Dicyanoanthracene [DCA]	422	1.99	-0.91	--	--	459852	<i>Chem. Rev.</i> 2016 , 116, 10075	<i>J. Am. Chem. Soc.</i> 1988 , 110, 3677
21	1,2,3,5-Tetrakis(carbazol-9-yl)-4,6-dicyanobenzene [4CzIPN]	435	1.35	-1.21	-1.04	1.52	901817	<i>ACS Catal.</i> 2016 , 6, 873	<i>ACS Catal.</i> 2016 , 6, 873
22	Mes-(MeO)4Acr-Ph-Bf ₄	412	1.62	-0.84	--	--	900693	<i>J. Org. Chem.</i> 2016 , 81, 7244	<i>J. Org. Chem.</i> 2016 , 81, 7244
23	Mes-(MeO)4Acr-Ar-Bf ₄ , Ar = 3,5-dimethoxyphenyl	414	1.65	-0.82	--	--	900694	<i>J. Org. Chem.</i> 2016 , 81, 7244	<i>J. Org. Chem.</i> 2016 , 81, 7244
24	Mes-Acr-Me-Bf ₄	425	2.08	-0.57	--	--	794171	<i>Chem. Rev.</i> 2016 , 116, 10075	<i>J. Am. Chem. Soc.</i> 2013 , 135, 9588
25	Mes-(t-Bu)2Acr-Ph-Bf ₄	420	2.08	-0.59	--	--	900421	<i>J. Org. Chem.</i> 2016 , 81, 7244	<i>Science</i> 2015 , 349, 1326
26	Mes-Me2Acr-Ph-Bf ₄	438	2.09	-0.58	--	--	793876	<i>Nature Chem.</i> 2014 , 6, 720, <i>Acc. Chem. Res.</i> 2016 , 49, 1997	<i>Nature Chem.</i> 2014 , 6, 720
27	Mes-Acr-Ph-Bf ₄	432	2.17	-0.5	--	--	793221	<i>Nature Chem.</i> 2014 , 6, 720, <i>Acc. Chem. Res.</i> 2016 , 49, 1997	<i>Org. Lett.</i> 2015 , 17, 1316
28	2,4,6-tris(4-methoxyphenyl)pyrylium-Bf ₄ [p-MeO-TPT]	470	1.84	-0.5	--	--	900692	<i>Chem. Ber.</i> 1993 , 126, 1671	<i>Chem. Sci.</i> 2013 , 4, 2625
29	2,4,6-tri-p-tolylpyrylium-Bf ₄ [p-Me-TPT]	444	2.13	-0.42	--	--	900685	<i>Chem. Ber.</i> 1993 , 126, 1671	<i>J. Am. Chem. Soc.</i> 2015 , 137, 15684
30	2,4,6-Triphenylpyrylium-Bf ₄ [TPT]	416	2.39	-0.27	--	--	272345	<i>Chem. Ber.</i> 1993 , 126, 1671	<i>Chem. Ber.</i> 1993 , 126, 1671
31	10-Phenylphenothiazine [PTh]	<300	--	--	-2.1	0.68	903167	<i>Chem. Rev.</i> 2016 , 116, 10075	<i>J. Am. Chem. Soc.</i> 2014 , 136, 16096

Sigma-Aldrich®

Lab & Production Materials

Merck KGaA
Frankfurter Strasse 250
64293 Darmstadt, Germany

MerckMillipore.com

To place an order or receive technical assistance in Europe, please call Customer Service:

France: 0825 045 645

Spain: 901 516 645 Option 1

Germany: 069 86798021

Switzerland: 0848 645 645

Italy: 848 845 645

United Kingdom: 0870 900 4645

For other countries across Europe, please call: +44 (0) 115 943 0840

Or visit: **SigmaAldrich.com/offices**

For Technical Service visit: **SigmaAldrich.com/techservice**

Copyright © 2019 Merck KGaA, Darmstadt, Germany and/or its affiliates. All Rights Reserved. Merck, the vibrant M and Sigma-Aldrich are trademarks of Merck KGaA, Darmstadt, Germany or its affiliates. All other trademarks are the property of their respective owners. Detailed information on trademarks is available via publicly accessible resources.

Lit. No. MK_BR2471EN Ver. 1.0
2019 – 17128
02/2019